REINFORCED HOLES IN SHELLS

by

KEELAPATLA PRABHAKARA RAO, M.A., M.E.

A thesis submitted for the degree of
Doctor of Philosophy of the University of London
and for the Diploma of Membership of
Imperial College

1969

Summary

In this thesis some problems concerned with reinforced holes in cylindrical and spherical shells are considered. The flat plate theories are inadequate in describing the stress distributions around holes in shells and this thesis presents a method of applying shallow shell theory to such problems. Though only two types of shells are considered, the results are applicable to cases where the local structure can be assumed to be a cylinder or a sphere.

Firstly, the case of a reinforced circular hole in a cylindrical shell is investigated. This problem is representative of a window in a fuselage shell. The analysis is carried out using shallow shell theory with the assumption that the reinforcement is a compact bead of constant cross-section having finite extensional, bending and torsional rigidities. In the case of pressure loading the hole is assumed to be covered by a diaphragm which allows the hole edge to deflect and rotate, the pressure force being communicated to the shell as a suitably distributed shear around the hole edge. It is shown that it is possible to find an optimum reinforcement for a given set of dimensions describing the cut-out, and the cylinder. The theory proposed gives good results for the shell and reinforcement stresses as shown by comparison with the experimental results obtained from tests on an aluminium alloy cylinder with a reinforced circular hole, under torsion.

There are cases when the reinforcement has to be flush with the outer surface of a shell for aerodynamic or other reasons. In such a case the shear centre of the reinforcement cross-section does not lie on the shell middle surface which causes coupling between the bending and membrane stresses. It is found that this mostly leads to an increase in the principal stresses as compared with a symmetric reinforcement for pressure loading.

It is very often advantageous to use hole shapes other than circular. In order to solve such problems, a conformal mapping technique is used. Though the method is applied to only two shapes, ellipse and a square with rounded corners, it is applicable to holes of any shape provided there are no sharp corners. In the analysis, only first-order effects due to the given hole shape being different from a circle, are considered.

The next problem considered is that of a reinforced circular hole in a spherical shell under pressure. The shell is assumed to be shallow and the reinforcement is assumed to be a compact bead, with bending rigidity. In this case it is possible to find a neutral hole, i.e. a hole so reinforced to leave the stress distribution in the shell undisturbed. The reinforcement required is the same as for a flat plate under uniform tension. The case when the reinforcement is flush with either inside or outside of the shell is considered which showed that the stresses always increased with eccentricity.

Throughout the thesis an attempt has been made to develop and use methods of analysis which are applicable to real situations, mainly because all previous work on reinforced holes was restricted to a small curvature parameter quite unrepresentative of typical aircraft and pressure vessel configurations. Also in the case of reinforced circular and elliptical holes in cylindrical shells, two idealisations describing the transfer of pressure load acting on the cut-out portion to the shell are considered.

ACKNOWLEDGEMENTS

The author would like to express his grateful thanks to Dr. G.A.O. Davies for his helpful guidance and constant encouragement and also to Professor J.H. Argyris for all the help given by him during the course of this project. Thanks are also due to Miss M. Hudgell for transforming the draft to the present form and to Mrs. Bartley for the help in preparing the drawings.

The author would like to take this opportunity to thank the Commonwealth Scholarship Commission of the United Kingdom for the award of the scholarship without which the present work would not have been possible.

INDEX

LIST OF APPENDICES:

GENERAL NOTATION

a	:	Radius of the hole.
R	:	Radius of the shell middle surface.
t	:	Shell thickness
ν	:	Poisson's ratio.
F	:	Airy's stress function for the membrane stresses. (Non-dimensional)
w	:	Normal displacement. (Non-dimensional)
$\overline{F}$; $\overline{w}$	:	Asymptotic values of F and w away from the hole.
F^*	:	$F - \overline{F}$.
w^*	:	$w - \overline{w}$.
E_S ; E_R	:	Elastic moduli of shell and reinforcement.
$E_R A$	:	Extensional)
$E_R I$	:	Bending) Rigidities of reinforcement.
$\frac{E_R J}{2(1+\nu)}$	:	Torsional)
H_n^1	:	Hankel functions of the first kind, order n.
∇^2	:	Laplacian operator $= \frac{\partial^2}{\partial r^2} + \frac{1}{r} \cdot \frac{\partial}{\partial r} + \frac{1}{r^2} \frac{\partial^2}{\partial \theta^2}$.
∇^4	:	$\nabla^2 \nabla^2$.
λ	:	A/at.
μ	:	$1/At^2$.
D	:	$E_S t^3 / 12(1-\nu^2)$.
p	:	Pressure loading.
$w_{,rr}$	:	$\frac{\partial^2 w}{\partial r^2}$.
F'	:	Airy's stress function (dimensional).
w'	:	Normal displacement (dimensional).

ADDITIONAL NOTATION

CHAPTER I :

β^2 : Curvature parameter $= \frac{a^2}{8Rt}\,(12[1-\nu^2])^{1/2}$.

ξ : $r\cos\theta = x/a$.

η : $r\sin\theta = y/a$.

$(E_1 - iE_2)$: $\{\exp[(1-i)\beta\xi] + \exp[-(1-i)\beta\xi]\}/2$.

$(E_3 - iE_4)$: $\{\exp[(1-i)\beta\xi] - \exp[-(1-i)\beta\xi]\}\ \frac{(1+i)}{4}$.

A_n, B_n : Constants occurring in the complex stress function ϕ^*.

ϕ : $w - iF$

H_n^2 : Hankel function of the second kind, order n.

r' : $a\,r$.

Γ : Torsion bending constant.

Z : $r\,e^{i\theta}$.

CHAPTER II :

Z : $r\,e^{i\theta}$.

ζ : $\rho e^{i\gamma}$

$f(\zeta)$: Mapping function occurring in (1.1.1).

ψ : The angle between the normal at any point on the contour and the radial direction through that point.

C_n, D_n : Constants occurring in ϕ_1^*.

α : The angle between the normal to the hole contour at any point and the 'x axis'.

ds : An elemental length of the bead.

dn_o : Angle made by the projection of an element perpendicular to the generator at the axis of the cylinder.

$w(\zeta)$: $\zeta + \varepsilon f(\zeta)$, Mapping function.

L_1, L_2 : Operator defined in Appendix VIII.

ϕ_o^* : Complex stress function for the case of a circular hole in a cylindrical shell.

ϕ_1^* : Additional contribution to the complex stress function due to the hole contour perturbation.

ϕ^* : $\phi_o^* + \varepsilon\phi_1^*$.

Λ : $\frac{E_R}{E_S} \cdot \frac{A}{r_o t}$.

Π : $\frac{E_R}{E_S} \cdot \frac{I}{r_o t^3}$

Ω : $\frac{E_R}{E_S} \cdot \frac{J}{r_o t^3}$

r_o : Characteristic dimension of the problem.

β^2 : Curvature parameter = $\frac{r_o^2}{8Rt} (12(1-\nu^2))^{1/2}$.

$\overline{\zeta}$: Complex conjugate of ζ.

∇_Z^2 : $\frac{\partial^2}{\partial r^2} + \frac{1}{r}\frac{\partial}{\partial r} + \frac{1}{r^2}\frac{\partial^2}{\partial \theta^2}$.

∇_ζ^2 : $\frac{\partial^2}{\partial \rho^2} + \frac{1}{\rho}\frac{\partial}{\partial \rho} + \frac{1}{\rho^2}\frac{\partial^2}{\partial \gamma^2}$.

$(E_1-iE_2)_Z$, $(E_3-iE_4)_Z$: Krylov functions in (r,θ) coordinates.

$(E_1-iE_2)_\zeta$, $(E_3-iE_4)_\zeta$: Krylov functions in (ρ,γ) coordinates.

ζ : $\xi_1 + i\eta_1$

ε : Defined in (2.1.1).

ϕ_j^* : $w_j^* - iF_j^*$.

r_o : $\frac{(a+b)}{2}$ for an elliptical hole with 'a' and 'b' as semi-major and semi-minor axes.

: $\frac{6a}{5}$ for a square hole with rounded corners of side '2a'.

ξ : $r \cos\theta = x/r_o$.

η : $r \sin\theta = y/r_o$.

CHAPTER III :

β^2 : Curvature parameter = $\frac{a^2}{Rt}[12(1-\nu^2)]^{1/2}$.

A_1, A_2 and C : Constants occurring in complex stress function ϕ^*.

INTRODUCTION

In general cut-outs are introduced into aircraft and spacecraft structures in order to facilitate access or visibility. As these cut-outs weaken the structure, reinforcement is necessary to reduce the stress concentrations. To find an optimum reinforcement to reduce the stresses to given limits is the problem faced by engineers in general. An aeronautical engineer has the additional problem of reducing the weight of reinforcement to low values even if it means a small increase in stresses consistent with the requirements.

The typical cut-outs in an aircraft are windows, doors, and canopy, and the designer's problem is to contain the rise in stress level due to these discontinuities. The ideal would be to have a window frame of such a shape and section as to leave the stresses outside the frame unaltered. A hole with this kind of reinforcement is referred to as a "Neutral Hole" (1). In practice, however, even if one can make a hole neutral in the structure it is found that the reinforcement required is too heavy. The theory of neutral holes has been considered by Mansfield (1) and by Gurney (2) for flat plates. Mansfield arrives at the conclusion that a circular hole is the neutral hole for a flat plate in an axisymmetrical stress field and an elliptical hole for a plate subjected to a biaxial stress system of unequal principal stresses with the same sign.

It was hitherto assumed that flat plate theory could be used for solving problems connected with very shallow shells without causing much error in the estimation of stresses. As one can see, the application of flat plate theory to a shell is not truly representative of the actual conditions obtained in a shell since the bending stresses and the curvature effects on the membrane stresses are

ignored. In fact the neglect of the effect of curvature is shown theoretically to lead to errors of large magnitude by Lurie (3) and Vandyke (4) amongst others (5), (6), (7) and (8). Experiments conducted by Houghton and Rothwell (9), Jessop et al. (10), Richards (11) and Durelli et al. (12) have shown the significant differences in stresses between the flat plate and the shell. In some cases the bending stresses are of the same order as the membrane stresses and flat plate theory assumes zero bending stresses.

Experimental studies of the state of stress in shells around holes with sufficiently smooth contours show that the perturbation in the state of stress around the hole in a shell has a local character and the perturbations die away rapidly with the distance from the hole. This has been shown by Savin (13) who concludes that the entire perturbed zone lies within an ellipse with semi-axes "a' and 'b' (a = 1.5 d, b = d) in the case of a cylinder under pressure and tension. In the case of a sphere this perturbed region lies inside a circle of radius r = 1.5 d, 'd' being the diameter of the hole. So it is reasonable to assume that the influence of one hole on neighbouring holes is negligible as long as the distance between their centres is more than '3d'. This has been shown theoretically (14) to be true for a flat plate and the experiments conducted by Durelli et al. (15) do show that there is no interaction between the stress distributions in the neighbouring bays of a ribbed cylindrical shell.

One can optimise a structure if one has a clear picture of the structural behaviour of the individual components. Williams (16) proves that it is worthwhile to optimise the construction of a fuselage, which is of interest to us, by considering a typical example of a fuselage cabin. In the cabin with a main section 10 ft in diameter

and walls of 20 gauge (0.036"), the maximum stress is that associated with the hoop tension in the main section of 16,600 psi (approximately) for an internal operating pressure of 10 psi. For an ultimate stress in the sheet of 60,000 lb/in^2 the theoretical maximum pressure is therefore 36 lb/in^2. The introduction of a multiplicity of discontinuities must inevitably weaken the structure, but the maintenance, by good design, of a failing pressure of 30 lb/in^2 would not appear an unreasonable target to aim at, in spite of discontinuities. Suppose the figure achieved actually is 20 lb/in^2, the outcome is, that for the latter figure, the cabin is loaded to half its ultimate load at every flight, whereas for the target figure it is loaded only to one-third of its ultimate. Having regard to the shape of S-N curve, the value of such a reduction in the ratio of the working load to the ultimate load is obvious, increasing the working life some ten-fold. Also it is clear that a design, using a sheet thickness appropriate to the maximum stress existing would be inefficient in terms of the structural weight. (See Appendix I.) The edge reinforcement around windows and doors is a reasonable way of bringing the local high stresses to permissible levels. At the same time caution should be exercised not to overstiffen the hole region as it is shown that this defeats its objective by actually increasing the stresses in the sheet.

Richards (11) constructs a neutral hole for pressurised cylinder (17) and obtains significant stress concentrations. He goes further and shows that a circular hole with constant area reinforcement around, has the same performance as the neutral hole but the validity of these results is questionable since the bending stresses are 25% of the membrane stresses even at distances '5a' (a is radius of hole) from the centre of the hole. Some other unsatisfactory tests have been conducted by Houghton and Rothwell (41) who incorrectly resist the pressure load over the hole by external means.

All this leads us to search for an analysis which takes into account the effects not considered in flat plate theory. Among the various methods of solution to this problem are the analytical approach and the matrix displacement method. The types of element required for problems of this type for using matrix displacement method, has recently been proposed by Argyris (18) and (19), (CUBA and SHEBA elements). A representation of a shell by polyhedron surfaces may lead to serious errors especially in the presence of pronounced bending effects. In order to obviate this difficulty the SHEBA family of shell elements, for the matrix displacement method, take into account the curvature effects. In this thesis the method employed is analytical in nature, starting with the shallow shell equations. The boundary conditions are satisfied by collocation technique.

The flat plate theories are inadequate in describing the stress distribution around holes in shells and this thesis presents a method of applying shallow shell theory to such problems. Attempts made so far on reinforced holes in shells consider values of the curvature parameter $\beta << 1$ (44) which are quite unrepresentative of typical aircraft or pressure vessel configurations. Even in the case of unreinforced holes, the solutions were restricted to $\beta << 1$ (42) and in some cases (46) boundary conditions on moment and normal shear were not satisfied. By considering values of $\beta << 1$, it was concluded (42) that for tension loading shell stresses differ very little from flat plate solutions. It can be seen (43) that this conclusion is not correct for pressure loading. Throughout this thesis an attempt has been made to develop and use methods of analysis which are applicable to real situations (i.e. $\beta > 1$).

Any loading on the region around a window in an aircraft fuselage can be obtained as a superposition of three basic loadings, tension,

pressure and torsion. Also the usual shape of window is circular, elliptical or a square with rounded corners. A spherical shell that one comes across in spacecraft structures is generally subjected to pressure loading and the cut outs are circular in shape. All these cases have been considered in this thesis.

In the first chapter the problem of a reinforced hole in a cylindrical shell is considered. Firstly the results of Vandyke (4) have been extended for values of 'β' up to 7, for the case of an unreinforced hole. Theoretical estimates are made for a reinforced circular hole in a cylindrical shell under torsion in order to compare with experimental results obtained by Rothwell (20). It is shown that an optimum reinforcement can be found for a given value of β for pressure loading. As the number of parameters that can be varied is large, it is a formidable task to try to optimise and hence this is done only for the important pressure loading case. Cases do arise when it is preferable to make the outside of reinforcing ring lie flush with the outside of the shell skin for aerodynamic or other reasons. Results have been obtained to show the penalty of attaching the reinforcement eccentrically.

The second chapter deals with holes of shapes other than circular in a cylindrical shell subjected to pressure loading. Though the method employed is general, application is made to two specific cases, the hole shapes being an ellipse and a square with rounded corners. The reinforcement is assumed to be a compact bead with the shear centre of its cross-section lying in the shell middle surface.

The third chapter deals with a reinforced circular hole in a spherical shell under pressure. The theory is given for both symmetric and eccentric reinforcements. Experimental results obtained by Houghton and Rothwell (9) for an unreinforced circular hole agree well with theory proposed.

Though this thesis deals with two types of shells, the results are applicable to many cases where the local structure can be assumed to be either a shallow cylinder or a shallow sphere. This excludes, of course, structures with negative Gaussian curvature like the cooling towers or toroidal shells.

All the computations leading to the results in this thesis were carried out on the University of London Computer 'ATLAS' using EXCHLF autocode. Throughout this thesis the value of ν is taken as $\frac{1}{3}$.

CHAPTER I

CYLINDRICAL SHELL WITH A REINFORCED CIRCULAR HOLE

1.1: Introduction:-

In this chapter stresses due to the presence of a reinforced circular hole in a cylindrical shell, subjected to prescribed loads away from the hole, are obtained by the use of collocation technique. The reinforcement is taken to be a compact bead placed around the inside of the hole and the shell is assumed to be shallow. A shallow, cylindrical shell may be described as a shell whose ratio of rise to base length is small, which implies that its circumferential dimension is small compared with its radius of curvature. By limiting the ratio of the hole radius to the radius of curvature, $\frac{a}{R}$, the effects of the hole may be confined to an area which is within a small radial distance from the hole; this region of the shell may be considered as a shallow shell. The shell configuration is shown in fig. 1. The formulation has been done for the general case when the shear centre of the reinforcement cross-section does not lie in the shell middle surface. The symmetric reinforcement case is a particular case of this general formulation.

The application of edge reinforcement to holes in flat plates started as early as 1924 when Timoshenko (21) obtained an approximate solution of the problem by using the theory of curved bars. Gurney (2) attempted to find the optimum reinforcement of constant cross-section to make the hole neutral for a given loading. The theory developed by him indicates that as the size of the ring is increased, the maximum circumferential stress at the hole decreases, and that the maximum shear stress in the sheet near the hole increases. Hence it is not possible, using a uniform ring, for both

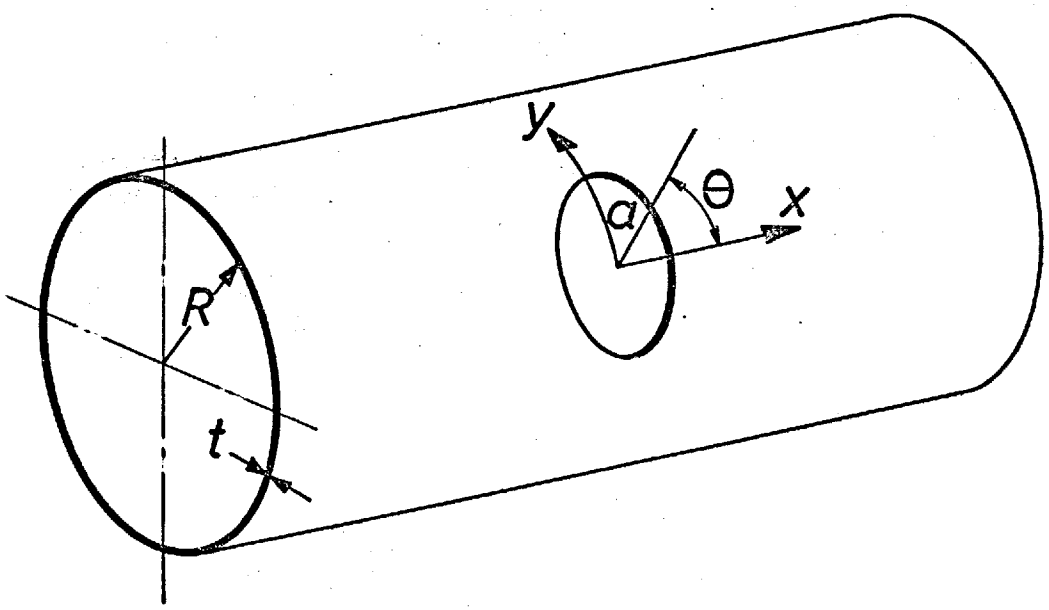

FIG. 1 CYLINDRICAL SHELL CONFIGURATION

these stress concentrations to be reduced simultaneously but it is possible to find an optimum reinfocement by compromising between the direct and shear stress concentrations. He also concludes that neutrality can be obtained only under special conditions.

Reissner and Morduchow (22) treated the problem of reinforced circular holes in plane sheets by permitting variations of the sectional area. Gurney (2) expresses the stress distribution in the sheet and the reinforcement by means of Airy's stress functions, the constants in which are evaluated by satisfying the boundary conditions. The approach used by Reissner (22) is different in that the reinforcement is a curved beam having extensional and bending rigidity.

Mansfield (1), (23), assuming the reinforcement to be a compact bead capable of carrying only tension, shows that for a given loading of the sheet it is possible to find the shape of the hole and the reinforcement which leaves the stress distribution unaltered everywhere in the sheet. He has discussed the design of neutral holes in pressurised shells (17) and shows that for a developable surface the neutral hole corresponds to that in the developed sheet. (These have been restudied more recently in (24) and (25).)

The case of an unreinforced circular hole in a cylindrical shell was first considered by Lurie (3). He obtained a perturbation solution, the results being valid for small values of the curvature parameter $\beta^2 = \frac{a^2}{8Rt}\,[12(1-\nu^2)]^{1/2}$. The shallow shell equations are solved exactly, expressing the solution in terms of the Hankel functions of the first kind, and of Krylov functions. Each of these functions are expanded in powers of 'β' retaining terms of the order of 'β^2'. The boundary conditions on the direct stress, shear stress, bending moment and Kirchoff shear are satisfied which leads to the solution of the unknowns assumed in the series solution.

Shevliakov and Zigel (7), using a perturbation method similar to that used by Lurie obtained a solution for the problem of a cylindrical shell with a circular hole for small values of 'β' (corresponding to torsion loading). The first extension of these results for larger, more practical values of 'β' was made by Withum (8) for a cylinder under torsion. Values of 'β' up to 2 were considered.

Lekkerkerker (5) expands the exponential functions in the exact solution of shallow cylindrical shell equations as a Fourier series involving Bessel functions and applying a numerical procedure obtains solutions for β up to 2.8, for tension and torsion loading cases. Each term in the Fourier series solution satisfied the hole boundary conditions. Experiments conducted by him on a steel cylinder for $\sqrt{2}\beta = 1$ showed good agreement with the theoretical estimates for torsion loading case.

Eringen and his coworkers (6) use a numerical procedure similar to that of Lekkerker (5), but the boundary conditions are satisfied by a collocation technique. Values of 'β' up to 1.75 are considered for tension, torsion and pressure loading cases.

Vandyke (4) using the exact solution and using collocation procedure for satisfying the boundary conditions extended the solution up to $\beta = 4$ for tension, torsion and pressure loading cases. The series solution is terminated when an increase in the number of terms does not alter the stress values. In fact the method suggested by Vandyke now seems to be applicable to all values of β, the only limitation being shallowness of the shell and the restriction that the deflections are not large.

For practical values of β ($\beta > 1$), no theoretical work on reinforced circular holes in cylindrical shells seems to have been published. This is so in the case of reinforced holes of arbitrary shape also.

The assumption that the hole reinforcement is a compact bead is a limitation (27) in the case of aircraft fuselages where windows and doors may have complex cross-sections to accommodate seals. However in this thesis the reinforcement is still idealised as a compact bead possessing flexural, torsional and extensional rigidities.

1.2 Formulation of the problem

The equations which govern the behaviour of a thin shallow shell were obtained in the non-linear form by Marguerre (28). For the cylindrical geometry the linearised form of the equations become

$$\nabla^4 w' + \frac{1}{RD} F'_{,xx} = \frac{p}{D} \qquad (1.2.1)$$

and

$$\nabla^4 F' - \frac{E_s t}{R} w'_{,xx} = 0 \qquad (1.2.2)$$

These equations can be obtained by using Donnell's approximations (26) for shallow shells. (See Appendix II.) It is assumed that the shell although shallow is not so shallow that the curvature due to deformation becomes as significant as the original curvature. If this were so then the edge effects around the hole would be confined to a boundary layer in which the non-linear equations would not be tractable in simple form (29). The sign convention for stress resultants and stress couples is shown in figure 2.

For the purpose of non-dimensionalising the stress resultants, a reference stress, N_{ref}, is chosen as the applied stress away from the hole in the case of tension and torsion loadings and hoop stress in the case of pressure loading.

Defining $F = F'/a^2 N_{ref}$

$$w = \frac{w' . E_s t^2}{a^2 N_{ref} [12(1-\nu^2)]^{1/2}} \qquad (1.2.3)$$

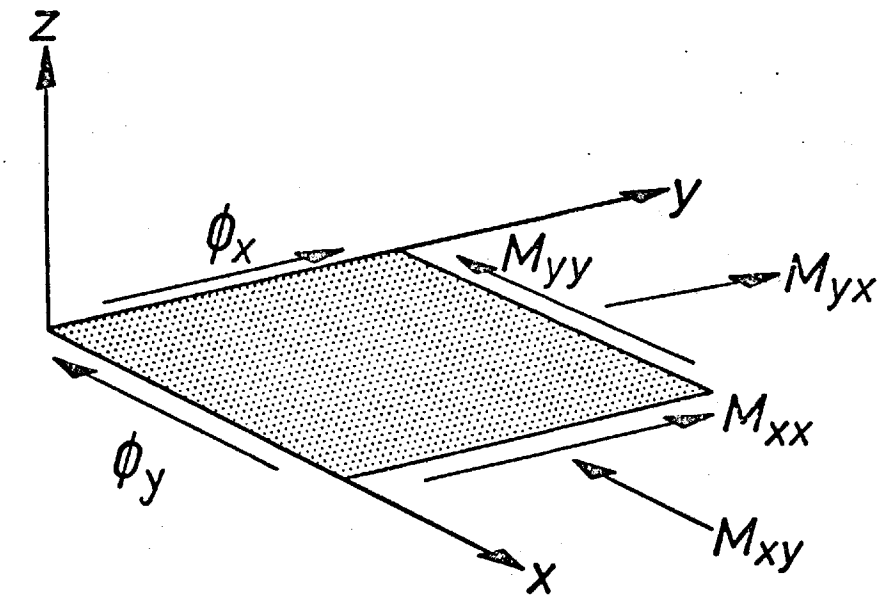

STRESS COUPLES & ROTATIONS

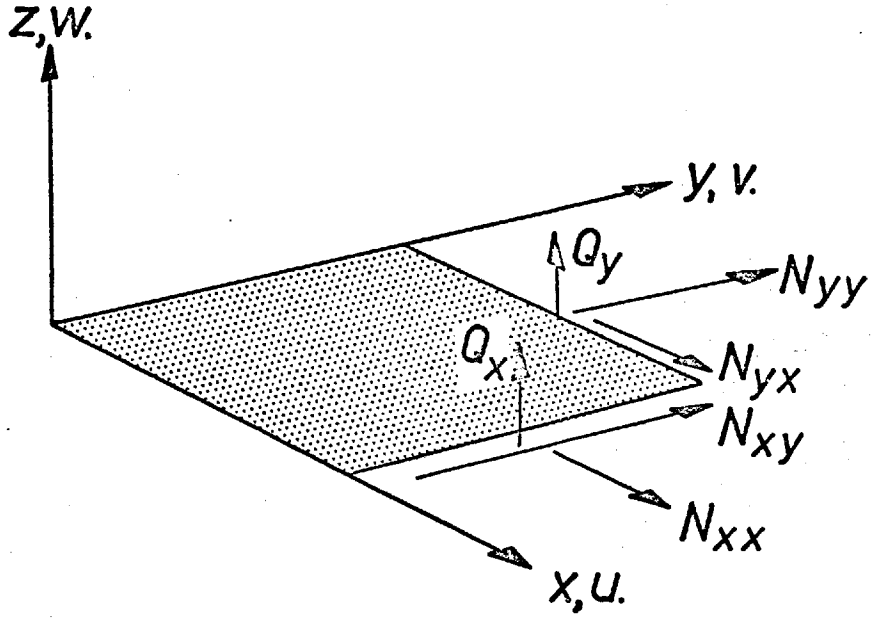

FIG. 2 STRESS RESULTANTS & DISPLACEMENTS

the two differential equations (1.2.1) and (1.2.2) can be combined into a single complex differential equation

$$\nabla^4\phi + 8i\beta^2\phi_{,\xi\xi} = 8\beta^2 \qquad (1.2.4)$$

where the right-hand side exists for pressure loading and is zero for other cases of loading,

and $\phi = w - iF.$

The effect of a hole in a shell is shown by Savin (13) to be confined to a local region around the hole. The stress function and normal deflection may therefore be written as,

$$F = \overline{F} + F^* \quad ; \quad w = \overline{w} + w^* \qquad (1.2.5)$$

where $\overline{F}$ and $\overline{w}$ are prescribed values of F and w away from the hole in which region F* and w* vanish.

$\overline{F}$ is given by $\eta^2/2$; $\xi\eta$; and $\frac{\xi^2}{2} + \frac{\eta^2}{4}$ for tension, torsion and pressure loading cases respectively.

Then the residual problem reduces to a homogeneous equation for all loadings and is given by,

$$\nabla^4\phi^* + 8i\beta^2\phi^*_{,\xi\xi} = 0 \qquad (1.2.6)$$

where $\phi^* = w^* - iF^*$ and tends to zero away from the hole.

1.3 The solution to the differential equation:

Equation (1.2.6) can be put in the operational form as,

$$L_1 L_2 \phi^* = 0 \qquad (1.3.1)$$

where $$L_1 = [\nabla^2 - 2(1-i)\beta\frac{\partial}{\partial\xi}]$$

and $$L_2 = [\nabla^2 + 2(1-i)\beta\frac{\partial}{\partial\xi}] \qquad (1.3.2)$$

As the operators L_1 and L_2 are commutative,

$$\phi^* = \phi_1^* + \phi_2^*$$

where $$L_1\phi_1^* = 0 \quad ; \quad L_2\phi_2^* = 0 \tag{1.3.3}$$

Choosing the form $$\phi_1^* = e^{(1-i)\beta\xi}\psi_1(\xi,\eta)$$

$$\phi_2 = e^{-(1-i)\beta\xi}\psi_2(\xi,\eta) \tag{1.3.4}$$

we find that the functions ψ_1 and ψ_2 must both satisfy the equation,

$$\nabla^2\psi + 2i\beta^2\psi = 0 \tag{1.3.5}$$

Equation (1.3.5) can be solved by separating the variables and assuming that $\psi = f_1(r) \begin{matrix}\cos\\ \sin\end{matrix} (n\theta)$. (1.3.6)

The problems concerned with tension and pressure loadings are symmetric in ξ and η whereas for torsion loading the problem is anti-symmetric. It can be seen that in both cases it is sufficient to satisfy the boundary conditions in a quadrant of the circular hole. It is convenient to form Krylov functions (3) which are symmetric and antisymmetric in ξ as follows,

$$(E_1 - iE_2) = [e^{(1-i)\beta\xi} + e^{-(1-i)\beta\xi}]/2$$

$$(E_3 - iE_4) = [e^{(1-i)\beta\xi} - e^{-(1-i)\beta\xi}](1+i)/4 \tag{1.3.7}$$

For problems which are symmetrical in ξ and η (1.3.6) takes the form

$$\psi = \sum_{-\infty}^{\infty} C_n H_n^1 (\beta r\sqrt{2i}) \cos n\theta + \sum_{-\infty}^{\infty} D_n H_n^2(\beta r\sqrt{2i}) \cos n\theta$$

in which the part containing the Hankel functions of the second kind should be discarded as they grow larger with the argument. Also, $H_{-n}^1 (\beta r\sqrt{2i}) = e^{in\pi} H_n^1 (\beta r\sqrt{2i})$, and C_n and D_n are complex constants.

Hence the solution to a problem symmetrical in ξ and η is,

$$\phi^* = (E_1 - iE_2) \sum_{0,2,..}^{\infty} (A_n + iB_n)\, H_n^1(\beta r\sqrt{2i}) \cos n\theta$$

$$+ (E_3 - iE_4) \sum_{1,3,..}^{\infty} (A_n + iB_n)\, H_n^1(\beta r\sqrt{2i}) \cos n\theta \qquad (1.3.8)$$

where the unknown real coefficients A_n and B_n are to be determined. For antisymmetrical problems 'cos nθ' terms must be replaced by 'sin nθ' and the even summation started at 2.

Applicability of present theory is discussed in Appendix XII.

1.4 Formualtion of the boundary conditions

Reissner and Morduchow (22) and Mansfield (1) considered the problem of a reinforced hole in a plane sheet and concluded that for compact beads the bending rigidity of reinforcement could be neglected. Mansfield considers the problem of a typical reinforced circular hole in a flat plate subjected to uniform stress away from the hole and shows that the energy stored in bending is only 1% of the extensional energy. This is so even for a reinforced elliptical hole, though the ratio of the bending energy to the extensional energy is slightly higher. Clearly in this problem the bending stiffness of the reinforcement cannot be ignored since we have shell shear forces to react around the boundary. However (like the flat plate) we will ignore the ring bending forces in the local tangential plane of the shell boundary. For beads whose cross-section does not differ drastically from a square, it can be formally shown that this assumption leads to fractional errors in the shell boundary conditions of the order of $(d/a)^2$ and in the reinforcement stresses of the order of (d/a), where 'd' is a typical dimension of the bead cross-section.

The assumption that the reinforcement is a compact bead is a severe limitation. Shin-Ichi-Suzuki (51) has shown that for a flat plate under tension, stresses begin to vary through the depth of reinforcement when $h/t > 6$ where 'h' is the depth of the bead and 't' is the sheet thickness. This puts a limitation on the values of the bending efficiency μ.

For the pressure loading case, unless we analyse a window as a shell, some assumption has to be made for the mechanism by which the pressure over the cut-out portion is communicated to the hole edge. All the previous works referred to in this thesis make the assumption that the pressure over the cut-out region is distributed as a uniform shear - that is the hole is covered by a plate the edge of which is supported by a very flexible seal. This will be referred to as 'Case A' and is included in the results of this chapter.

However aircraft windows are not in general very flexibly supported and an alternative mechanism can be found if we assume that the curved 'window' is infinitely rigid in planes normal to the cylinder axis compared to planes parallel to the cylinder generators.* The relative rigidities in these directions can be shown to be of order β^4 (for the window) and consequently this becomes more valid for large β. This model also has the singular advantage that for the neutral hole it provides the necessary edge shear to completely balance the normal component of the reinforcement tension and so ensure that the hole is neutral in the curved cylinder. This idealisation will be referred to as 'Case B' and the results are presented in Appendix XIII.

If the hole is neutral then 'Case B' clearly gives no stress concentrations for all β but for the circular hole it will be difficult to assess the realism of either model (A) or (B) unless β is large or, un-

---

* The author wishes to thank Dr. E.H. Mansfield for suggesting this idealisation.

less, for small β, the two models give similar answers.

Equilibrium Equations:

Figure 3, shows the reinforcement forces and moments and the shell forces and moments per unit length. The equations of equilibrium are given below taking into account the eccentricity of the reinforcing bead. The expressions for a symmetric reinforcement can readily be obtained by putting $h = b = 0$.

$$N_{rr} = T/a \tag{1.4.1}$$

$$N_{r\theta} = -\frac{1}{a}\left(1 - \frac{b}{a}\right) T_{,\theta} \tag{1.4.2}$$

$$M_{rr} + N_{rr}h = \frac{M}{a} + \frac{1}{a} H_{,\theta} + Q.b + \frac{pa}{2} b \tag{1.4.3}$$

$$M_{r\theta} + N_{r\theta}.h = -\frac{1}{a} M_{,\theta} + \frac{H}{a} - P \tag{1.4.4}$$

$$Q = \frac{1}{a} P_{,\theta} + \frac{T}{R} \cos^2\theta - \frac{pa}{2} \tag{1.4.5}$$

The component of tension in (1.4.5) is obtained as follows. Consider an element of length 'ds' whose projection perpendicular to generators of the cylinder makes an angle '$d\psi$' at the axis of the cylinder.

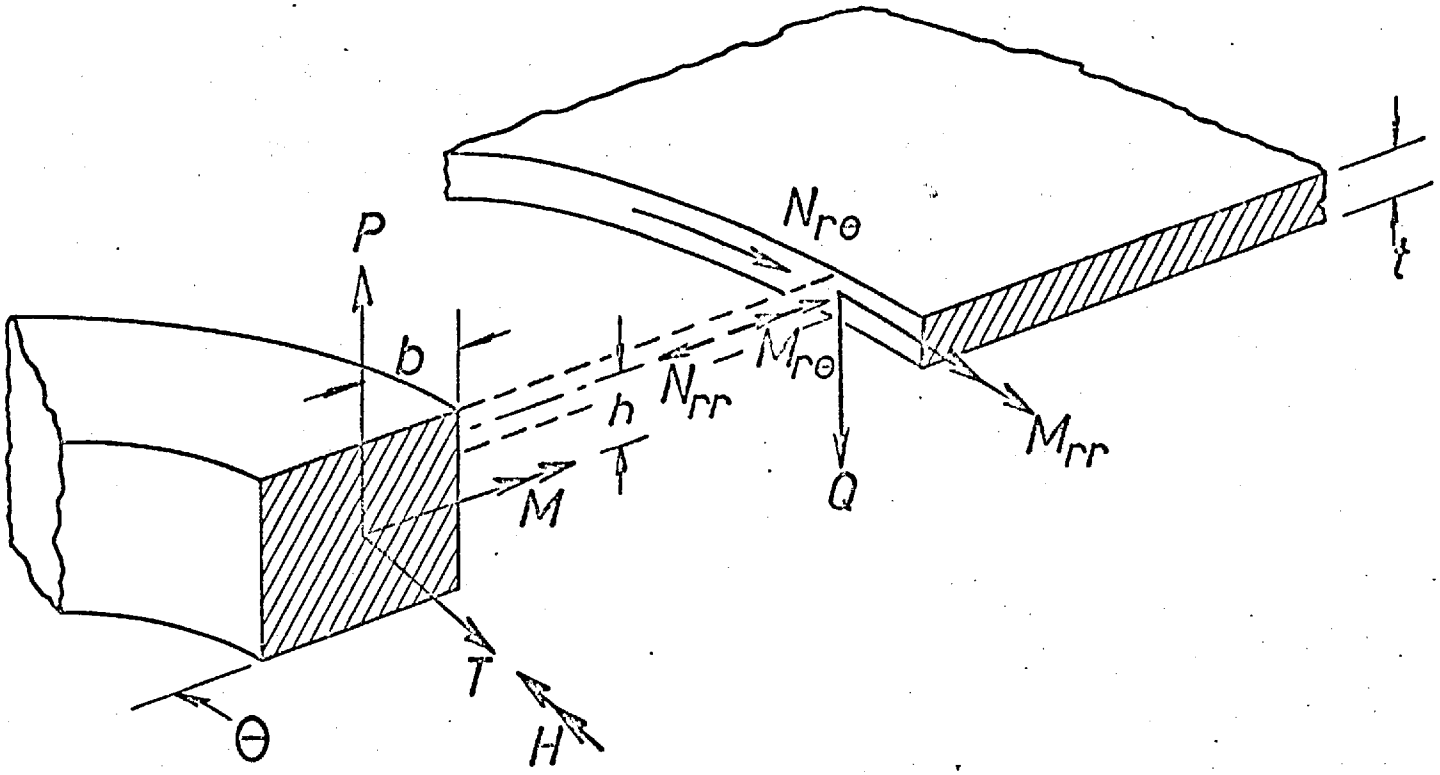

FIGURE 3

Component of tension in the bead normal to the shell middle surface per unit length is,

$$T \cos\theta . \frac{d\psi}{ds} \quad .$$

But we have $a \sin\theta = R\psi$ and $ds = ad\theta$, using which the required component becomes,

$$\frac{T \cos^2\theta}{R}$$

Compatibility Conditions:

It is assumed that the normal displacement and its derivatives at $r = 1$, are the same for the reinforcement and the middle plane of the sheet. This ensures compatibility of deflections, slopes and curvatures in both the reinforcement and the shell. This leads to,

$$M = -\frac{E_R I}{a^2} w'_{,\theta\theta} - \frac{E_R I}{a^2} w'_{,r} \qquad \text{(see Appendix III)}$$

$$\text{and} \quad H = \frac{E_R J}{2(1+\nu)a^2} w'_{,r\theta} \qquad (1.4.6)$$

The tangential strains of the reinforcement and the middle plane of the shell at $r = 1$ are equal. Here the effect of bending (29) has been taken into account.

$$\frac{T}{AE_R} + \frac{Mh}{E_R I} = \frac{1}{E_S t}(N_{\theta\theta} - \nu N_{rr}) \qquad (1.4.7)$$

For the stress resultants and couples in the shell, the usual flat plate relations hold. All the forces, moment and Kirchoff shear can now be eliminated in terms of F' and w'. After non-dimensionalising, the four boundary conditions are obtained as given in Appendix IV.

1.5 Method of Solution:

The boundary conditions are satisfied by a collocation procedure for the three loading cases of internal pressure, longitudinal tension and pure torsion of the cylinder which leads to the finding of unknowns in the series for ϕ^*. For a symmetric reinforcement the only coupling between F and w occurs in the normal shear equilibrium equation, where the shell curvature produces a component of the bead tension to the same degree of approximation as in the shallow shell equations. There is no other coupling if it is assumed that the shell is connected to the bead at its shear centre, which coincides with the centroid ($h = b = 0$).

For the symmetric loading cases the series (1.3.8) is truncated at an odd value of n leaving $(2n+2)$ coefficients A_n and B_n to be determined. The necessary equations are generated by satisfying the equations given in Appendix IV at $(n+1)/2$ equally spaced discrete points in the first quadrant of the circular hole. The procedure is identical for antisymmetrical loading with the series truncated at an even value of n and using $n/2$ collocation points. The series for ϕ^* is terminated at successively higher values of n until all the stresses calculated remain essentially the same.

For an eccentric reinforcement, there is additional coupling between the membrane and bending forces but the numerical procedure for obtaining the unknowns in ϕ^* is the same as for symmetrical reinforcement case.

The numerical calculations for this procedure were carried out on an ATLAS Computer. In all the numerical calculations $\nu = 1/3$ was assumed. Appendix V shows the flow diagram used for computation.

1.6 Results and discussion:

To start with the problem of a cylinder with an unreinforced circular hole was solved for values of β in the range $4 \leqslant \beta \leqslant 7$. This is done in order to verify the validity of projected connection suggested by Vandyke (4) who obtained an asymptotic solution for large β by using boundary layer techniques (between $\beta = 4$ and very large values of β). For the pressure loading (case) the tangential direct and tangential bending stresses are plotted in figures 4 and 5, and figures 6 and 7 correspond to tension loading. The effect of shell curvature is particularly marked in the pressure loading case, the membrane stress concentrations increasing from 2.5 to 50 as β increases from 0 to 7.

As the required Hankel functions $H_n^1(\beta r\sqrt{2i})$ in ϕ^* are generated using the recurrence relations, it is necessary to use accurate values of $H_o^1(\beta r\sqrt{2i})$ and $H_1^1(\beta r\sqrt{2i})$ (available to 10 places of accuracy in tables) as well as the value of (βr). Errors in the starting values get amplified particularly for large values of n.

At $\theta = \pi/2$, for tension loading case the agreement between the values obtained now and those by Vandyke's suggested formula,

$$\frac{\sigma_{\theta\theta}}{\sigma_\infty} \simeq 3.05\ \beta^{2/3} + 1 \qquad (1.6.1)$$

is very good. The bending stresses in this case also show a trend of having reached a maximum value. For the pressure loading case at $\theta = \pi/2$, the suggested formula

$$\frac{\sigma_{\theta\theta}}{\sigma_\infty} \simeq -1.65\ \beta^{4/3} + 1/2 \qquad (1.6.2)$$

gives slightly lower values. At $\theta = 0$, the membrane stresses seem to tend to the values predicted by boundary layer theory at a much slower rate. The bending stresses do not show any trend of having

reached a maximum value. For $\sqrt{2}\beta = 10$, values of n up to 39 were necessary for convergence. In the case of unreinforced and symmetrically reinforced holes the largest difference between the stresses calculated by the two longest series is less than 1% and the corresponding value for the eccentrically reinforced case is about 3%.

For symmetric reinforcement case it was found that the convergence depended almost entirely on the curvature parameter β, the larger the value of β, the slower the convergence. The effect of the various reinforcement parameters was marginal. It was also found unfortunately that only for $\beta < 0.3$ could the bending and torsional rigidities of the bead be ignored. This confirms our suggestion that for reinforced holes in practical shells it is not possible to use the concept of a compact flexible bead possessing only extensional rigidity.

Experimental results for a reinforced circular hole have been obtained at the College of Aeronautics by Rothwell (20). In the experiment a light alloy cylinder with a reinforced circular hole was subjected to torque loading and both the reinforcement and the shell were strain gauged on both inner and outer surfaces to separate the bending and the membrane stresses. The dimensions of the specimen are,

$$R = 8 \text{ ins}; \quad a = 3.15 \text{ ins}; \quad t = 0.064 \text{ ins};$$

so that we require our parameter to be,

$$\beta = 2.824; \quad \nu = \frac{1}{3}; \quad \frac{A}{at} = 0.1687;$$

$$\frac{I}{At^2} = 0.3763; \quad \frac{J}{I} = 2.6206; \quad \bar{w} = 0; \quad \bar{F} = \xi\eta.$$

Convergence was sufficient at n = 20.

Figure 8 shows the bending and membrane stresses in the reinforcement and figure 9 shows the tangential strain distribution at r = 1.05 in the shell. The agreement between theory and experiment is reasonable whereas, in the shell, the experimental results are somewhat

sparse and unreliable as the strains were small. It was also observed that the scatter increased as one moves away from the hole centre. Figures 10 and 11 give the stresses in the shell for the reinforced and unreinforced cases. The volume of this particular reinforcement is small (being only one-third of the volume of the shell removed by the hole), even so the maximum principal stress is $\frac{\sigma}{\sigma_\infty} = 19.5$ compared with $\frac{\sigma}{\sigma_\infty} = 38.8$ for the unreinforced hole. The value for the reinforced flat plate (30) is a mere 2.51.

Stress concentrations of the order of 20 are clearly intolerable and one must select a better reinforcing ring. However there are five independent non-dimensional structural parameters in the equations given in Appendix IV and the selection of an optimum configuration is a formidable task particularly if one attempts to show the penalty of departing from the optimum. This has been done for the most important pressure loading case (including the effect of eccentrically attaching the reinforcement).

The non-dimensional parameters naturally arising in the solution are the curvature parameter β, the elastic moduli $\frac{E_R}{E_S}$, and the extensional, bending and torsional rigidities $\frac{A}{at}$, $\frac{I}{at^3}$ and $\frac{J}{at^3}$. To simplify the results it is now assumed firstly the ring and the shell are made of the same material, that is $E_R/E_S = 1$. Secondly that the ring cross-section is either a closed tube or solid section not differing greatly from a circle, in which case J/I is of order 2. The problem is now defined by the three parameters β, $\lambda = A/at$ and $\mu = I/At^2$.

(It has actually been found that the stresses decrease if J/I is increased and vice versa as shown for some typical sections by figure 12. Very small J/I implies that the section must be a thin-walled open tube and it has been found that one can then not ignore the torsion bending rigidity (figure 13). Details are given in Appendix VI.

In the examples chosen, it is assumed that the web and flange have the same dimensions.)

The values of the shell curvature parameter are chosen as $\sqrt{2}\beta = 2$, 3 and 4, as this covers most typical aircraft configurations. The parameter λ is a measure of the extensional rigidity and also of the weight penalty since it is equal to a half the volume of the ring referred to the volume of the shell removed by the hole - the range chosen is $0.4 \leqslant \lambda \leqslant 2.0$. The paremeter μ is a measure of the bending efficiency of the ring cross-section since it is equal to the square of its radius of gyration referred to the shell thickness, the range chosen is $1 \leqslant \mu \leqslant 8$. The stress concentration in the shell is obtained by searching around the edge of the ring for the maximum principal tensile stress, σ_p, and referring it to the maximum shell stress at infinity.

The carpet diagrams, figures 14, 15 and 16 show how the stress varies with both λ and μ. For constant μ (or λ) the stress falls as λ (or μ) increases until a minimum is reached and then the stress rises. It clearly pays to increase μ if the bending stresses can be consequently reduced. Since this does not imply a weight penalty, but by examining the 'constant λ' curves, it is clear that there may be a critical value at which the stress is a pronounced minimum. The 'constant μ' curves tend to produce minimum stresses at excessively large values of λ, for example if $\sqrt{2}\beta = 4$ and $\mu = 5$, the value of $\lambda = 2$ produces a stress concentration of 3.1 whereas if λ is reduced to 0.8 (a 60% reduction in weight), the stress is increased to only 3.25. The stresses increase with β and for the smallest practical value of $\sqrt{2}\beta = 2$, the minimum is about 1.75 occurring at the largest chosen value of $\lambda = 1.8$. This compares with Wittrick's (32) minimum stress of 1.306 for the flat plate ($\beta = 0$) at a value of $\lambda = 1.0$.

All these comments are not applicable to loading case B which is discussed in detail in Appendix XIII.

In assessing the effects of eccentrically attaching the reinforcement and to restrict the embarrassing number of additional parameters, we assume that the ring has a doubly-symmetrical rectangular cross-section whose centre is offset distances 'b' and 'h' from the edge of the hole as shown in figure 3. Although the boundary conditions produce further coupling between the bending and membrane forces the numerical solution converges only slightly slower than that for a symmetrical reinforcement.

The results are given in figures 17, 18 and 19 and are clearly markedly different from the corresponding symmetrical cases. The stresses are invariably higher and the deleterious effect of using too high a bending efficiency (μ) is more pronounced.

Mansfield's 'Efficiency factor':

For reinforcements around holes which are neutral or nearly neutral Mansfield (17) has suggested that an eccentric reinforcement may be effectively replaced by a symmetrical reinforcement whose cross-sectional area is reduced by a factor which turns out to be 1/4 for a rectangular cross-section. His argument is restricted to an axisymmetrically loaded flat plate which offers no bending resistance to rotation of the reinforcement and so to test Mansfield's assertion we must choose reinforcements which produce little bending in the shell. On examining the bending stresses it is found that they are small only when $\mu > 7$, particularly for large values of β.

In table I, the stress concentration factors are given for eccentric reinforcement with a cross-sectional area $\lambda = 1.6$, and compared to the symmetrical case with $\lambda = \frac{1}{4}(1.6) = 0.4$. The agreement is remarkable, especially when one considers that these holes are far from neutral and the stress system is infinitely more complex than Mansfield's simple model.

TABLE I

	$\sqrt{2}\beta = 2$		$\sqrt{2}\beta = 3$		$\sqrt{2}\beta = 4$	
μ	Symmetric $\lambda = 0.4$	Eccentric $\lambda = 1.6$	Symmetric $\lambda = 0.4$	Eccentric $\lambda = 1.6$	Symmetric $\lambda = 0.4$	Eccentric $\lambda = 1.6$
4	2.48	2.50				
5	2.50	2.55	3.23	2.93		
6	2.54	2.58	3.05	2.97	4.0	3.66
7			2.91	2.99	3.78	3.46
8					3.60	3.52

In conclusion therefore it appears that figures 14, 15 and 16 may be used, with care, for any shape of reinforcement, symmetrical or eccentric.

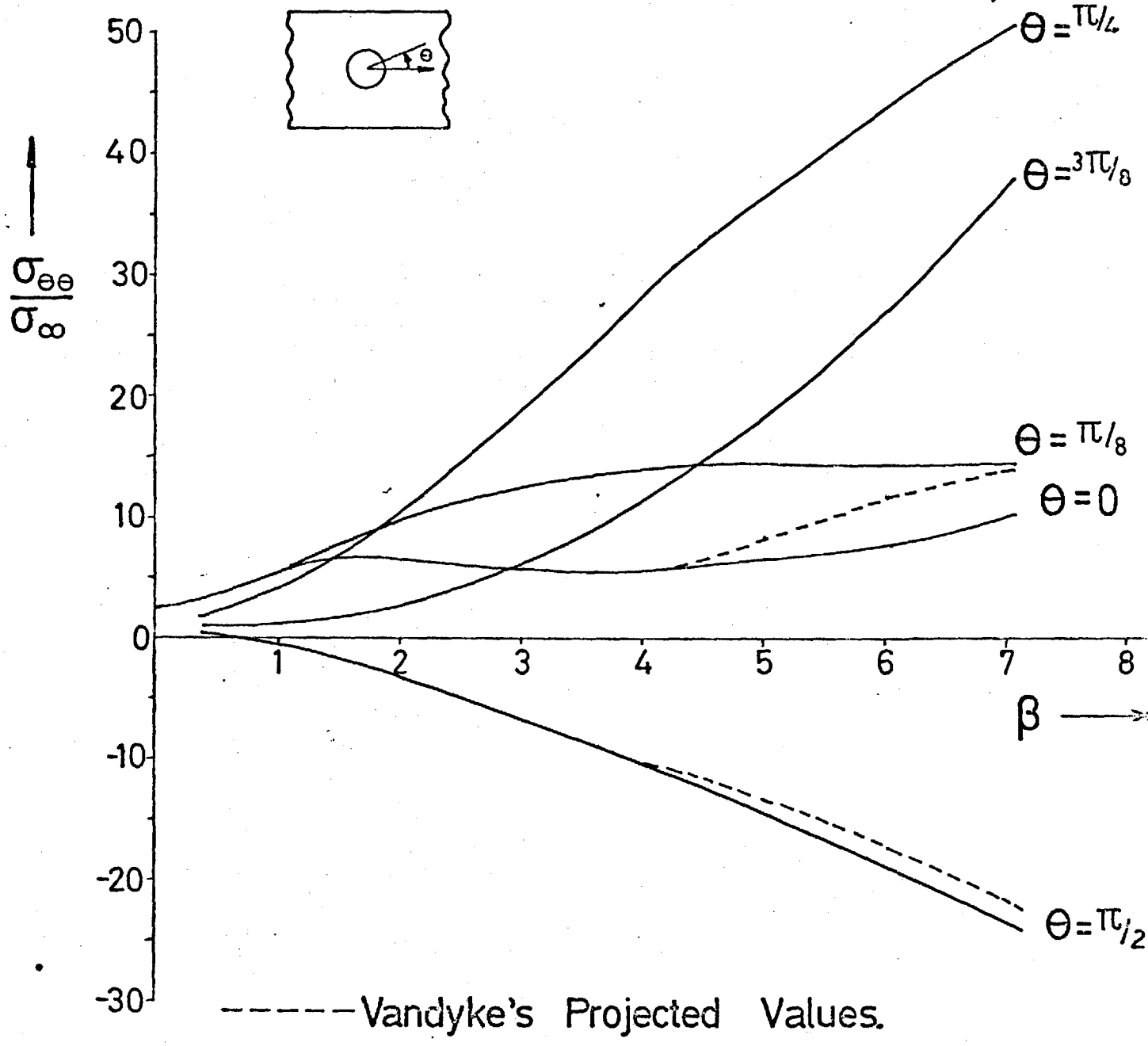

FIG. 4 DIRECT STRESSES AT HOLE EDGE (PRESSURE LOADING).

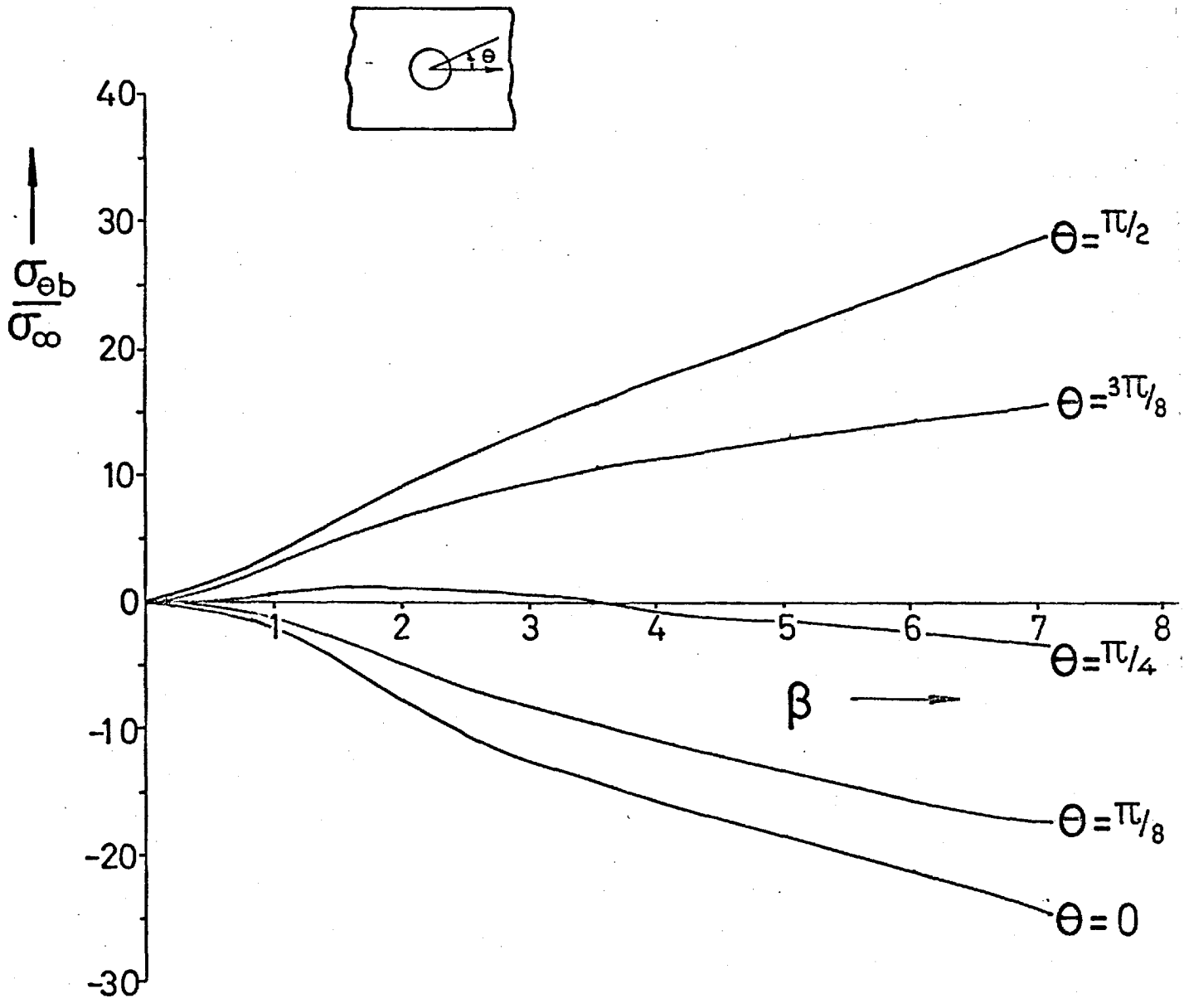

FIG. 5 BENDING STRESSES AT HOLE EDGE (PRESSURE LOADING) (UPPER SHELL SURFACE).

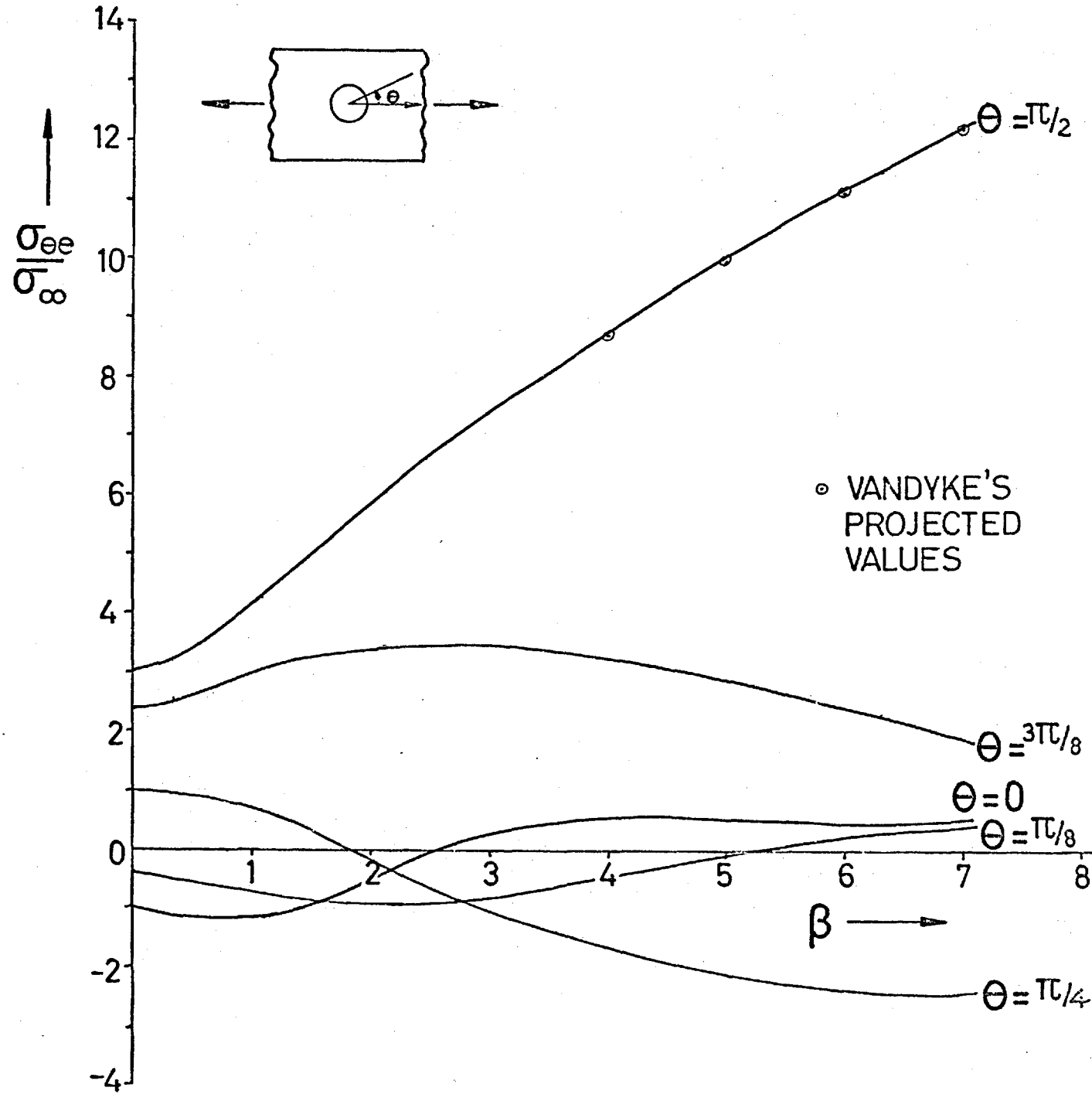

FIG. 6 MEMBRANE STRESSES AT HOLE EDGE (TENSION CASE).

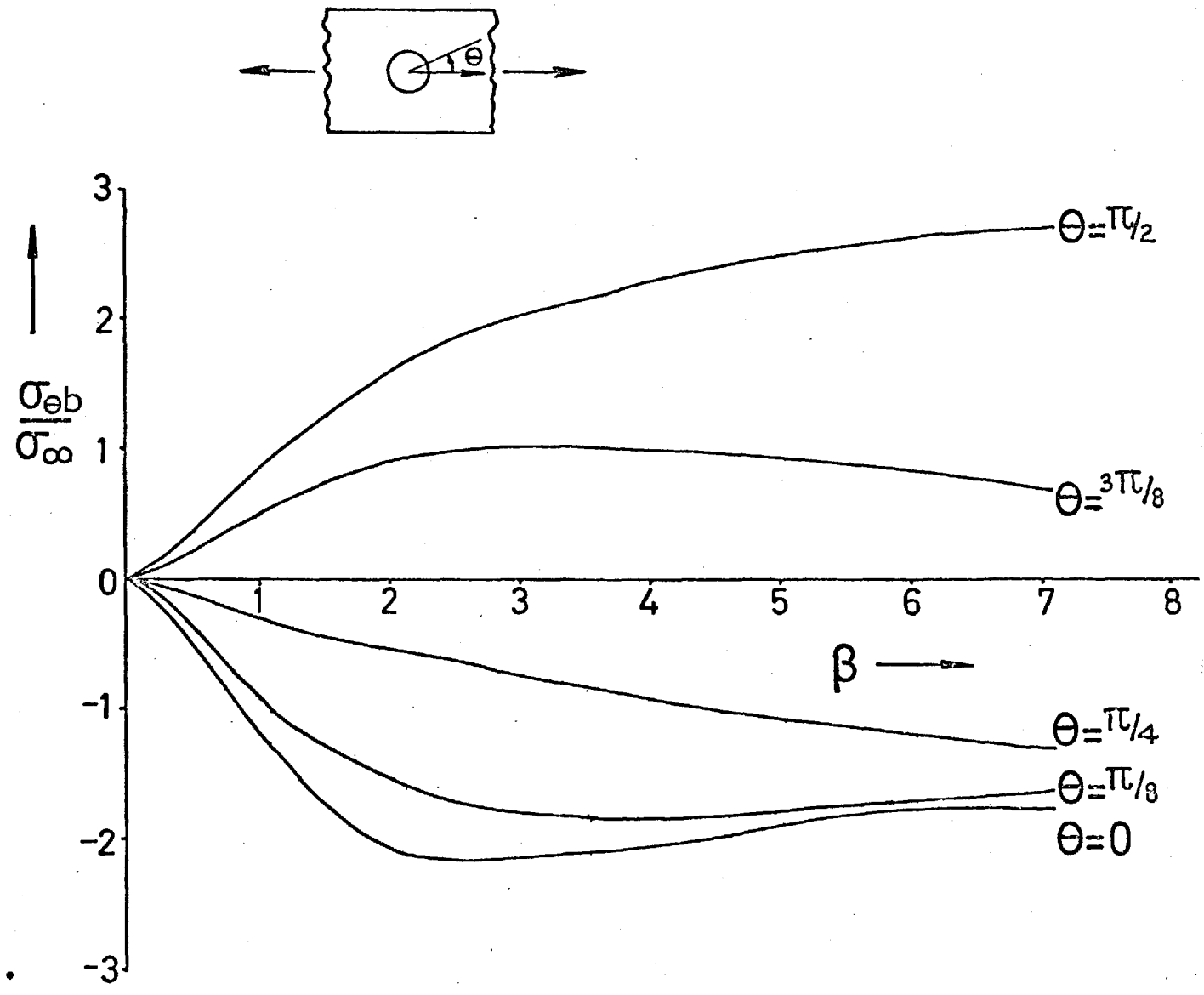

FIG. 7 BENDING STRESSES AT HOLE EDGE (TENSION CASE) (LOWER SHELL FACE).

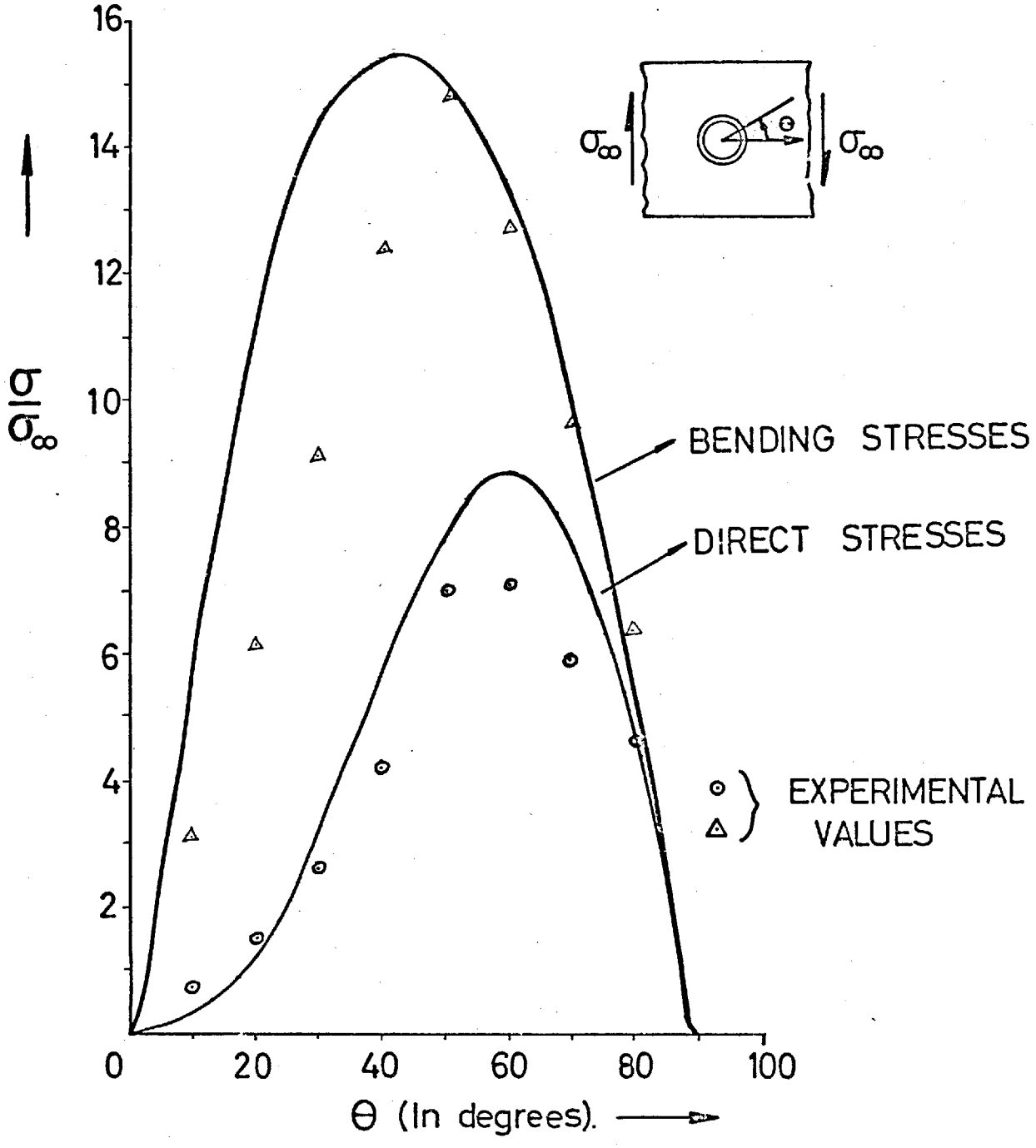

FIG. 8 STRESSES AROUND HOLE IN REINFORCEMENT

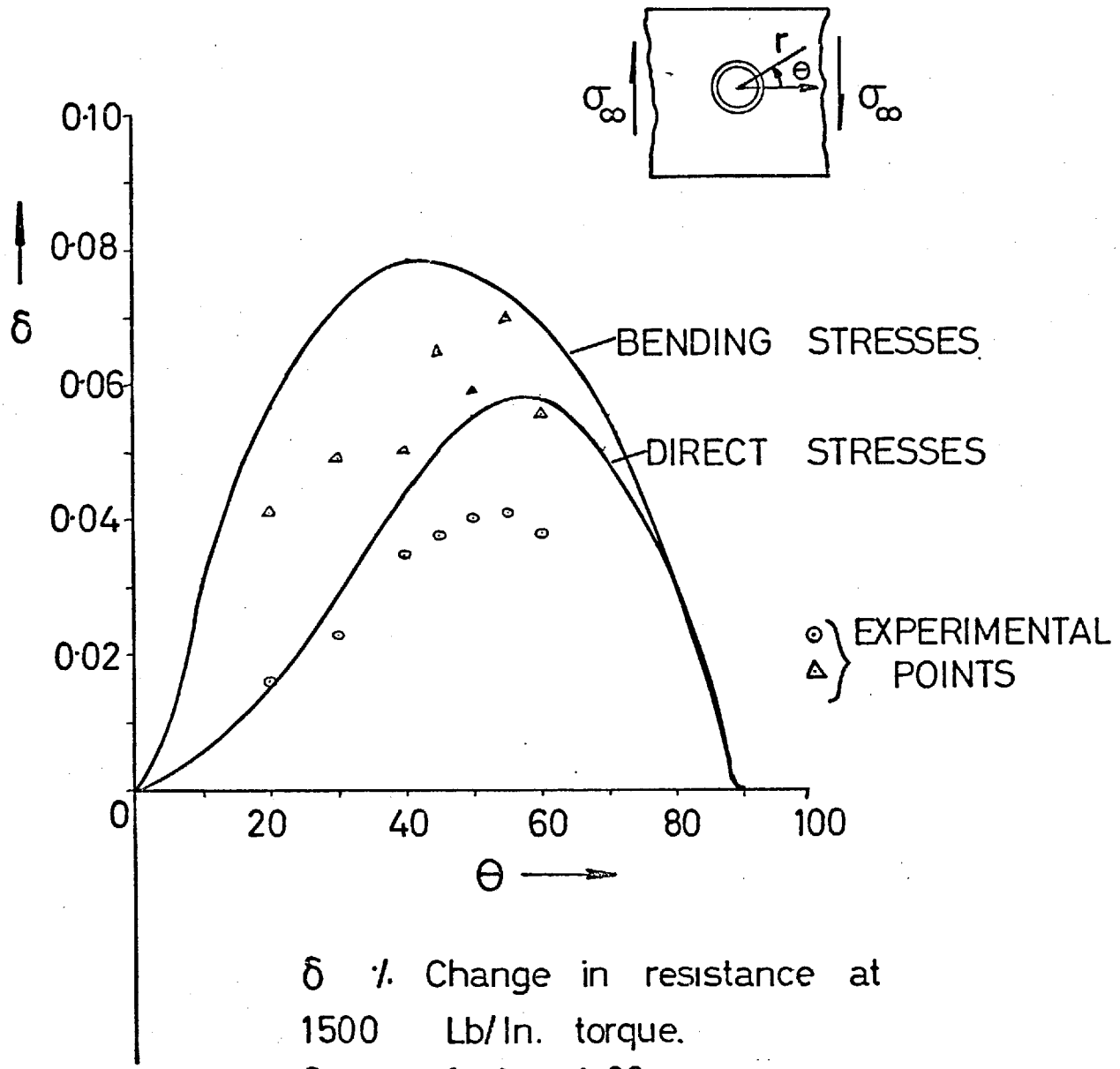

δ % Change in resistance at
1500 Lb/In. torque.
Guage factor 1·99
Shunt factor 10
$E = 10{\cdot}3 \times 10^6$ lb/sq. in.

FIG. 9 STRAIN DISTRIBUTION AT r = 1·05

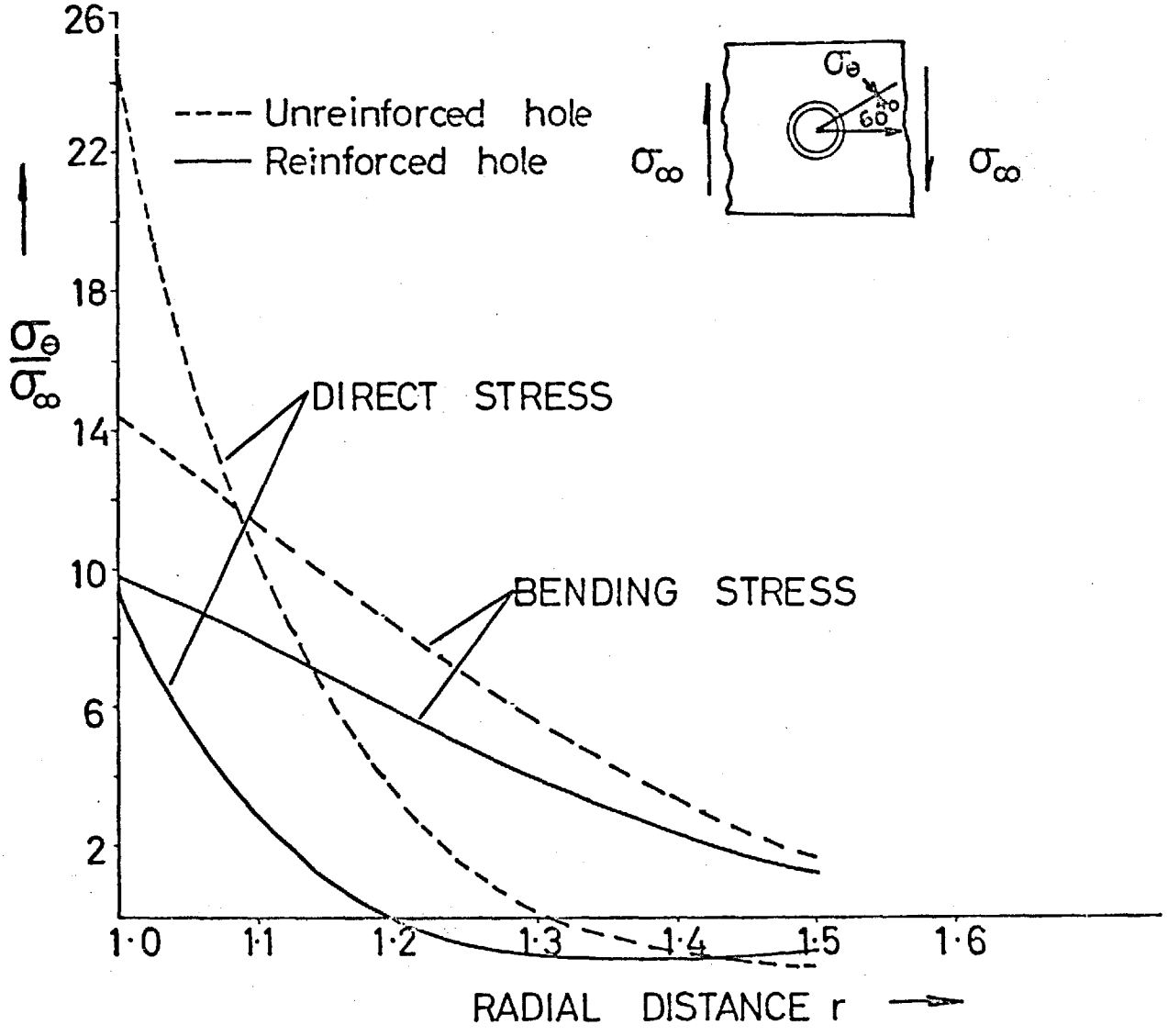

FIG. 10 SHELL STRESSES ALONG $\Theta = 60°$ (TORSION).

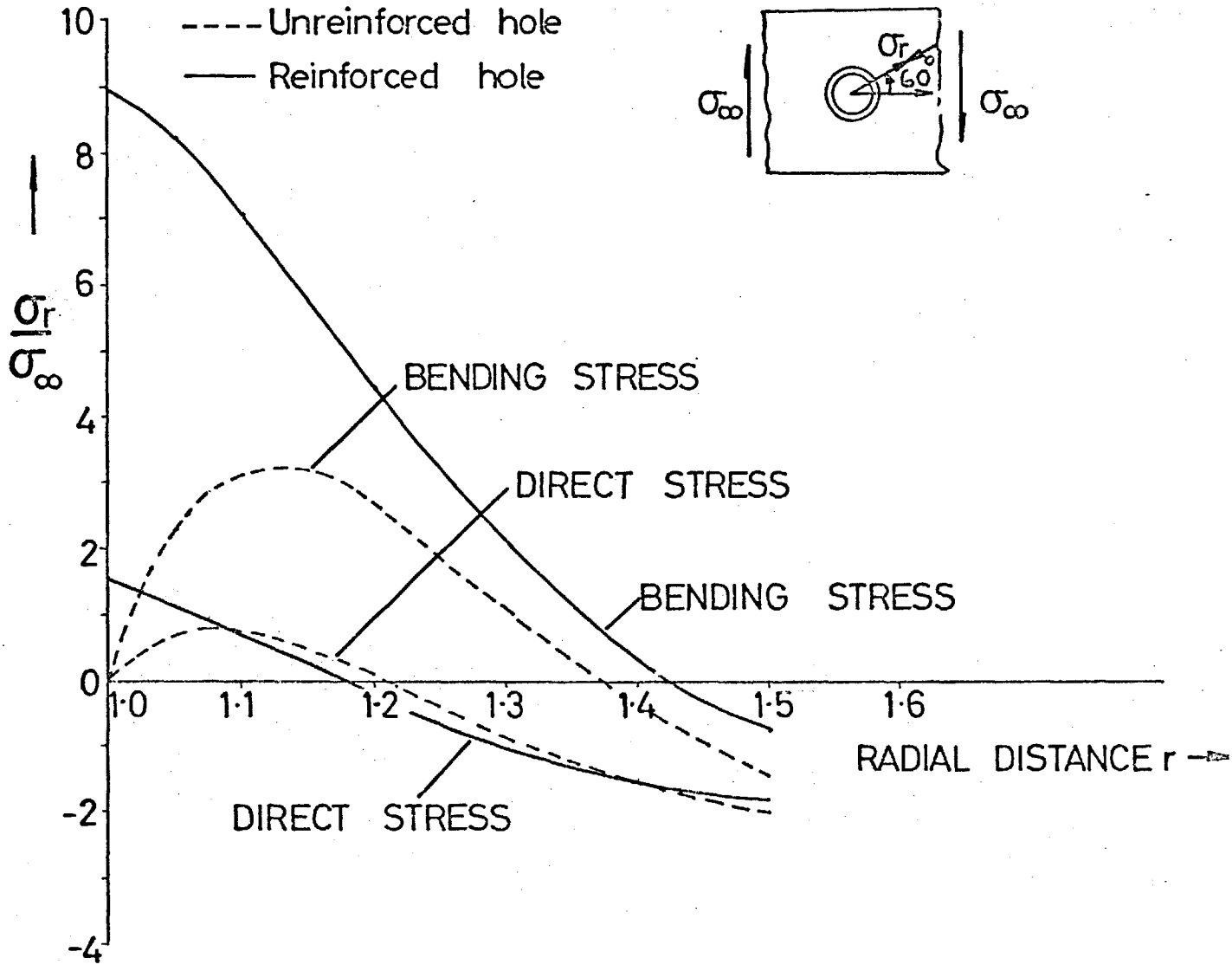

FIG. 11 SHELL STRESSES ALONG $\theta = 60^\circ$ (TORSION).

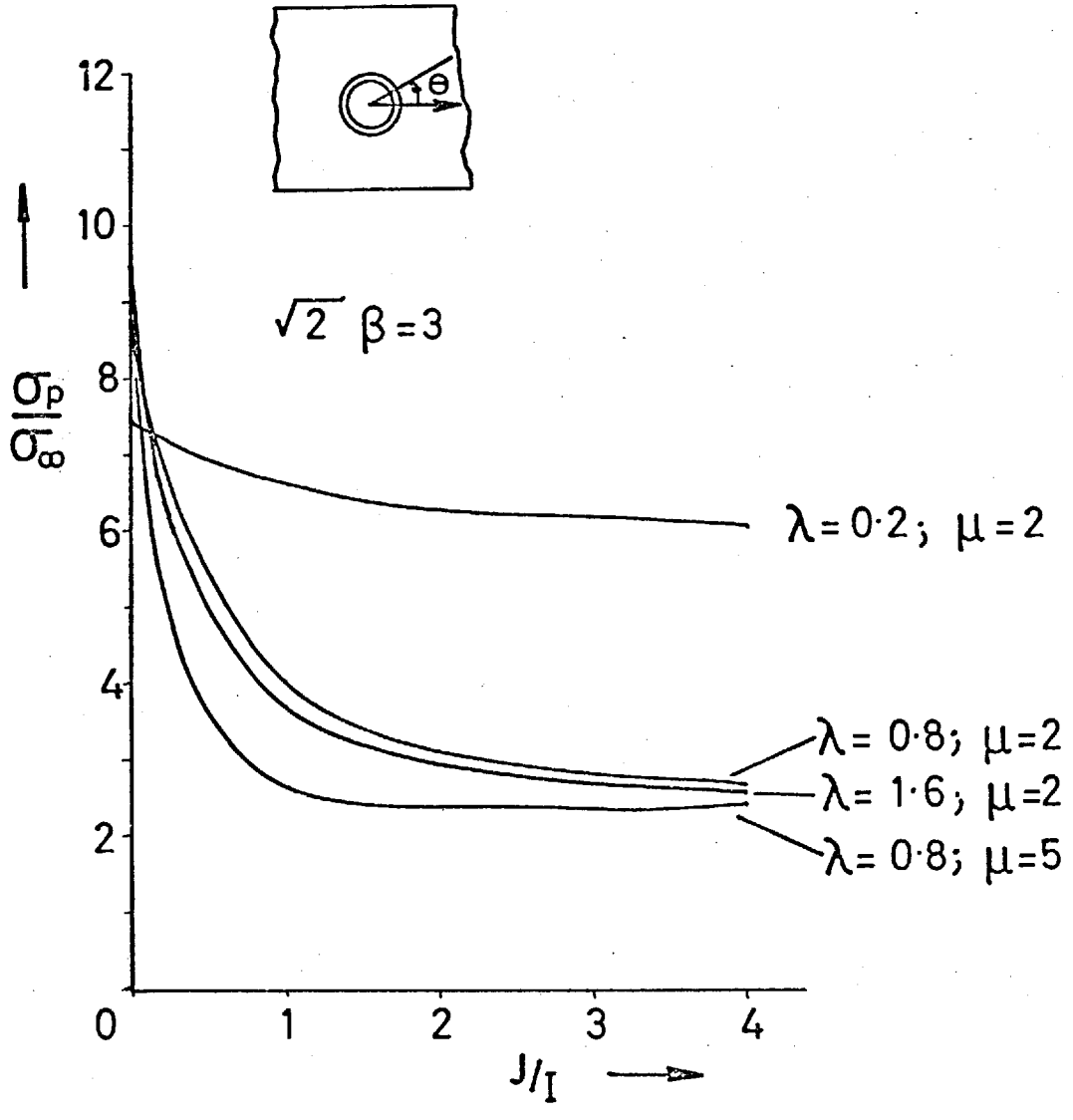

FIG 12 VARIATION OF MAXIMUM PRINCIPAL STRESSES WITH J / I.
(PRESSURE)

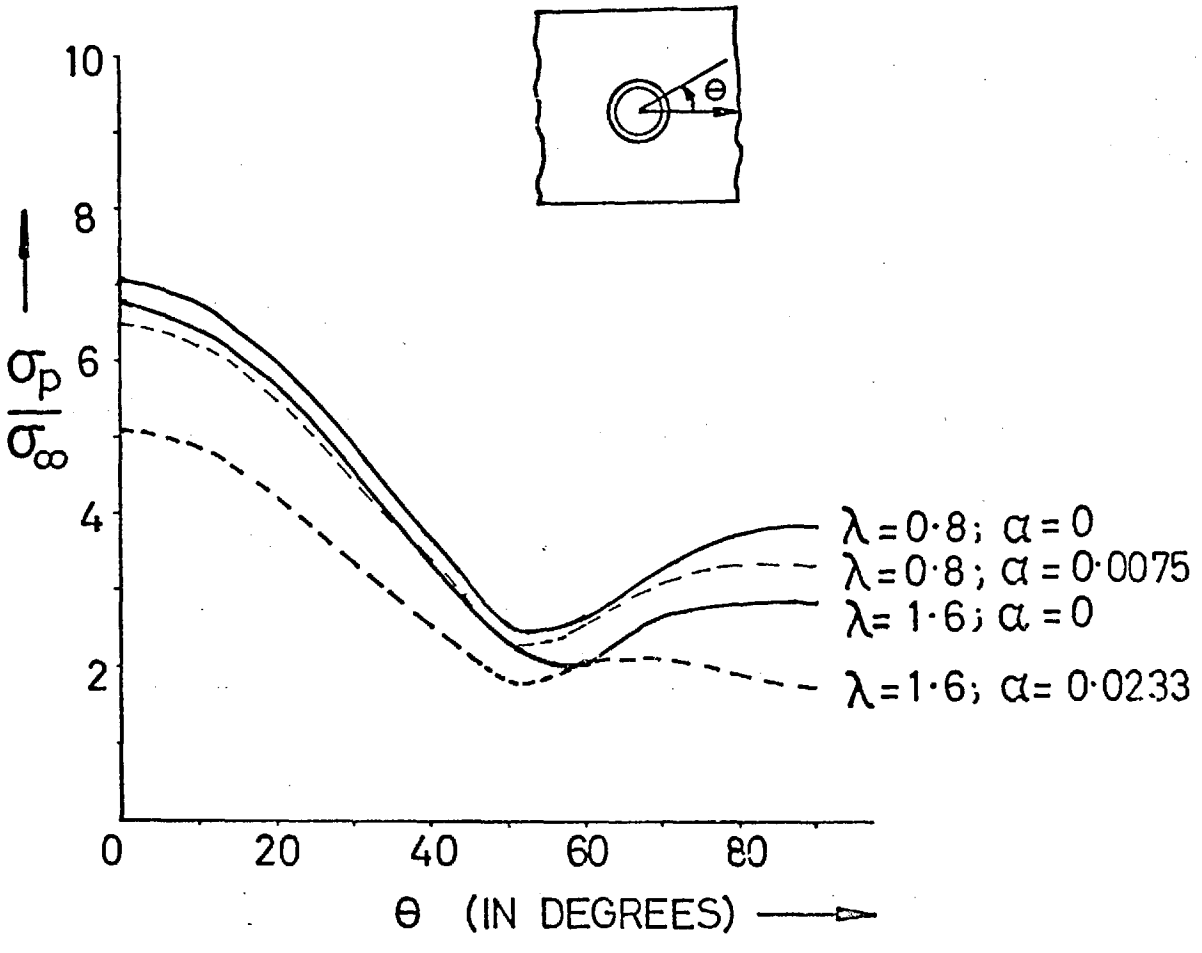

$\sqrt{2}\ \beta = 3; \quad \frac{E_R}{E_S} = 1; \quad \frac{J}{I} = 0{\cdot}16; \quad \mu = 2; \quad \alpha = \frac{\Gamma}{a^2 I}$

FIG.13 INFLUENCE OF TORSION BENDING ON SHELL STRESSES. (PRESSURE).

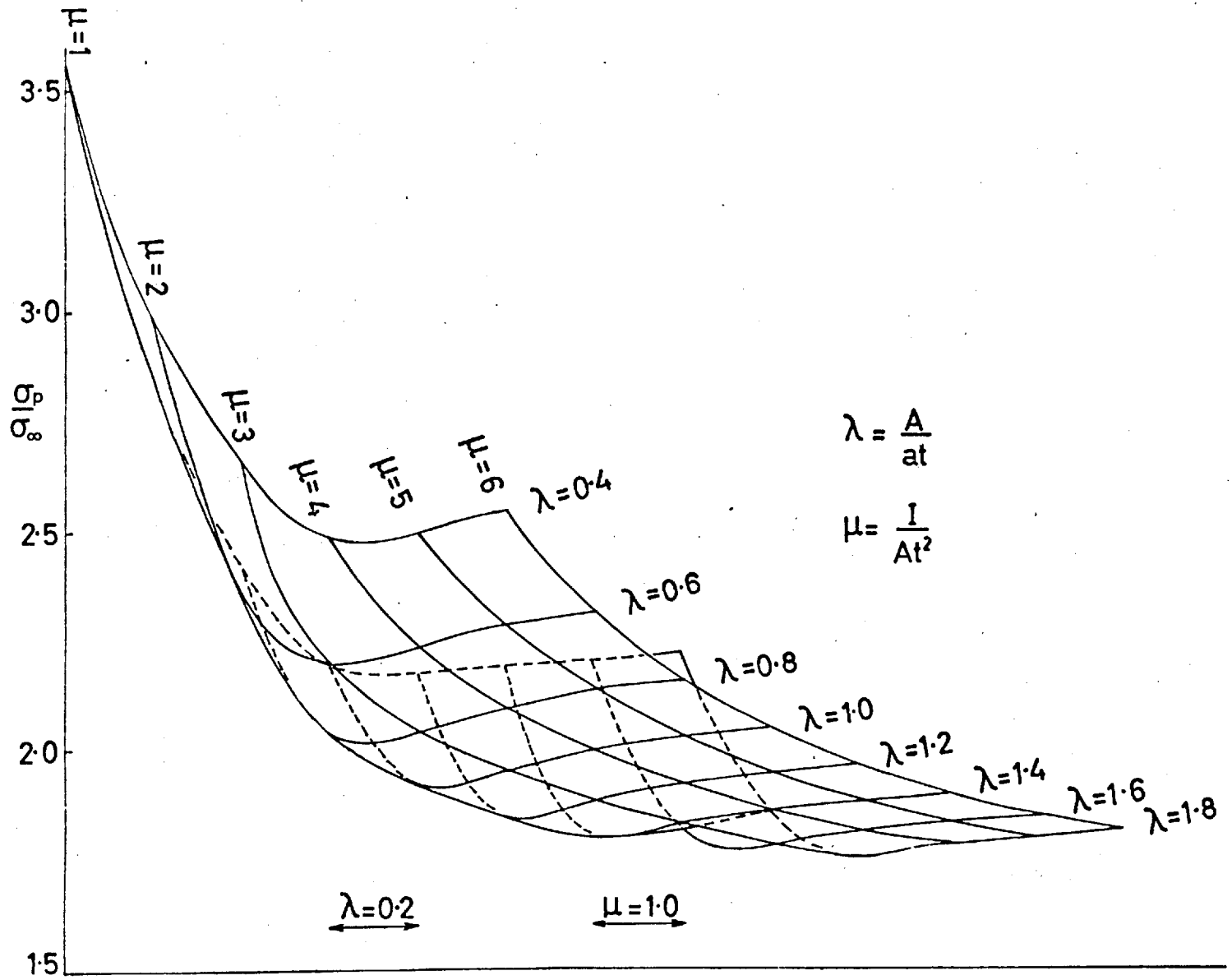

FIGURE 14 SYMMETRIC REINFORCEMENT, $\sqrt{2}\,\beta = 2$

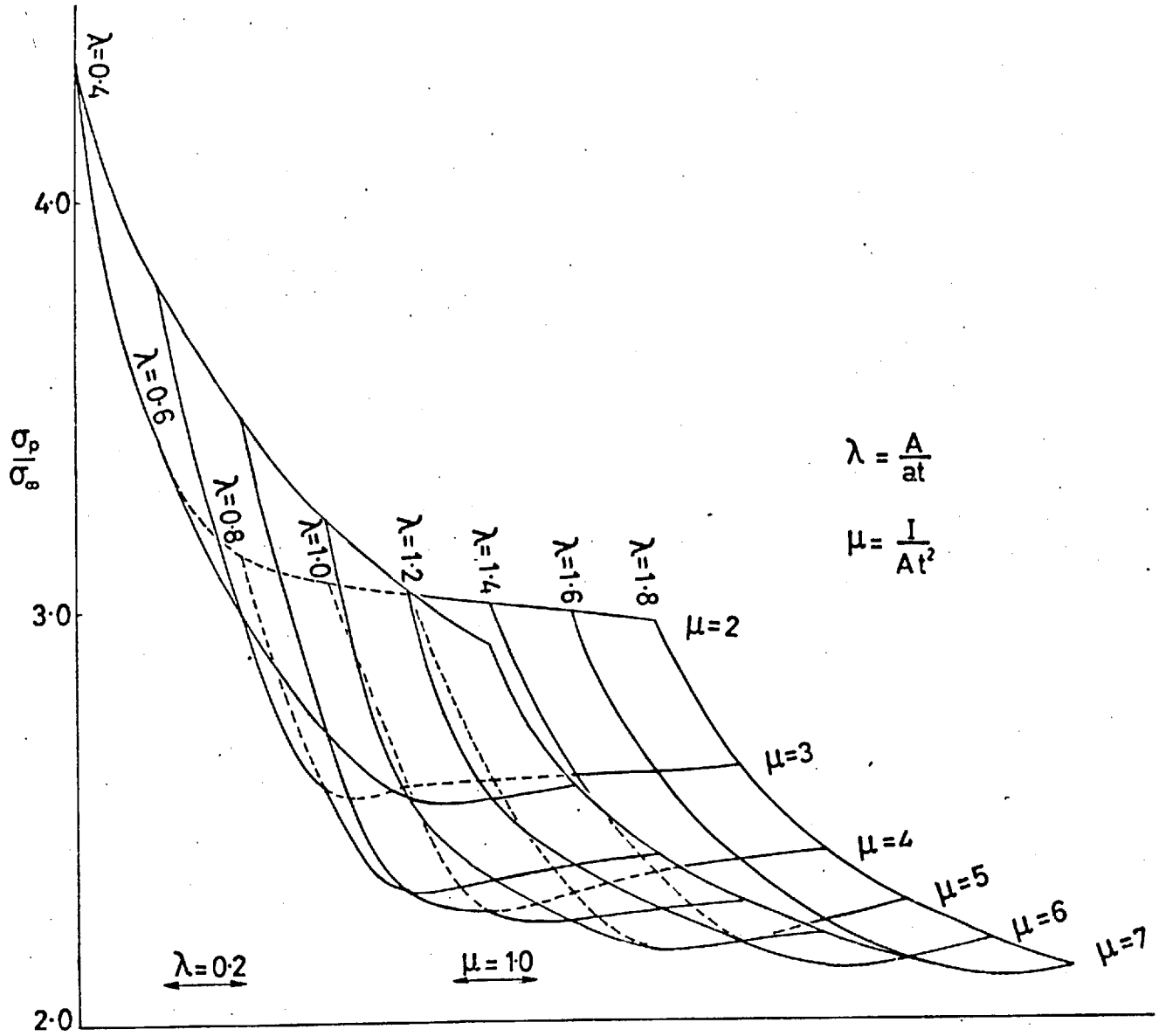

FIGURE 15 SYMMETRIC REINFORCEMENT, $\sqrt{2}\,\beta = 3$.

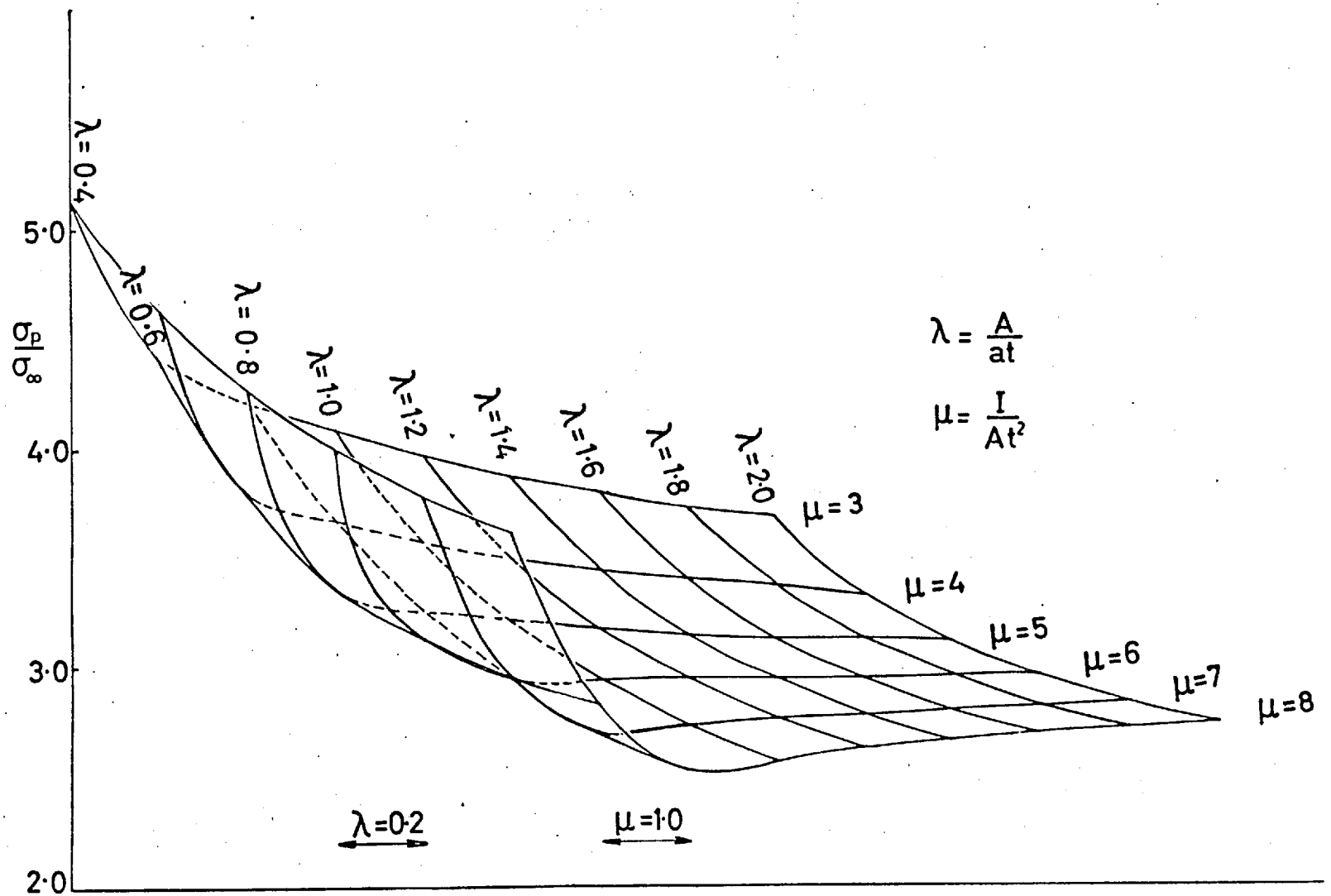

FIGURE 16 SYMMETRIC REINFORCEMENT, $\sqrt{2}\beta = 4$.

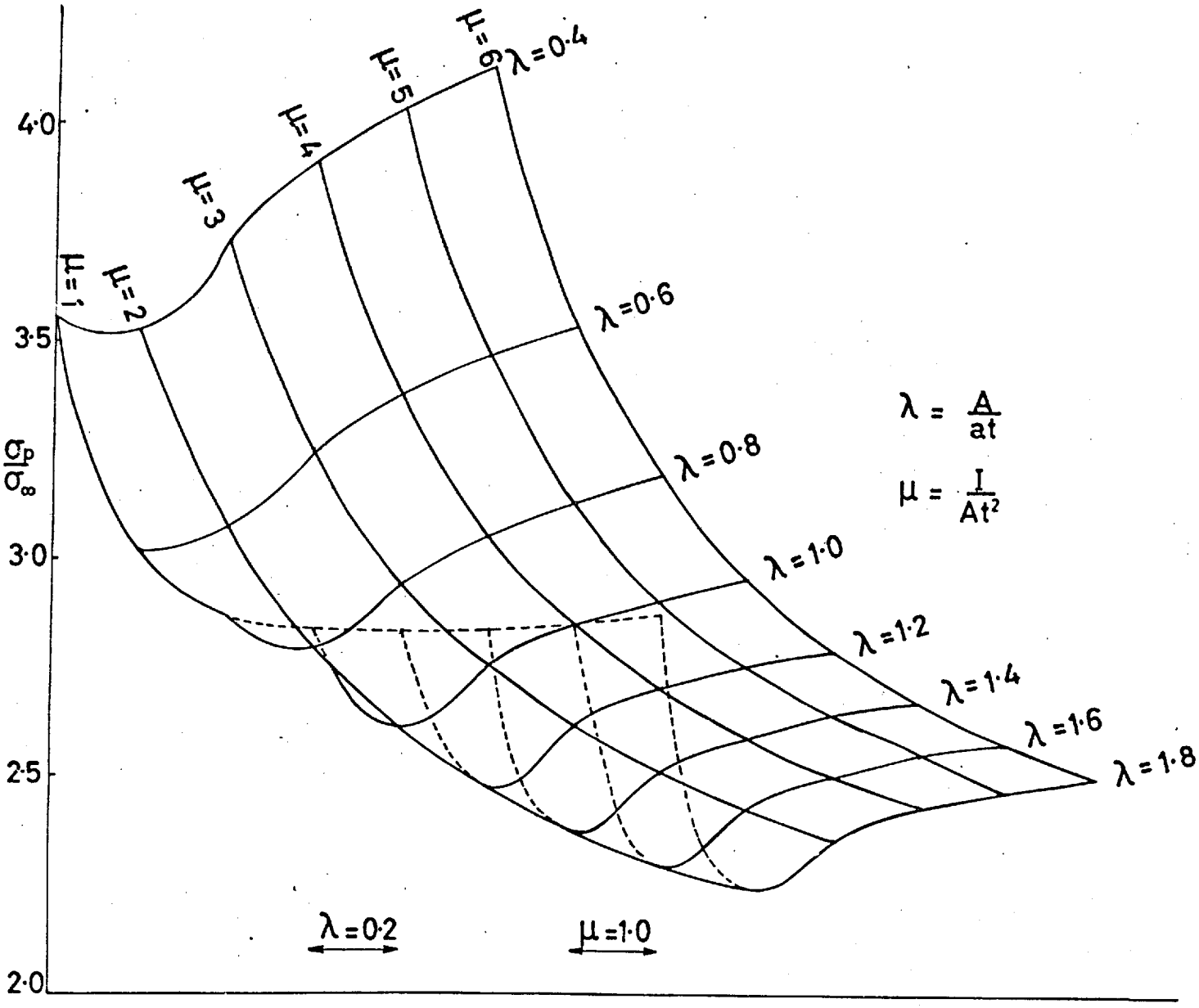

FIGURE 17 ECCENTRIC REINFORCEMENT, $\sqrt{2}\beta = 2$

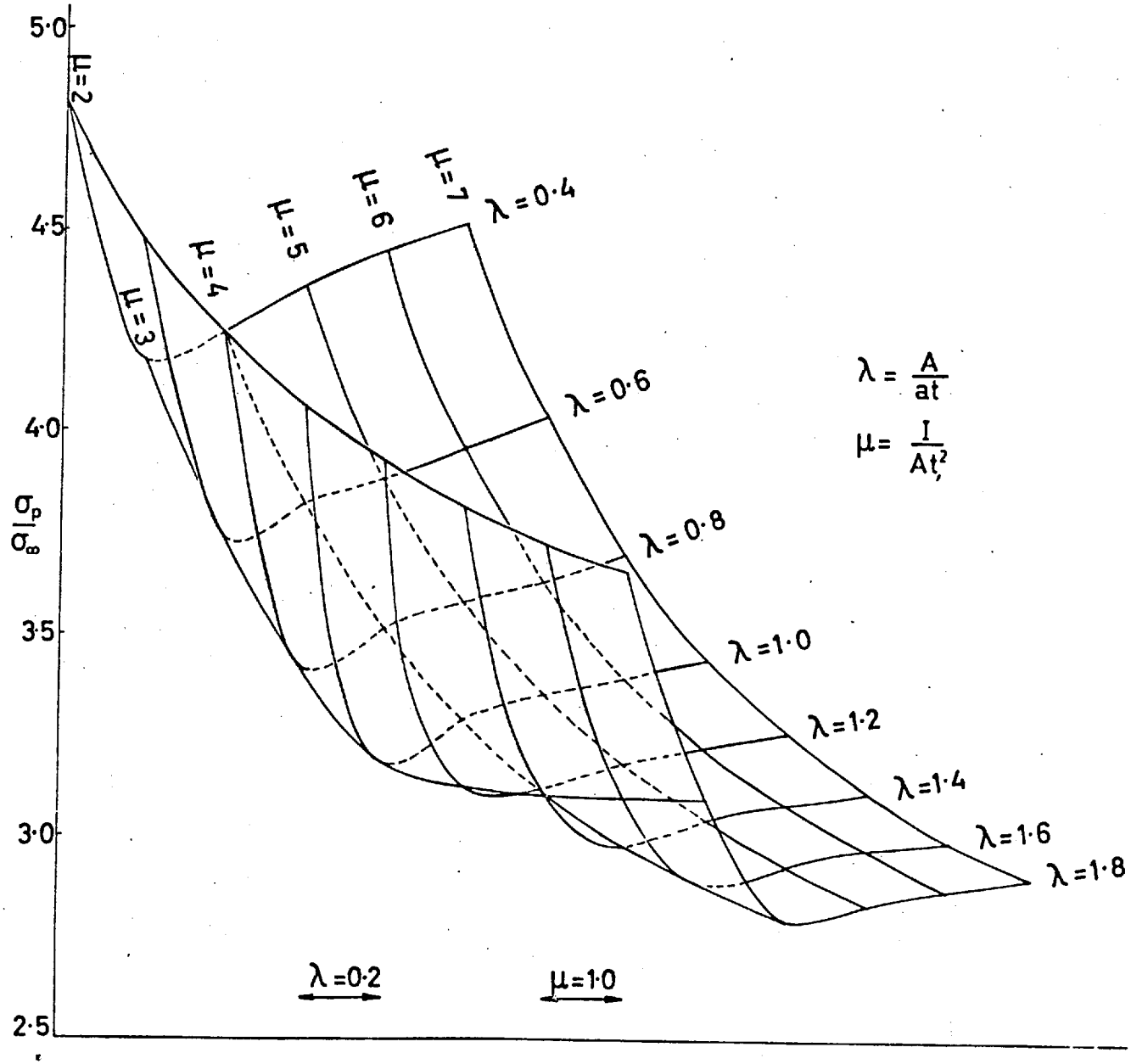

FIGURE 18 ECCENTRIC REINFORCEMENT, $\sqrt{2}\beta = 3$.

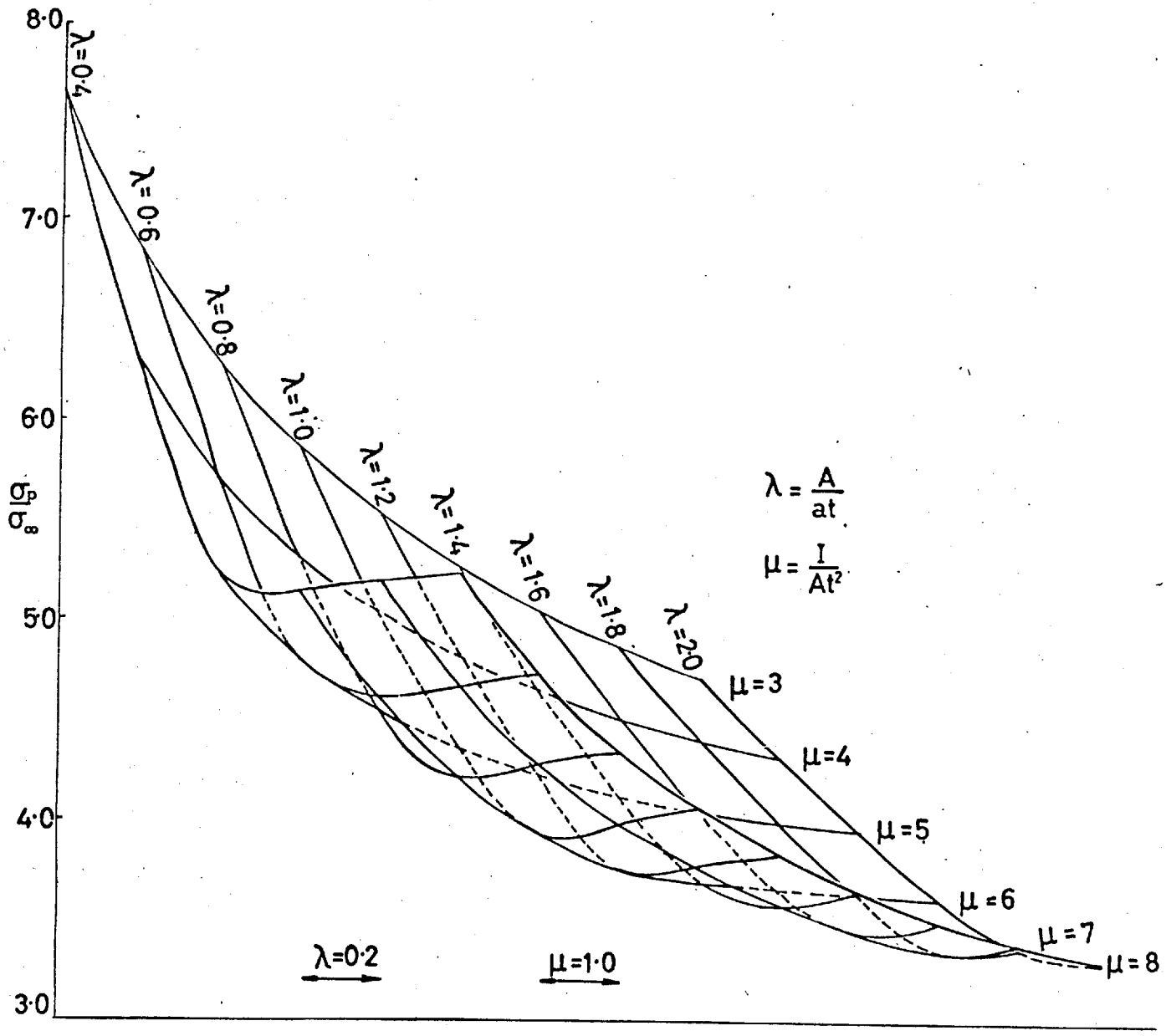

FIGURE 19 ECCENTRIC REINFORCEMENT, $\sqrt{2}\beta = 4$

CHAPTER II

CYLINDRICAL SHELL WITH REINFORCED ARBITRARY SHAPED HOLES

2.1 Introduction:

In aircraft structures one comes across cutouts of shapes other than a circle like ellipses (Viscount, Friendship and Jetstream have elliptical windows), square with rounded corners (most other aircraft), or a triangle with rounded corners (Caravelle windows). Hence it is logical to consider a method to estimate the stress distribution around such types of cutouts. In this chapter an approximate method is given to estimate the stresses around a reinforced hole of arbitrary shape in a circular cylindrical shell. Though the method is general, particular application is made to elliptical and square holes with rounded corners in cylindrical shells under pressure loading.

The problem of an unreinforced elliptical hole was first solved by Inglis (33) and using his solution the problem was extended to reinforced elliptical holes in plane sheet in (34) and (35). In plane stress problems concerning a plate with an arbitrary shaped hole, the usual technique employed is conformal mapping, developed by Muskhelishvili (36). Once the solution for the case of a circular hole in a plate under a given loading is known, the solution for an arbitrary shaped hole can be readily obtained as long as a conformal transformation function can be found. Such a function maps the region outside the boundary of the hole on to the region outside the unit circle and one can always find such a function provided the given contour of the hole does not have sharp corners. Extensive theoretical work has been done (27,32,37,38, and 39) on holes in plates and the results predicted by theory agreed well with experimental values (40) and (41). Wittrick (32) arrives at the conclusion that for an

elliptical hole with the axes in the ratio $\sqrt{2}$: 1, a stress concentration factor of 1.09 can be achieved by using a uniform reinforcement whose weight is only about half that required for Mansfield's neutral hole.

The problem of an unreinforced arbitrary shaped hole in a cylindrical shell has been solved approximately for small values of β, in recent years by Guz and Savin (42) and (43) and the method has been extended to reinforced curvilinear holes (44). Reference (45) gives the stresses around an elliptical hole in a cylindrical shell subjected to longitudinal tension for $\beta << 1$ and for any value of eccentricity.

The technique used by Guz and Savin, 'theory of perturbations', makes it possible to evaluate the stresses everywhere in the shell. This method of perturbing the boundary shape consists in choosing a mapping function of the form

$$Z = \zeta + \varepsilon f(\zeta) \qquad (2.1.1)$$

where $\varepsilon < 1$; $Z = re^{i\theta}$; $\zeta = \rho e^{i\gamma}$. If $f(\zeta) = \zeta^{-N}$, then N is a number which defines the shape of the hole. N = 1, 2 or 3 correspond to an ellipse, a triangle with rounded corners and a square with rounded corners respectively. Also such a transformation implies that the stress distribution in the shell can be obtained as the sum of the solution for a circular hole and a perturbation component caused by the departure of the given hole contour from a circle. The solution for the circular hole case is used to evaluate the additional perturbations.

In (42), for the circular hole problem, the complex stress function ϕ^* is expanded in powers of the curvature parameter 'β' ($\beta < 1$) and terms of order β^2 are only retained. This implies that their solution is only applicable to cases where the hole size is small

whereas for the aircraft windows the range of β is given by $2 \leqslant \sqrt{2}\beta \leqslant 4$. Also they conclude (not unnaturally) that flat plate solution can be used without much error for a cylindrical shell with a hole of arbitrary shape under tension loading. It can be seen from the first chapter that the bending stresses for this particular loading is about a fifth of the membrane stresses even for $\beta = 4$. On the other hand if one considers either pressure or torsion loading the bending stresses are of the order of membrane stresses. Hence one can expect that a change in hole shape will alter the direct as well as the bending stresses, especially if one considers pressure loading. This happens for large values of β thus proving that the predictions by flat plate theory are not applicable to problems of shells with holes.

In (42) it is shown that the solution one obtains to the order of 'ε' is quite a good approximation to the true solution. In this chapter solutions are obtained to the order of 'ε' as the equations become very cumbersome if one tries to include higher order terms. Exact solutions are either impossible or very cumbersome. As long as one can obtain a mapping function for the given hole contour in the form (2.1.1), this method can be employed to predict the stresses in the shell.

In this chapter also, the shell is assumed to be shallow and the bead is placed symmetrically on the hole edge. It is also assumed that the shear centre of the bead cross-section coincides with the C.G. and they lie on the shell middle surface. Cylindrical shell configuration with an arbitrary shaped hole is given in figure 20.

2.2 Formulation of the problem

The governing differential equation for the residual problem of a cylinder with a cutout is given in (1.2.6). In the case of a cir-

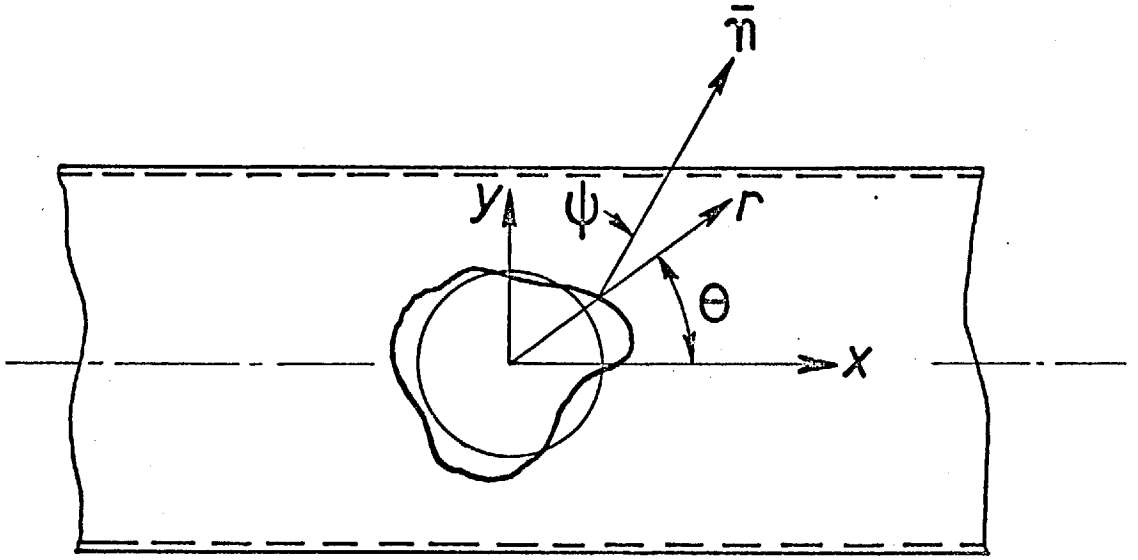

FIG. 20

cular hole the radius of the hole forms a characteristic dimension. In this case we define a characteristic dimension based on the dimensions of the cut-out.

Governing differential equation is given by

$$\nabla_Z^4 \phi^* + 8\, i\beta^2 \phi,^*_{\xi\xi} = 0 \tag{2.2.1}$$

Assume the following relations in the form of a power series in parameter ε,

$$\begin{aligned}
\phi^* &= \phi_o^* + \varepsilon\phi_1^* + \varepsilon^2\phi_2^* + \ldots \\
N_{nn} &= N_{nn}^{(o)} + \varepsilon N_{nn}^{(1)} + \varepsilon^2 N_{nn}^{(2)} + \ldots \\
N_{ss} &= N_{ss}^{(o)} + \varepsilon N_{ss}^{(1)} + \varepsilon^2 N_{ss}^{(2)} + \ldots \\
N_{ns} &= N_{ns}^{(o)} + \varepsilon N_{ns}^{(1)} + \varepsilon^2 N_{ns}^{(2)} + \ldots \\
M_{nn} &= M_{nn}^{(o)} + \varepsilon M_{nn}^{(1)} + \varepsilon^2 M_{nn}^{(2)} + \ldots \\
M_{ss} &= M_{ss}^{(o)} + \varepsilon M_{ss}^{(1)} + \varepsilon^2 M_{ss}^{(2)} + \ldots \\
M_{ns} &= M_{ns}^{(o)} + \varepsilon M_{ns}^{(1)} + \varepsilon^2 M_{ns}^{(2)} + \ldots \\
Q_n &= Q_n^{(o)} + \varepsilon Q_n^{(1)} + \varepsilon^2 Q_n^{(2)} + \ldots
\end{aligned} \tag{2.2.2}$$

(2.2.3)

(see figure 21) where $N_{nn}^{(o)}$, $N_{ss}^{(o)}$,..represent the solution for the case of a circular hole and $N_{nn}^{(1)}$, $N_{nn}^{(2)}$, $N_{ss}^{(1)}$, $N_{ss}^{(2)}$, ... are the additional contributions due to the fact that the given hole contour departs from the circle.

Using (2.2.2) in (2.2.1),

$$[\nabla_Z^4\, \phi_o^* + 8i\beta^2 \phi_o^*,_{\xi\xi}] + \varepsilon[\nabla_Z^4\, \phi_1^* + 8i\beta^2 \phi_1^*,_{\xi\xi}] = 0 \tag{2.2.4}$$

(From now on we retain only terms of order ε.)

First the problem is solved assuming $\varepsilon = 0$, which gives

$$\nabla_Z^4 \phi_o^* + 8i\beta^2 \phi_o^*{}_{,\xi\xi} = 0 \qquad (2.2.5)$$

This yields a solution for ϕ_o^* corresponding to the problem of a circular hole, as in Chapter I, using ϕ_o^*, the various stress components $N_{nn}^{(o)}$, $N_{ss}^{(o)}$, etc. can be obtained for the circular hole case. Then for any given ε,

$$\nabla_Z^4 \phi_1^* + 8i\beta^2 \phi_1^*{}_{,\xi\xi} = 0 \qquad (2.2.6)$$

the solution ϕ_1^* of which is used together with ϕ_o^* to evaluate the additional components $N_{nn}^{(1)}$, $N_{ss}^{(1)}$, etc.

Both ϕ_o^* and ϕ_1^* tend to zero away from the hole.

We must now proceed to use the solutions ϕ_o^* and ϕ_1^* to satisfy the boundary conditions on the arbitrary shaped hole. It will be found impossible to convert the boundary conditions by merely transforming the dependent variables and all differential operators in terms of r,θ to those in terms of ϱ,γ. In fact the solution of (2.2.1) could have been obtained in this manner and the formal equivalance of this approach with the solution of (2.2.5) and (2.2.6) is shown in Appendix VII.

2.3 Conformal Transformation:

The mapping function which transforms the region outside the boundary of the hole in the plane $Z = re^{i\theta}$ on to the region outside the unit circle in the plane $\zeta = \rho e^{i\gamma}$ is,

$$Z = w(\zeta) = \zeta + \varepsilon f(\zeta) \qquad (2.3.1)$$

From this transformation one gets,

$$r = \{\zeta\bar{\zeta} + \varepsilon[\bar{\zeta}f(\zeta) + \zeta\overline{f(\zeta)}] + \varepsilon^2 f(\zeta)\,\overline{f(\zeta)}\}^{1/2}$$

$$= \rho\left(1 + \frac{\varepsilon}{2\rho^2}\,[\bar{\zeta}\,f(\zeta) + \zeta\overline{f(\zeta)}]\right) \qquad (2.3.2)$$

$$\theta = \tan^{-1}\left[\frac{\sin\gamma + \frac{\varepsilon}{\rho}\left(\frac{f(\zeta) - \overline{f(\zeta)}}{2i}\right)}{\cos\gamma + \frac{\varepsilon}{\rho}\left(\frac{f(\zeta) + \overline{f(\zeta)}}{2}\right)}\right]$$

$$= \gamma + \varepsilon\left[\frac{(f(\zeta) - \overline{f(\zeta)})}{2i\rho}\cdot\cos\gamma - \frac{(f(\zeta) + \overline{f(\zeta)})}{2\rho}\sin\gamma\right] \qquad (2.3.3)$$

and $$e^{2i\psi} = e^{2i\gamma}\,\frac{[\overline{w(\zeta)}]^2[w'(\zeta)]^2}{|w(\zeta)|^2|w'(\zeta)|^2} \qquad (2.3.4)$$

(see figure 20)

$$\psi = \varepsilon\left[\frac{\zeta\overline{f(\zeta)} - \bar{\zeta}f(\zeta)}{2i\zeta\bar{\zeta}} + \frac{(f'(\zeta) - \overline{f'(\zeta)})}{2i}\right] \qquad (2.3.5)$$

In all the expressions given above only terms of order ε are retained.

Also,

$$Z = \varepsilon + i\eta = \rho(\cos\gamma + i\sin\gamma) + \varepsilon\left[\frac{f(\zeta) + \overline{f(\zeta)}}{2} + i\cdot\frac{f(\zeta) - \overline{f(\zeta)}}{2i}\right]$$

$$\xi = \rho\cos\gamma + \varepsilon\,\frac{(f(\zeta) + \overline{f(\zeta)})}{2} \qquad (2.3.6)$$

2.4 Solution to the differential equation:

Equation (2.2.5) is solved exactly as in (1.3) giving a complex stress function for the symmetric problem of a circular hole in a cylindrical shell, ϕ_o^* as,

$$\phi_o^* = (E_1 - iE_2)Z \sum_{0,2,..}^{\infty} (A_n + iB_n)\,H_n^1(\beta r\sqrt{2i})\cos n\theta\,..$$

$$+ (E_3 - iE_4)Z \sum_{1,3,..}^{\infty} (A_n + iB_n)\,H_n^1(\beta r\sqrt{2i})\cos n\theta \qquad (2.4.1)$$

Now let us consider the solution to equation (2.2.6)-

$$\nabla_Z^4 \phi_1^* + 8i\beta^2 \phi_1^*{}_{,\xi\xi} = 0 \qquad (2.4.2)$$

The coordinate transformation effected is given by,

$$Z = \zeta + \varepsilon f(\zeta) \qquad (2.4.3)$$

To the order of 'ε', one can write the solution of (2.4.2)

$$\phi_1^*(r,\theta) = \phi_1^*(\rho,\gamma) + \Delta\rho \frac{\partial \phi_1^*}{\partial \rho} + \Delta\gamma . \frac{\partial \phi_1^*}{\partial \gamma} \qquad (2.4.4)$$

where $r = \rho + \Delta\rho$; $\theta = \gamma + \Delta\gamma$ given in (2.3.2) and (2.3.3) respectively. It is readily seen that $\Delta\rho$, and $\Delta\gamma$ are of order 'ε'.

Also, $$\nabla_Z^2 = \{1 - \varepsilon[f'(\zeta) + \overline{f'(\zeta)}]\}\nabla_\zeta^2 \qquad (2.4.5)$$

giving $$\nabla_Z^4 = \{1 - \varepsilon[f'(\zeta) + \overline{f'(\zeta)}]\}\{\nabla_\zeta^4 - \varepsilon \nabla_\zeta^2(f'(\zeta) + \overline{f'(\zeta)})\nabla_\zeta^2\} \qquad (2.4.6)$$

Using (2.4.4) and (2.4.6) in (2.4.2),

$$\{1 - \varepsilon[f'(\zeta) + \overline{f'(\zeta)}]\}\{\nabla_\zeta^4 - \varepsilon[\nabla_\zeta^2(f'(\zeta) + \overline{f'(\zeta)})\nabla_\zeta^2]\}$$

$$\{\phi_1^*(\rho,\gamma) + \Delta\rho \frac{\partial \phi_1^*}{\partial \rho} + \Delta\gamma . \frac{\partial \phi_1^*}{\partial \gamma}\}$$

$$+ 8i\beta^2[\phi_1^*(\rho,\gamma)_{,\xi_1\xi_1} + \text{Terms } 0(\varepsilon)] = 0 \qquad (2.4.7)$$

where $\zeta = \xi_1 + i\eta_1$.

As only 'ε' order terms are needed in the solution for $\phi^* = \phi_o^* + \varepsilon\phi_1^*$, (2.4.7) reduces to

$$\nabla_\zeta^4 \phi_1^*(\rho,\gamma) + 8i\beta^2 \phi_1^*(\rho,\gamma)_{,\xi_1\xi_1} = 0 \qquad (2.4.8)$$

This equation is of identical form to (2.2.5) except that the variables are changed from (r,θ) to (ρ,γ) and hence the solution can be written as,

$$\phi_1^* = (E_1 - iE_2)_\zeta \sum_{0,2,..}^{\infty} (C_n + iD_n)\, H_n^1(\beta\rho\sqrt{2i})\cos n\gamma$$

$$+ (E_3 - iE_4)_\zeta \sum_{1,3,..}^{\infty} (C_n + iD_n)\, H_n^1(\beta\rho\sqrt{2i})\cos n\gamma \qquad (2.4.9)$$

where the unknown coefficients C_n and D_n are to be determined.

2.5 Formulation of the boundary conditions:

In the case of a hole of arbitrary shape also, it is assumed that the bending rigidity of the reinforcing bead in the local tangential plane of the shell is negligible. Only the important pressure loading case will be considered and the two alternative models (A) and (B) will again be taken for the shear distribution around the window edge. 'Case A' is examined here and the results for 'Case B' are given in Appendix XIV.

Equilibrium equations:

Figure 21, shows the reinforcement forces and moments and the shell forces and moments per unit length. By considering the equilibrium of an element 'ds', we obtain,

$$N_{nn} = T.\alpha_{,s} \qquad (2.5.1)$$

$$N_{ns} = -T_{,s} \qquad (2.5.2)$$

$$M_{nn} = M.\alpha_{,s} + H_{,s} \qquad (2.5.3)$$

$$M_{ns} = -M_{,s} + H.\alpha_{,s} - P \qquad (2.5.4)$$

$$Q_n = P_{,s} + T.\cos\alpha.n_{o,s} - q \qquad (2.5.5)$$

where q is the distributed shear.

α is given by the equation

$$e^{i\alpha} = e^{i\gamma}\frac{w'(\zeta)}{|w'(\zeta)|}$$

$$= e^{i\gamma}\left[1 + \varepsilon\frac{(f'(\zeta) - \overline{f'(\zeta)})}{2}\right] \qquad (2.5.6)$$

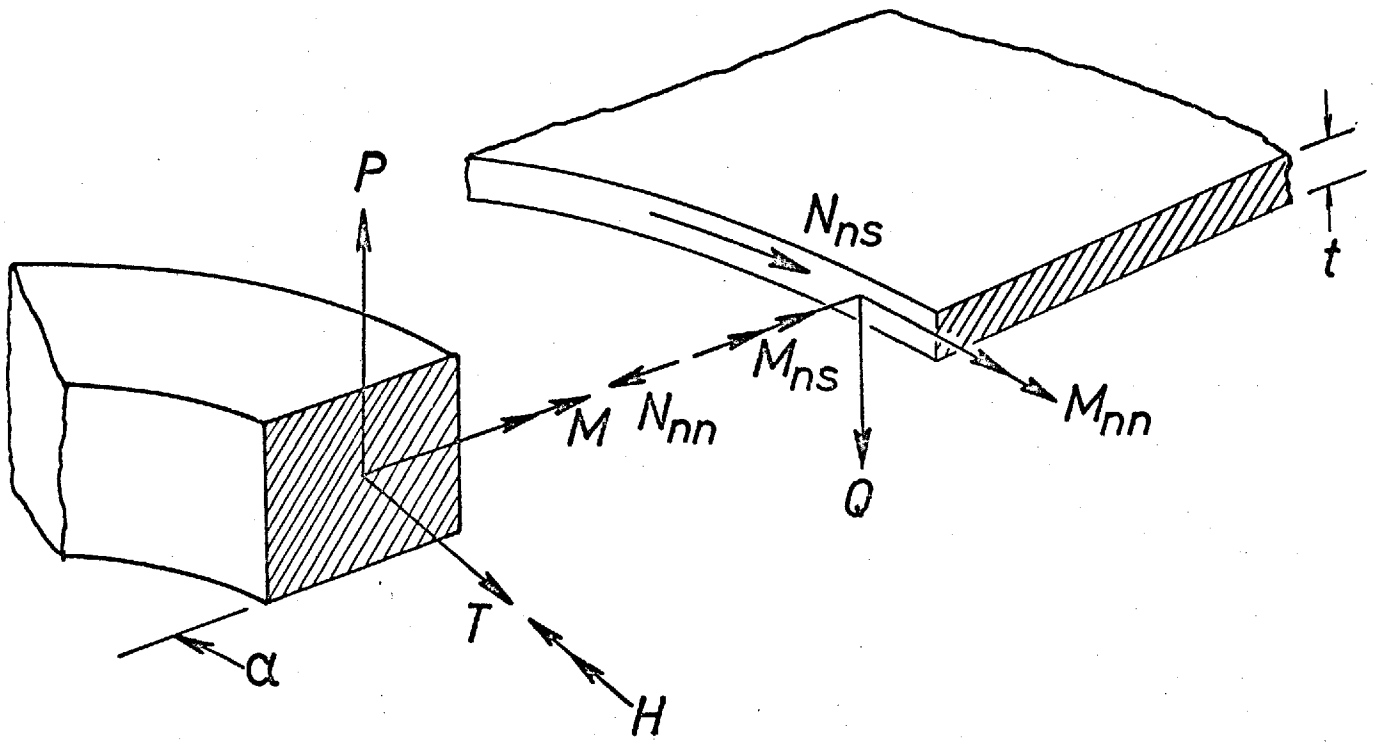

FIG. 21

α : is the angle between the normal to the hole contour at any point and the 'x' axis.

$d\eta_o$: is the angle made by the projection of an element 'ds' perpendicular to the generator at the axis of the cylinder.

Compatibility conditions:

The compatibility conditions are formed just similar to the case of the circular hole (1.4). In doing so, we ensure that the tangential strains of the bead and the middle surface of the shell are equal at the junction. Also normal deflections and slopes must be equal for the bead and the shell at the hole edge.

$$\frac{T}{AE_R} = \frac{1}{E_s t}(N_{ss} - \nu N_{nn}) \qquad (2.5.8)$$

$$M = -E_R I\, w'_{ss} - \frac{E_R I}{r_o}\, w'_n \qquad (2.5.9)$$

and

$$H = \frac{E_R J}{2(1+\nu)} \cdot w'_{ns} \qquad (2.5.10)$$

The stress resultants and couples in the shell around the curvilinear boundary must now be expressed in terms of the complex stress function ϕ^* as shown in Appendix VIII. All the forces, moments and Kirchoff shear can consequently be obtained in terms of F' and w'.

The complete formulation of the boundary conditions is algebraically very complex so a few of the salient steps will now be developed and the final four expressions presented in Appendices IX and X for two special cases.

CORRIGENDUM There is an error in equation (2.5.9) where the average curvature $1/r_o$ appears, instead of the actual curvature $\alpha_{,s}$. The correct expression should be read as,

$$M = -E_R I\, w'_{ss} - E_R I\, w'_n \cdot \alpha_s$$

This modification gives rise to some extra terms on the right hand sides of the moment and normal shear equilibrium equations of order 'ε' in Appendices IX and X. A few typical cases considered showed that the errors thus caused in the maximum principal stresses are not significant. For example $\sqrt{2}\beta = 4$, $\frac{E_R}{E_s} = 1$, $\lambda = 0.8$, $\mu = 6$ and $\frac{J}{I} = 2$, $\frac{(\sigma_p)_{max}}{\sigma_\infty}$ changes from 2.258 to 2.224 for an elliptical hole and 7.721 to 7.897 for a square hole with rounded corners (an error of about 2%).

2.6 Some details used in obtaining the boundary conditions:

The conformal transformation is given by

$$Z = \zeta + \varepsilon f(\zeta) \tag{2.6.1}$$

The elemental length 'ds' in the (ρ,γ) set of coordinates is given by,

$$(ds)^2 = r_o^2[(d\rho)^2 + \rho^2(d\gamma)^2](1 + \varepsilon[f'(\zeta) + \overline{f'(\zeta)}])$$

on the hole boundary $d\rho = 0$.

$$\therefore \quad \frac{d\gamma}{ds} = \frac{1}{r_o\rho}\left[1 - \frac{\varepsilon}{2}(f'(\zeta) + \overline{f'(\zeta)})\right] \tag{2.6.2}$$

To obtain, for example, the expression for the Kirchoff shear $\overline{Q}_n$ in terms of the complex stress function, we proceed as follows,

$$\overline{Q}_n = Q_r \cos\psi + Q_\theta \sin\psi + \frac{\partial M_{ns}}{\partial s} \quad .$$

Using results in Appendix VIII, and (2.6.2)

$$\overline{Q}_n = Q_r^{(o)} + \varepsilon[Q_r^{(1)} + L_1 Q_r^{(o)} + \frac{L_2}{2} Q_\theta^{(o)}]$$

$$+ \frac{1}{r_o}\left[1 - \frac{\varepsilon}{2}(f'(\zeta) + \overline{f'(\zeta)})\right] \frac{1}{\rho} \cdot \frac{\partial}{\partial\gamma} (M_{ns})$$

i.e.
$$\overline{Q}_n = Q_r^{(o)} + \varepsilon[Q_r^{(1)} + L_1 Q_r^{(o)} + \frac{L_2}{2} Q_\theta^{(o)}]$$

$$+ \frac{1}{r_o}\left[1 - \frac{\varepsilon}{2}(f'(\zeta) + \overline{f'(\zeta)})\right] \frac{1}{\rho} \cdot \frac{\partial}{\partial\gamma} [M_{r\theta}^{(o)} + \epsilon M_{r\theta}^{(1)} + \varepsilon L_1 M_{r\theta}^{(o)}$$

$$+ \frac{\varepsilon L_2}{2} (M_{\theta\theta}^{(o)} - M_{rr}^{(o)})] \tag{2.6.3}$$

where $Q_r^{(o)}$, $Q_\theta^{(o)}$ ...etc. are given in terms of the stress function in Appendix VIII.

To obtain the component of tension to normal shear

The required component is

$$C = T \cos\alpha \cdot \frac{\partial\eta_o}{\partial s} \tag{2.6.4}$$

α is given by, $e^{i\alpha} = e^{i\gamma}\left[1 + \varepsilon \frac{(f'(\zeta) - \overline{f'(\zeta)})}{2}\right]$ (2.6.5)

Also, $r'\sin\theta = R\eta_o$ (2.6.6)

(η_o is defined in the notation).

Using results in (2.3),

$$\rho\left[1 + \frac{\varepsilon}{2\rho^2}(\zeta\,\overline{f(\zeta)} + \bar{\zeta} f(\zeta))\right] \times \left\{\sin\gamma + \varepsilon\cos\gamma\left[\frac{f(\zeta) - \overline{f(\zeta)}}{2i\rho}\cos\gamma - \frac{f(\zeta) + \overline{f(\zeta)}}{2\rho}\sin\gamma\right]\right\} = \frac{R}{r_o}\eta_o \quad (2.6.7)$$

from which $\frac{\partial \eta_o}{\partial \gamma}$ can be found.

(2.6.4) gives,

$$C = \frac{T\cos\alpha}{r_o\rho}\left(1 - \frac{\varepsilon}{2}[f'(\zeta) + \overline{f'(\zeta)}]\right)\frac{\partial \eta_o}{\partial \gamma} \quad (2.6.8)$$

<u>To obtain a typical equation given in (2.7) or (2.8):</u>

Consider equation (2.5.1)

$$N_{nn} = T\,\alpha_{,s} \quad (2.6.9)$$

$$\alpha_{,s} = \left[1 - \frac{\varepsilon}{2}(f'(\zeta) + \overline{f'(\zeta)})\right]\frac{\alpha_{,\gamma}}{r_o}$$

$$= \frac{1}{r_o}\left[1 - \frac{\varepsilon}{2}(f'(\zeta) + \overline{f'(\zeta)})\right]\left[1 + \frac{\varepsilon}{2}(f''(\zeta)\,e^{i\gamma} + \overline{f''(\zeta)}\,e^{-i\gamma})\right]$$

(using (2.6.5)

$$= \frac{1}{r_o}\left[1 - \frac{\varepsilon}{2}(f'(\zeta) + \overline{f'(\zeta)}) + \frac{\varepsilon}{2}(f''(\zeta)e^{i\gamma} + \overline{f''(\zeta)}e^{-i\gamma})\right] \quad (2.6.10)$$

Also $N_{nn} = N_{nn}^{(o)} + \varepsilon N_{nn}^{(1)}$

$N_{ss} = N_{ss}^{(o)} + \varepsilon N_{ss}^{(1)}$

From (2.6.9)

$$N_{nn}^{(o)} + \varepsilon N_{nn}^{(1)} = \frac{AE_R}{E_S.tr_o}(N_{ss}^{(o)} - \nu N_{nn}^{(o)})$$

$$+ \varepsilon.\frac{AE_R}{E_S.tr_o}.(N_{ss}^{(1)} - \nu N_{nn}^{(1)})$$

$$+ \frac{\varepsilon}{2}.\frac{AE_R}{E_S.tr_o}\{(f''(\zeta)\, e^{i\gamma} + \overline{f''(\zeta)}\, e^{-i\gamma}) - (f'(\zeta) + \overline{f'(\zeta)})\}$$

$$\times (N_{ss}^{(o)} - \nu N_{nn}^{(o)})$$

Comparing the coefficients of equal powers of ε,

$$\varepsilon^o: \quad N_{nn}^{(o)} = \frac{AE_R}{E_S.tr_o}(N_{ss}^{(o)} - \nu N_{nn}^{(o)}) \tag{2.6.11}$$

$$\varepsilon: \quad N_{nn}^{(1)} = \frac{AE_R}{E_S.tr_o}(N_{ss}^{(1)} - \nu N_{nn}^{(1)}) + \tfrac{1}{2} N_{nn}^{(o)} \{(f''(\zeta)e^{i\gamma} + \overline{f''(\zeta)}e^{-i\gamma}) - (f'(\zeta) + \overline{f'(\zeta)})\}$$

[Using (2.6.11)] (2.6.12)

Equation (2.6.12) gives (2.7.5) for the elliptical case and (2.8.5) for the square hole with rounded corners.

Moments on the bead:

$$\text{Define} \quad M = M^{(o)} + \varepsilon M^{(1)}$$

$$H = H^{(o)} + \varepsilon H^{(1)} \tag{2.6.13}$$

The expression for H is derived below.

$$H = \frac{E_R J}{2(1+\nu)}\, w'_{,ns} \tag{2.6.14}$$

$$H = \frac{E_R J}{2(1+\nu)r_o}\,\frac{\partial}{\partial s}\left[\frac{\partial w'^{(o)}}{\partial \rho} + \varepsilon\frac{\partial w'^{(1)}}{\partial \rho} + \varepsilon L_1\frac{\partial w'^{(o)}}{\partial \rho} + \varepsilon\frac{L_2}{2}.\frac{\partial w'^{(o)}}{\partial \gamma}\right]$$

$$H = \frac{E_R J}{2(1+\nu)r_o^2}\left(1 - \frac{\varepsilon}{2}[f'(\zeta) + \overline{f'(\zeta)}]\right)\frac{\partial}{\partial \gamma}\left[\frac{\partial w'^{(o)}}{\partial \rho} + \varepsilon\frac{\partial w'^{(1)}}{\partial \rho} + \varepsilon L_1\frac{\partial w'^{(o)}}{\partial \rho} + \varepsilon.\frac{L_2}{2}.\frac{\partial w'^{(o)}}{\partial \gamma}\right] \tag{2.6.15}$$

$$N_{nn} = \overline{N_{nn}^{(o)}} + N_{nn}^{(o)}* + \epsilon(\overline{N_{nn}^{(1)}} + N_{nn}^{(1)}*) \qquad \text{(see Appendix VIII)}$$

where,

$\overline{N_{nn}^{(o)}}$ = Normal stress around the circle for the uncut cylinder.

$N_{nn}^{(o)}*$ = Perturbation stress to be added to $\overline{N_{nn}^{(o)}}$ for obtaining stress distribution for the case of a circular hole.

$\epsilon\overline{N_{nn}^{(1)}}$ = Additional normal stress to be added to $\overline{N_{nn}^{(o)}}$ to obtain the stress distribution around the non-circular hole, for an uncut cylinder.

$\epsilon N_{nn}^{(1)}*$ = Perturbation stresses to be added to $(\overline{N_{nn}^{(o)}} + N_{nn}^{(o)}* + \epsilon\overline{N_{nn}^{(1)}})$ to obtain the stress distribution for the case of a non-circular hole in a cylinder.

$N_{nn}^{(o)}*$ is obtained from the stress function ϕ_o*.

$N_{nn}^{(1)}*$ is obtained from the stress functions ϕ_o*, and ϕ_1*.

To obtain $\overline{N_{nn}^{(1)}}$, $\overline{N_{ss}^{(1)}}$ and $\overline{N_{ns}^{(1)}}$:

Let q_1, q_2 represent the principal stresses in x and y directions far away from the hole.

Then,

$$\overline{N_{nn}} = q_1 \cos^2\alpha + q_2 \sin^2\alpha$$

$$= \frac{(q_1 + q_2)}{2} + \frac{(q_1 - q_2)}{2} \cos 2\alpha \qquad (2.6.16)$$

But $e^{2i\alpha} = e^{2i\gamma}(1 + \epsilon[f'(\zeta) - \overline{f'(\zeta)}])$ (2.6.17)

given

$$\cos 2\alpha = \cos 2\gamma + i\,\epsilon \sin 2\gamma\,.[f'(\zeta) - \overline{f'(\zeta)}]$$

$$\sin 2\alpha = \sin 2\gamma - i\,\epsilon\cos 2\gamma\,.[f'(\zeta) - \overline{f'(\zeta)}] \qquad (2.6.18)$$

(2.6.16) gives:

$$\overline{N_{nn}} = \left(\frac{q_1+q_2}{2}\right) + \frac{(q_1-q_2)}{2} \cos 2\gamma + \frac{(q_1-q_2)}{2}$$

$$\times \{i\,\varepsilon \sin 2\gamma \,.(f'(\zeta) - \overline{f'(\zeta)})\}$$

$$\overline{N_{nn}^{(o)}} = \frac{(q_1+q_2)}{2} + \frac{(q_1-q_2)}{2} \cos 2\gamma$$

$$\overline{N_{nn}^{(1)}} = \frac{(q_1-q_2)}{2}\, i \sin 2\gamma \,.(f'(\zeta) - \overline{f'(\zeta)}) \qquad (2.6.19)$$

Similar expressions can be found for $N_{ss}^{(1)}$ and $N_{ns}^{(1)}$ in non-dimensional form.

For the elliptical hole, (pressure loading)

$$\overline{N_{nn}^{(1)}} = \frac{1}{2} \sin^2 2\gamma$$

$$\overline{N_{ss}^{(1)}} = -\frac{1}{2} \cdot \sin^2 2\gamma$$

$$\overline{N_{ns}^{(1)}} = \frac{\sin 4\gamma}{4} \qquad (2.6.20)$$

For the square hole with rounded corners, (pressure loading)

$$\overline{N_{nn}^{(1)}} = \frac{3}{2} \cdot \sin 2\gamma \cdot \sin 4\gamma$$

$$\overline{N_{ss}^{(1)}} = -\frac{3}{2} \sin 2\gamma \cdot \sin 4\gamma$$

$$\overline{N_{ns}^{(1)}} = \frac{3}{2} \cdot \cos 2\gamma \cdot \sin 4\gamma \qquad (2.6.21)$$

2.7 Application to the case of an elliptical hole:

The transformation function required in this case is

$$Z = w(\zeta) = \zeta + \frac{\varepsilon}{\zeta} \qquad (2.7.1)$$

giving; $e^{i\alpha} = e^{i\gamma}(1 + i\,\varepsilon \sin 2\gamma)$, using (2.5.6)

from which $$\frac{\partial \alpha}{\partial s} = \frac{1}{r_o}(1 + 3\varepsilon\cos 2\gamma), \text{ at } \rho = 1 \qquad (2.7.2)$$

Also $$L_1 = \frac{\bar{\zeta} f(\zeta) + \zeta \overline{f'(\zeta)}}{2\rho} \frac{\partial}{\partial \rho} + \left[\frac{(f(\zeta) - \overline{f(\zeta)})}{2i\rho} \cos\gamma - \left(\frac{f(\zeta) + \overline{f(\zeta)}}{2\rho}\right) \cdot \sin\gamma\right] \frac{\partial}{\partial \gamma}$$

$$= \frac{\cos 2\gamma}{\rho} \cdot \frac{\partial}{\partial \rho} - \frac{\sin 2\gamma}{\rho^2} \cdot \frac{\partial}{\partial \gamma} \qquad (2.7.3)$$

$$L_2 = 2\left[\frac{\zeta \overline{f(\zeta)} - \bar{\zeta} f(\zeta)}{2i\rho^2} + \frac{f'(\zeta) - \overline{f'(\zeta)}}{2i}\right]$$

$$= \frac{4 \sin 2\gamma}{\rho^2} \qquad (2.7.4)$$

Using the relations given in (2.5), to the order of ε at $\rho = 1$, the equations to be satisfied are:

$$\left(6 + 2\frac{E_R}{E_S} \cdot \frac{A}{r_o t}\right) N_{nn}^{(1)} - 6 \cdot \frac{E_R}{E_S} \cdot \frac{A}{r_o t} \cdot N_{ss}^{(1)} = 18 \cos 2\gamma \, N_{nn}^{(o)} \qquad (2.7.5)$$

$$6N_{ns}^{(1)} + 2 \cdot \frac{E_R}{E_S} \cdot \frac{A}{r_o t} \cdot \left(3\frac{\partial N_{ss}^{(1)}}{\partial \gamma} - \frac{\partial N_{nn}^{(1)}}{\partial \gamma}\right) = 6 N_{ns}^{(o)} \cos 2\gamma \qquad (2.7.6)$$

$$M_{nn}^{(1)} = \frac{M^{(1)}}{r_o} + \frac{1}{r_o}\frac{\partial H^{(1)}}{\partial \gamma} + 3\frac{M^{(o)}}{r_o}\cos 2\gamma + \frac{\cos 2\gamma}{r_o}\frac{\partial H^{(o)}}{\partial \gamma} \qquad (2.7.7)$$

$$\overline{Q_n^{(1)}} = -\frac{1}{r_o^2}\frac{\partial^2 M^{(1)}}{\partial \gamma^2} + \frac{1}{r_o^2} \cdot \frac{\partial H^{(1)}}{\partial \gamma} + \frac{AE_R}{E_S \cdot t \cdot R} \cdot \left(N_{ss}^{(1)} - \frac{N_{nn}^{(1)}}{3}\right) \cos^2\gamma$$

$$- \frac{AE_R}{E_S \cdot t \cdot R} \cdot \sin^2 2\gamma \cdot \left(N_{ss}^{(o)} - \frac{N_{nn}^{(o)}}{3}\right) - \frac{2\cos 2\gamma}{r_o^2}\frac{\partial^2 M^{(o)}}{\partial \gamma^2}$$

$$+ \frac{2 \sin 2\gamma}{r_o^2}\frac{\partial M^{(o)}}{\partial \gamma} + \frac{4\cos 2\gamma}{r_o^2}\frac{\partial H^{(o)}}{\partial \gamma} - \frac{6H^{(o)}}{r_o^2}\sin 2\gamma. \qquad (2.7.8)$$

(Refer to Appendix IX for details of these four equations in terms of ϕ_o^* and ϕ_1^*.)

2.8 Application to the case of a square hole with rounded corners:

The transformation function required in this case is,

$$Z = w(\zeta) = \zeta - \frac{1}{6\zeta^3} \tag{2.8.1}$$

giving $e^{i\alpha} = e^{i\gamma}(1 + \varepsilon .3i \sin 4\gamma)$

from which $\frac{\partial \alpha}{\partial s} = \frac{1}{r_o}(1 + 15\,\varepsilon \cos 4\gamma)$, at $\rho = 1$ (2.8.2)

Also $L_1 = \frac{\cos 4\gamma}{\rho^3} \cdot \frac{\partial}{\partial \rho} - \frac{\sin 4\gamma}{\rho^4} \cdot \frac{\partial}{\partial \gamma}$ (2.8.3)

$$L_3 = \frac{8 \sin 4\gamma}{\rho^4} \tag{2.8.4}$$

Using the relations given in (2.5), to the order of ε at $\rho = 1$, the equations to be satisfied are,

$$(6 + 2.\frac{E_R}{E_S} \cdot \frac{A}{r_o t}) N_{nn}^{(1)} - 6 \frac{E_R}{E_S} \cdot \frac{A}{r_o t} \cdot N_{ss}^{(1)} = 90 \cos 4\gamma . N_{nn}^{(o)} \tag{2.8.5}$$

$$6N_{ns}^{(1)} + 2 \frac{E_R}{E_S} \cdot \frac{A}{r_o t} \cdot (3 \frac{\partial N_{ss}^{(1)}}{\partial \gamma} - \frac{\partial N_{nn}^{(1)}}{\partial \gamma}) = 18 \cos 4\gamma . N_{ns}^{(o)} \tag{2.8.6}$$

$$M_{nn}^{(1)} = \frac{M^{(1)}}{r_o} + \frac{1}{r_o} \frac{\partial H^{(1)}}{\partial \gamma} + \frac{15 \cos 4\gamma}{r_o} M^{(o)} + \frac{3 \cos 4\gamma}{r_o} \cdot \frac{\partial H^{(o)}}{\partial \gamma} \tag{2.8.7}$$

$$\overline{Q_n^{(1)}} = -\frac{1}{r_o^2} \cdot \frac{\partial^2 M^{(1)}}{\partial \gamma^2} + \frac{1}{r_o^2} \frac{\partial H^{(1)}}{\partial \gamma} + \frac{AE_R}{E_S . t . R} (N_{ss}^{(1)} - \frac{1}{3} N_{nn}^{(1)}) \cos^2 \gamma$$

$$- \frac{AE_R}{E_S . t . R} 3 . \sin 2\gamma . \sin 4\gamma . (N_{ss}^{(o)} - \frac{1}{3} N_{nn}^{(o)}) - \frac{6 \cos 4\gamma}{r_o^2} \frac{\partial^2 M^{(o)}}{\partial \gamma^2}$$

$$+ \frac{12 \sin 4\gamma}{r_o^2} \frac{\partial M^{(o)}}{\partial \gamma} + \frac{18 \cos 4\gamma}{r_o^2} \frac{\partial H^{(o)}}{\partial \gamma} - \frac{60 \sin 4\gamma}{r_o^2} . H^{(o)} \tag{2.8.8}$$

(Refer Appendix X for details of these four equations in terms of ϕ_o^* and ϕ_1^*.)

2.9 Method of solution:

The boundary conditions (Appendix IX for an elliptical hole and X for a square hole with rounded corners) are satisfied by collocation procedure. First solution of the problem of a circular hole gives the coefficients A_n and B_n. Having got ϕ_o^*, the boundary conditions give the unknowns C_n and D_n in ϕ_1^*. The series for ϕ_1^* is truncated at an odd value of n, leaving (2n+2) unknowns to be determined. The required equations are obtained by satisfying the boundary conditions at (n+1)/2 collocation points in the first quadrant. The series for ϕ_1^* is terminated at successively higher values of n until the stresses calculated remained essentially the same. The stresses are obtained by using the relations given in Appendix VIII. The flow diagram used for computation is shown in Appendix XI. In all the numerical calculation, as in Chapter I, ν is taken as 1/3.

2.10 Results and discussion:

Firstly solutions for ϕ_1^* alone (that is for arbitrary ε) were obtained for unreinforced elliptical holes and square holes with rounded corners, in cylindrical shells and are presented in figures 22, 23, 24 and 25. The results cover a range $0 \leqslant \beta \leqslant 7$. (The values of β considered in (42) and (45) were less than unity.) It was necessary to evaluate the coefficients A_n and B_n in ϕ_o^*, to 9 places of accuracy in order to make the residual errors low for $\sqrt{2}\beta = 10$. The number of terms required in ϕ_1^* was about the same as the number of terms chosen in ϕ_o^* for any given β.

For any given β and ε: the following is the procedure to obtain the stress distribution. Let us consider the case of an elliptical hole. Figures 4 and 5 give the membrane and bending stresses for the given value of β for a circular hole. Figures 22 and 23 give

the perturbations in membrane and bending stresses.

$$\frac{\sigma_{ss}}{\sigma_\infty} = \frac{\sigma_{ss}^{(o)}}{\sigma_\infty} + \varepsilon \cdot \frac{\sigma_{ss}^{(1)}}{\sigma_\infty} \qquad (2.10.1)$$

where $\frac{\sigma_{ss}^{(o)}}{\sigma_\infty}$, $\frac{\sigma_{ss}^{(1)}}{\sigma_\infty}$ are taken from figures 4 and 22 respectively. The procedure is identical for the bending stresses.

It should be noted that the angle 'γ' refers to the unit circle in the 'ζ' plane and the corresponding angle 'θ' in the plane of the cut-out is given by

$$\tan\theta = \left(\frac{1-\varepsilon}{1+\varepsilon}\right) \tan\gamma \qquad (2.10.2)$$

for the elliptical hole and,

$$\tan\theta = \frac{\sin\gamma - \varepsilon\sin 3\gamma}{\cos\gamma + \varepsilon\cos 3\gamma} \qquad (2.10.3)$$

for the square hole with rounded corners.

It can be seen that the bending stresses as well as membrane stresses are affected to a large extent for larger values of ε. The conclusion, that flat plate theory is applicable to non-circular holes in cylindrical shells under tension, by Guz and Savin (42) is true for small values of β only. The increase in membrane stresses in the case of a square hole with rounded corners ($\varepsilon = -1/6$) for large values of 'β' is about 100% as compared with circular hole solution. Though we are restricting ourselves to terms of order 'ε' only, the convergence is reasonable as shown by Guz and Savin (42) for small values of β. It is, thus, expected that the inclusion of 'ε^2' order terms do not contribute substantially to the stresses for all values of β and for practical values of 'ε'.

To check the solution given by Savin (43) for the case of an elliptical hole in a cylindrical shell under pressure a value of $\sqrt{2}\beta = 0.5$, $\varepsilon = \pm 1/6$ was chosen. The tangential stress given by

Savin to the order of 'ε' is,

$$\frac{\sigma_{ss}}{\sigma_\infty} = (1.5 + \cos 2\gamma) + \varepsilon(3\cos 2\gamma + \cos 4\gamma) + \pi\beta^2(1 + 1.25 \cos 2\gamma) + \pi\beta^2.\varepsilon\,[5 + 16 \cos 2\gamma + 5 \cos 4\gamma] \qquad (2.10.4.)$$

where $\beta^2 = \frac{r_o^2}{8Rt} \cdot 12(1-\nu^2)$

It has been pointed out by Vandyke (4) and others (5,6) that there is an error in Lurie's solution in the term containing β^2 and that the correct values were one half of Lurie's values. It is found that there is a similar error in the term containing '$\varepsilon\beta^2$' and the correct values are a quarter of those given in (2.10.4).

In reference (46), the expression for the tangential stress is obtained as,

$$\frac{\sigma_{ss}}{\sigma_\infty} = \frac{1.5 - [\varepsilon - \cos 2\gamma]}{(1 - 2\varepsilon \cos 2\gamma)} + \frac{\pi a^2}{8Rt} \frac{[3(1-\nu^2)]^{1/2}[2 + 3\varepsilon\cos 2\gamma + 2.5 \cos 2\gamma + \varepsilon\cos 2\gamma]}{(1 + 2\varepsilon - 2\varepsilon \cos 2\gamma)} \qquad (2.10.5)$$

$$= (1.5 - [\varepsilon - \cos 2\gamma])(1 + 2\varepsilon\cos 2\gamma) + \frac{\pi\beta^2}{2}(1 + 2\varepsilon)(2 + 4\varepsilon \cos 2\gamma + 2.5 \cos 2\gamma)(1-2\varepsilon +2\varepsilon \cos 2\gamma)$$

$$= (1.5+\cos 2\gamma) +\varepsilon(3 \cos 2\gamma+\cos 4\gamma) +\pi\beta^2(1 + 1.25 \cos 2\gamma) + \frac{\pi\beta^2\varepsilon}{4}(16 \cos 2\gamma + 5 \cos 4\gamma + 5) \qquad (2.10.6)$$

(2.10.6) is the same as the expression (2.10.4) except the factor 1/4 in the '$\varepsilon\beta^2$' term.

Figures 26 and 27 show $\frac{\sigma_{ss}}{\sigma_\infty}$ distribution for an elliptical hole with $\varepsilon = \pm 1/6$ ($\frac{a}{b}, \frac{b}{a} = 1.4$) and figure 28 shows the distribution for a square hole ($\varepsilon = -1/6$). The value $\sqrt{2}\beta = 0.5$ is chosen. The agreement between the present solution and Savin's solution is good, though

'β' is slightly greater than 0.3 which is the limit for applicability of Lurie's solution for the circular hole problem. The influence of curvature can be seen by considering the case of an elliptical hole with $\frac{b}{a} = 1.4$ (figure 27). The maximum stress that occurs is $\frac{\sigma_{ss}}{\sigma_\infty} = 2.32$ as compared with the value for the flat plate of 1.93.

In the case of a square hole with rounded corners, the requirement that the transformation is conformal implies, $\varepsilon < 1/3$. If $\varepsilon = + 1/6$ is chosen, the solution corresponds to the case when the diagonals are parallel to the x and y axes.

In order to study the influence of reinforcement Wittrick's (32) optimum bead with $\lambda = \frac{A}{r_o t} = 0.8$ was chosen. For $\mu = 6$; $J/I = 2$ and $E_R/E_S = 1$, figure 29 shows the variation of maximum principal stress with β. The reduction in shell stresses one obtains by choosing $\lambda = 1.489$ (reinforcement area giving weight equivalent to that required for Mansfield's neutral hole), $\mu = 6$; $J/I = 2$; $E_R/E_S = 1$; is also shown in figure 29. For $\sqrt{2}\beta = 4$ the maximum principal stress corresponding to Wittrick's optimum bead is 2.258, about twice that for the flat plate and increasing λ to 1.489 brings down the stress only to 1.729. For a reinforced elliptical hole with $\varepsilon = -1/6$, it is clear from figure 30, that it pays to increase the bending efficiency.

The influence of the shape of the cut-out is illustrated by the following table obtained for $E_R/E_S = 1$: $\lambda = 0.8$ and $J/I = 2$.

TABLE II

	$\sqrt{2}\beta = 2$		$\sqrt{2}\beta = 3$		$\sqrt{2}\beta = 4$	
μ	Ellipse S.C.F.	Square with rounded corners S.C.F.	Ellipse S.C.F.	Square with rounded corners S.C.F.	Ellipse S.C.F.	Square with rounded corners S.C.F.
2	1.679	5.191				
3	1.613	5.163				
4	1.581	5.086	1.932	6.173		
5	1.558	5.158	1.842	6.035		
6	1.543	5.161	1.805	6.171	2.258	7.721
7			1.780	6.179	2.165	7.874
8					2.098	8.010

In the case of square hole with rounded corners choosing $E_R/E_S = 1$; $\lambda = 1.489$; $\mu = 6$: $J/I = 2$, the stresses increase to 5.187, 6.26 and 8.659 for $\sqrt{2}\beta = 2$, 3 and 4 respectively showing that over-reinforcing defeats its own objective. More results need to be evaluated to enable the optimum λ and μ to be selected, specially for square holes with rounded corners as the stress concentrations are too high.

For details and results corresponding to the case B in the case of a reinforced elliptical hole, refer to Appendix XIV.

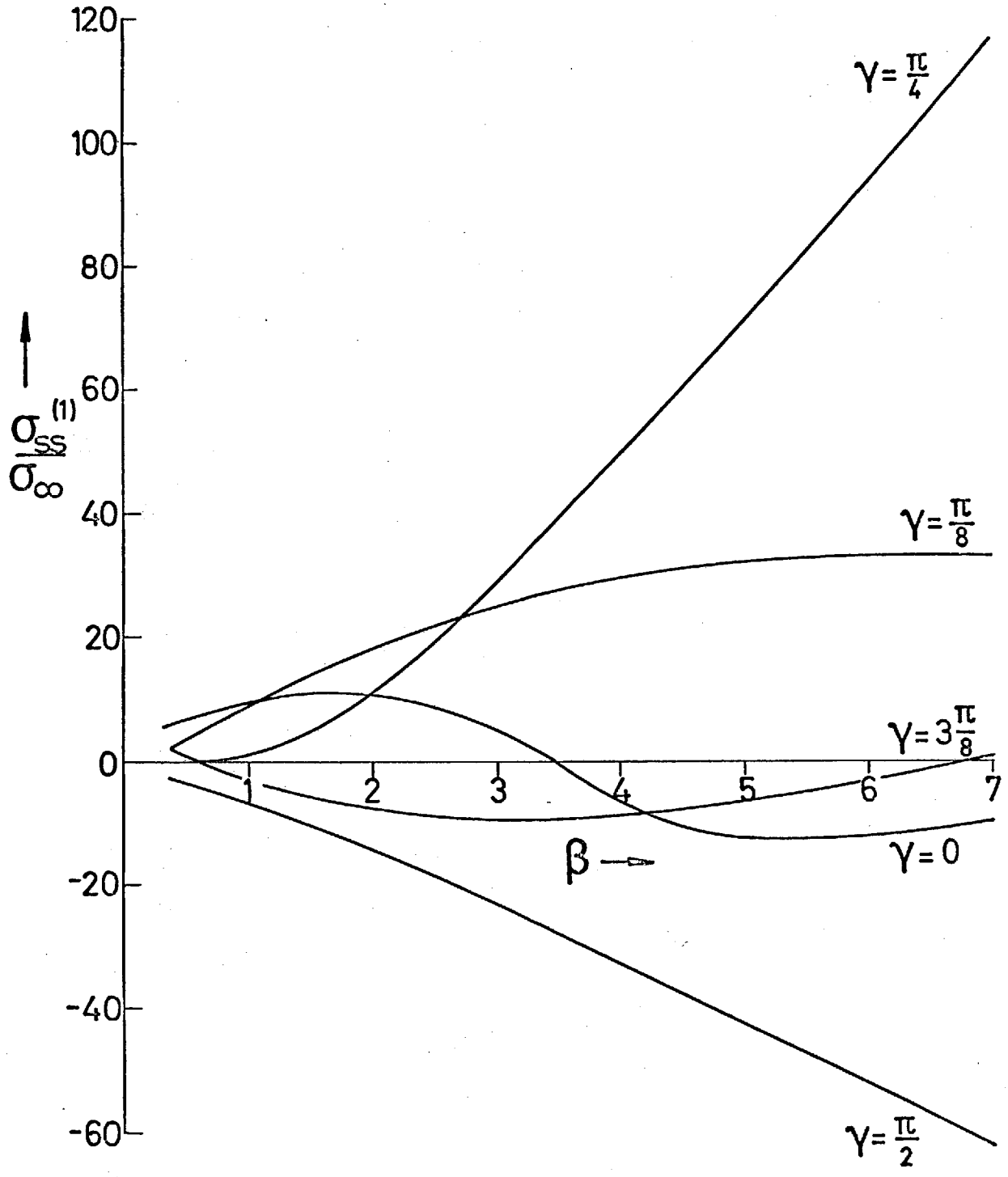

FIG. 22 MEMBRANE STRESSES (PRESSURE LOADING). (ELLIPTICAL HOLE.)

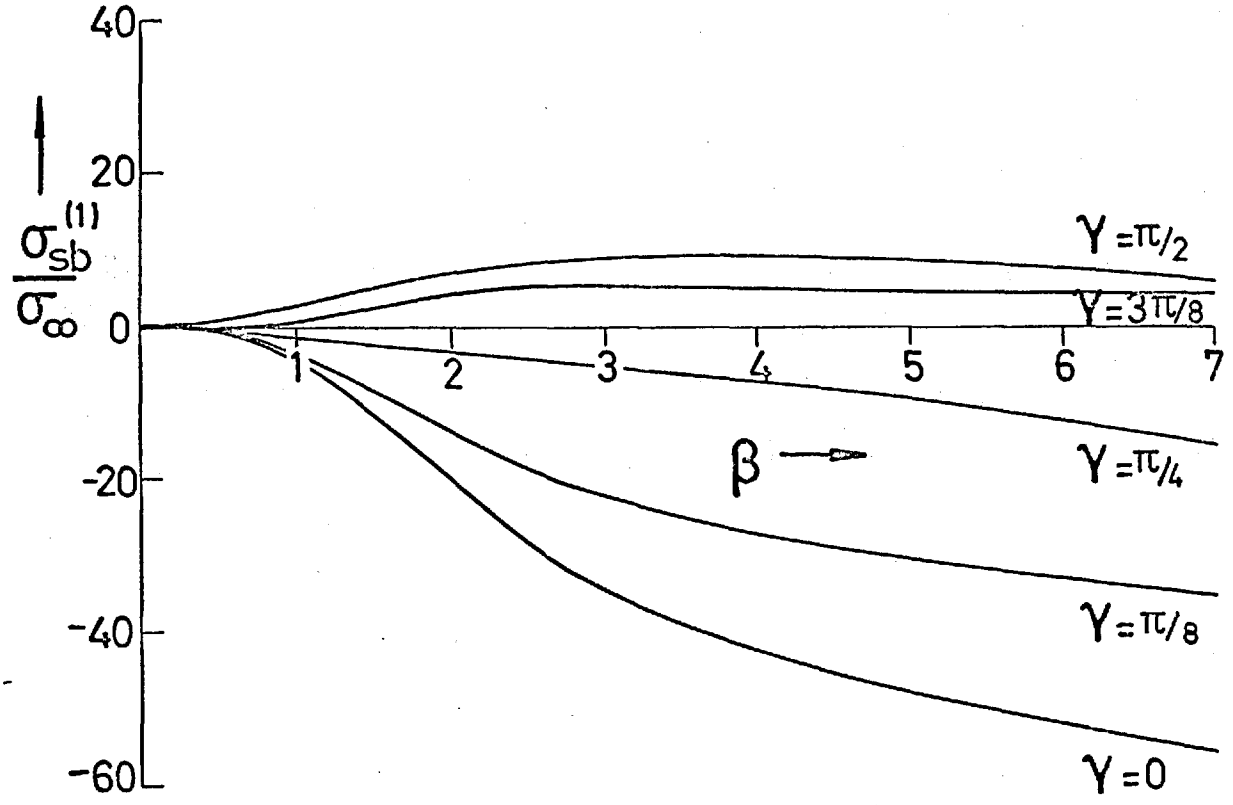

FIG. 23 BENDING STRESSES (PRESSURE LOADING). ELLIPTICAL HOLE. SHELL UPPER SURFACE

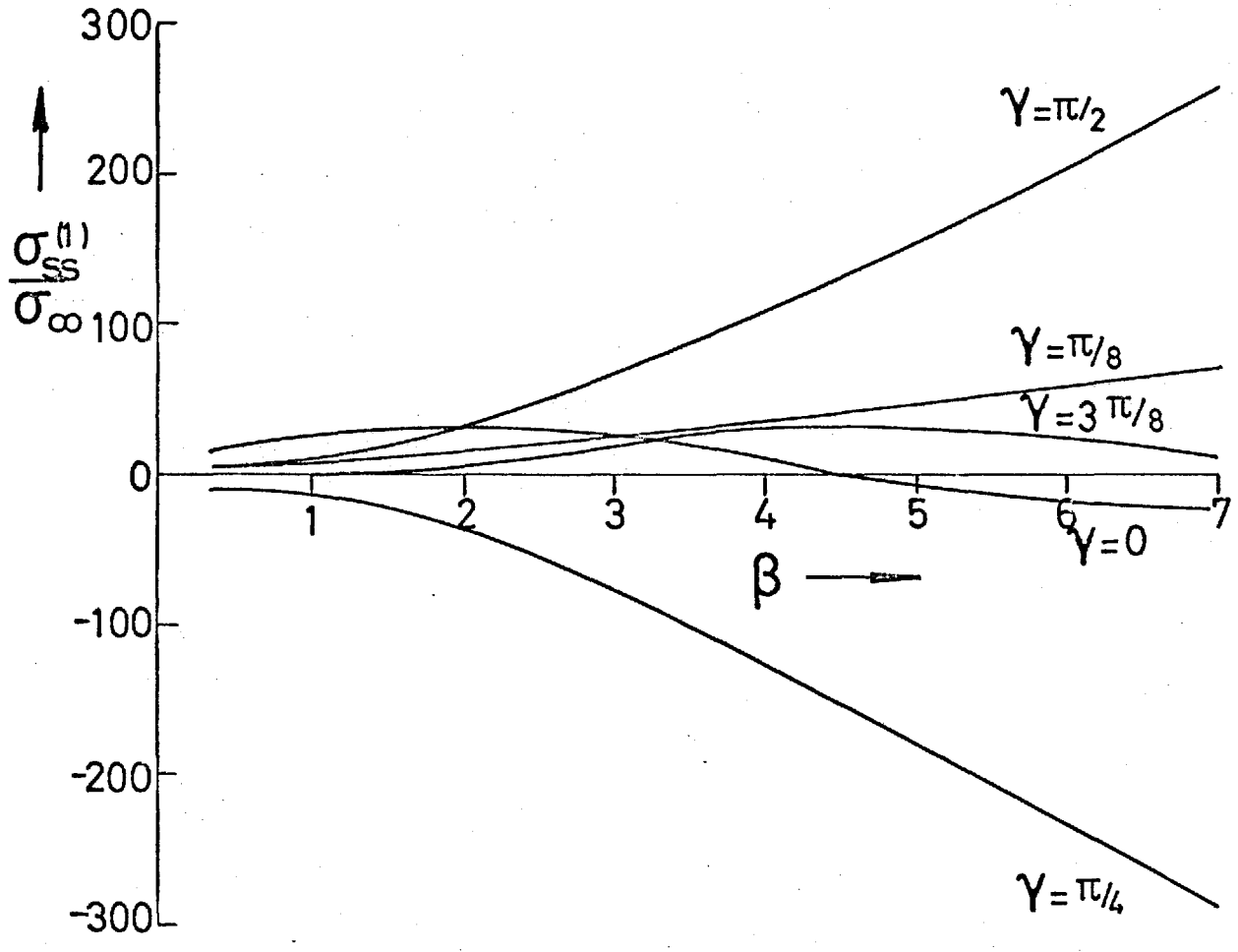

FIG. 24 MEMBRANE STRESSES (PRESSURE LOADING). (SQUARE HOLE.)

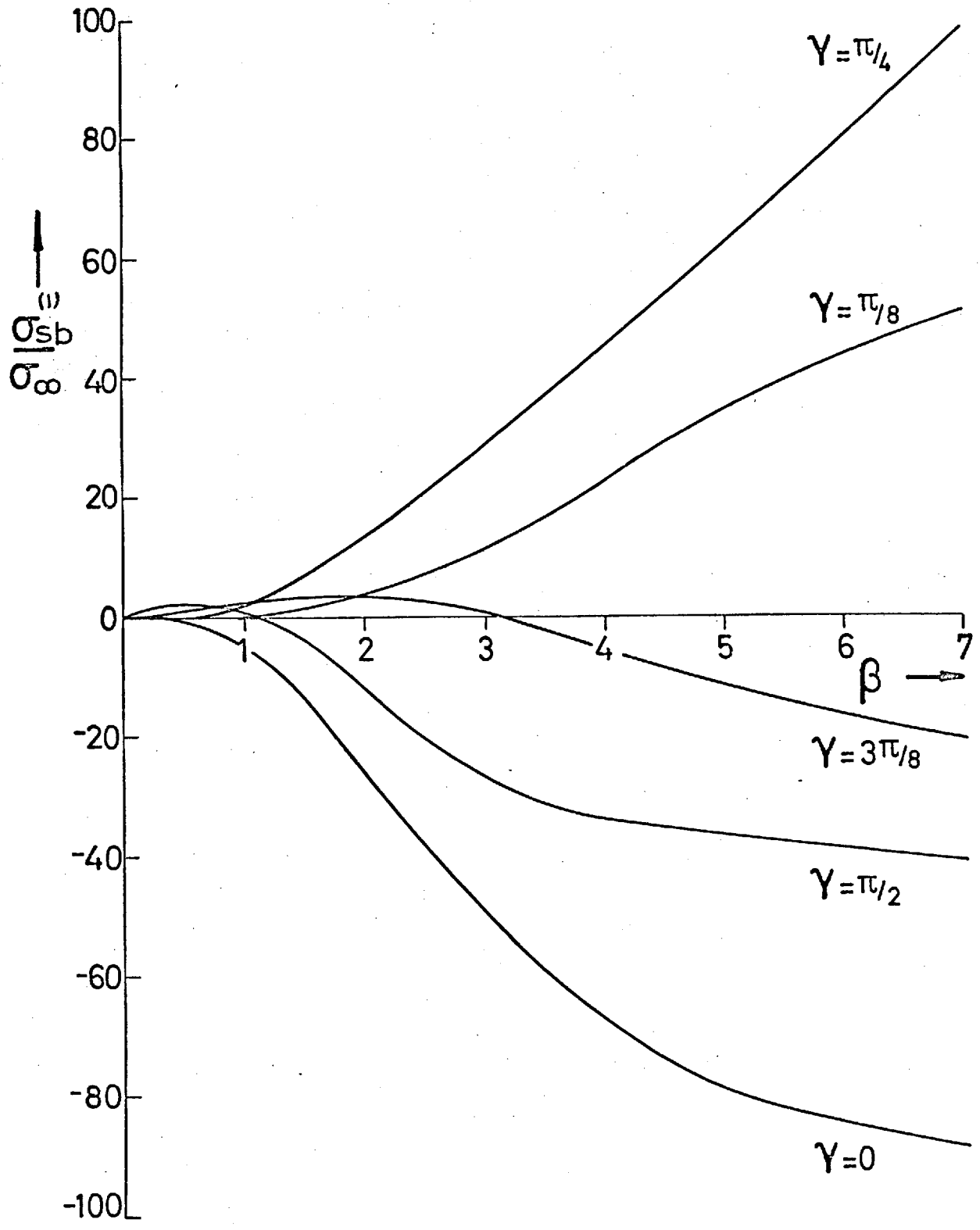

FIG. 25 BENDING STRESSES (PRESSURE LOADING). (SQUARE HOLE)
SHELL UPPER SURFACE

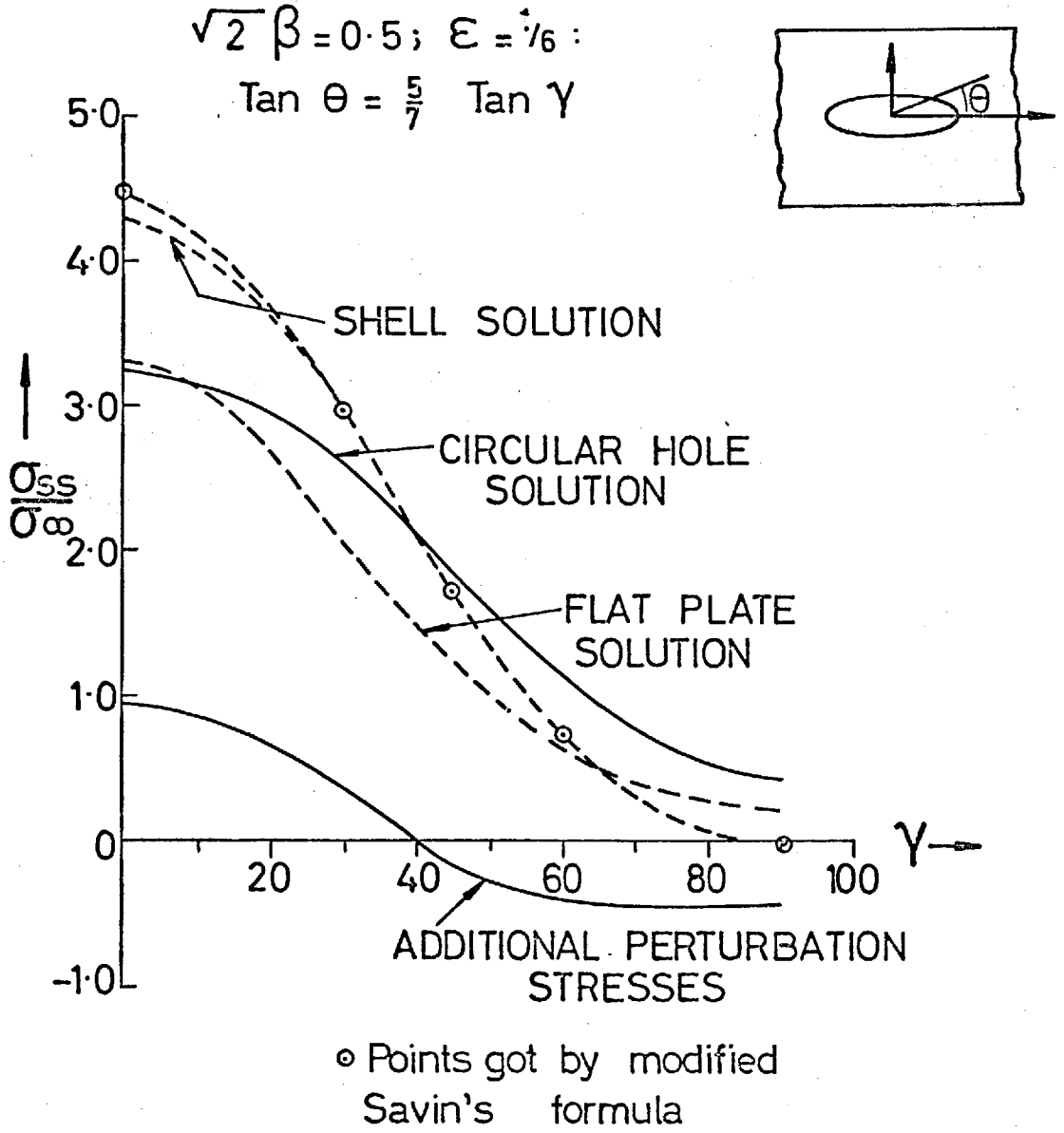

FIG. 26 ELLIPTICAL HOLE (PRESSURE LOADING)

$\sqrt{2}\,\beta = 0{\cdot}5;\ \varepsilon = -1/6$:

$\tan\theta = \frac{7}{5}\tan\gamma$

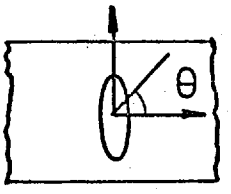

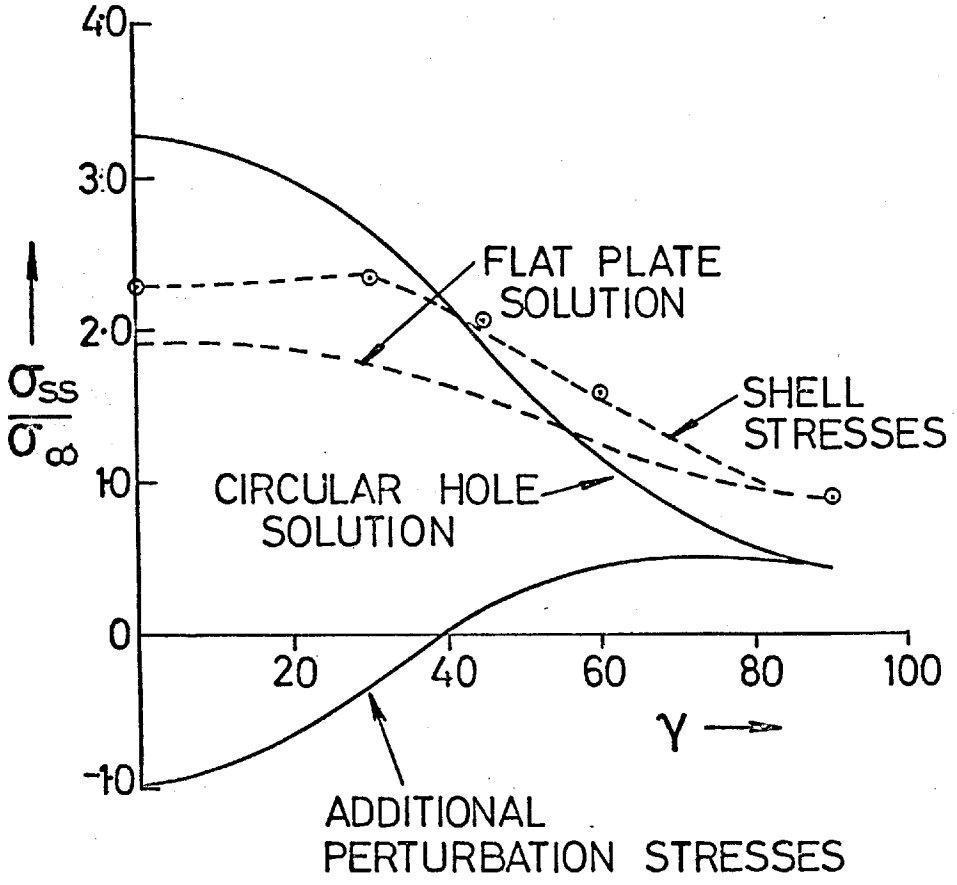

⊙ Points by using modified Savin's formula

FIG. 27 ELLIPTICAL HOLE (PRESSURE LOADING).

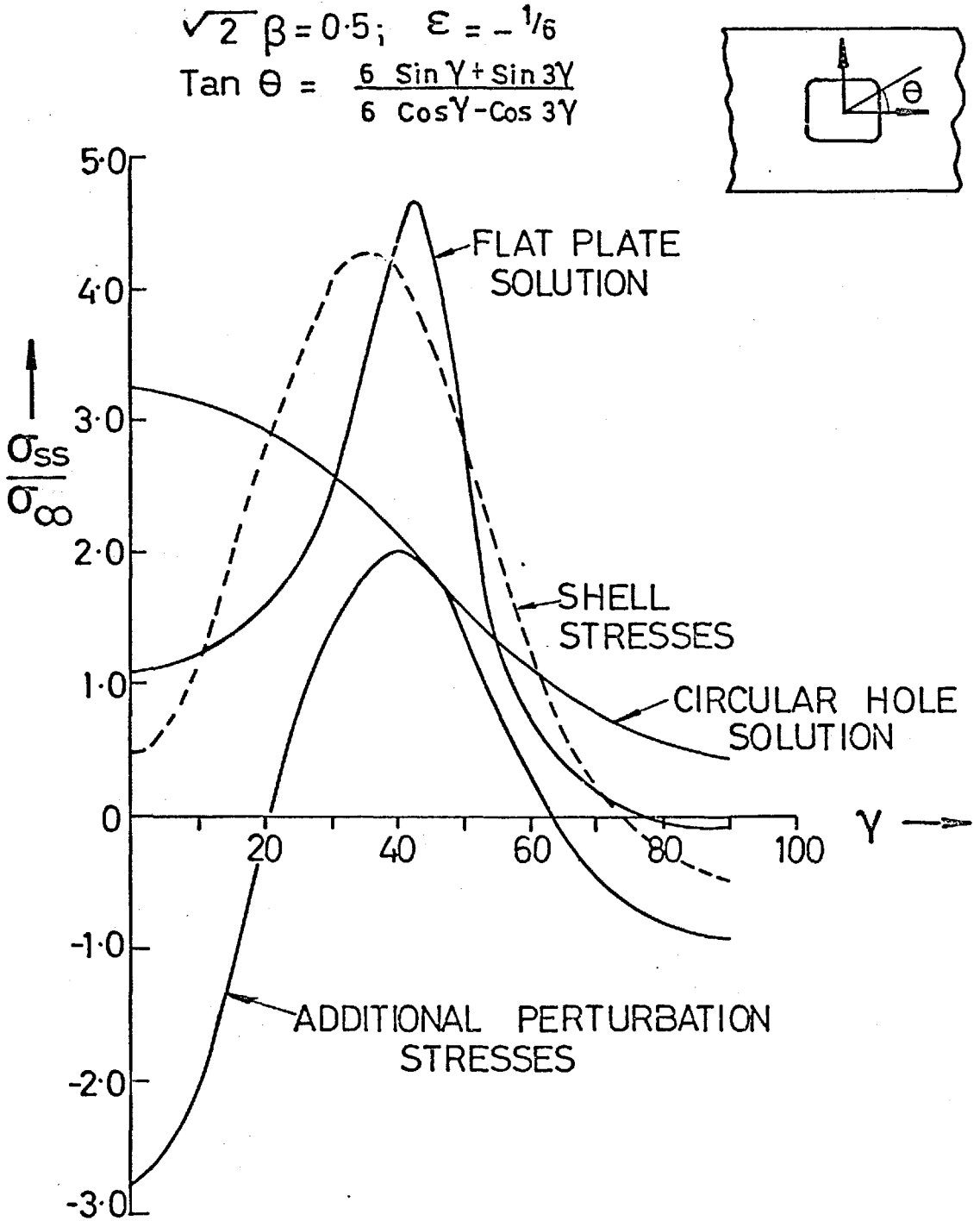

FIG. 28 SQUARE HOLE (PRESSURE LOADING)

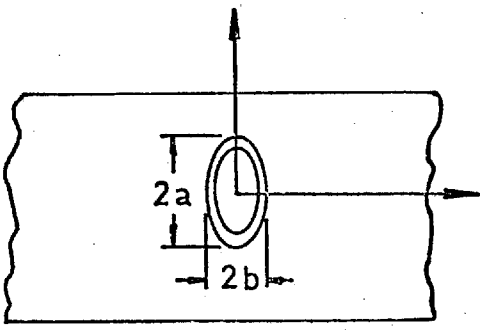

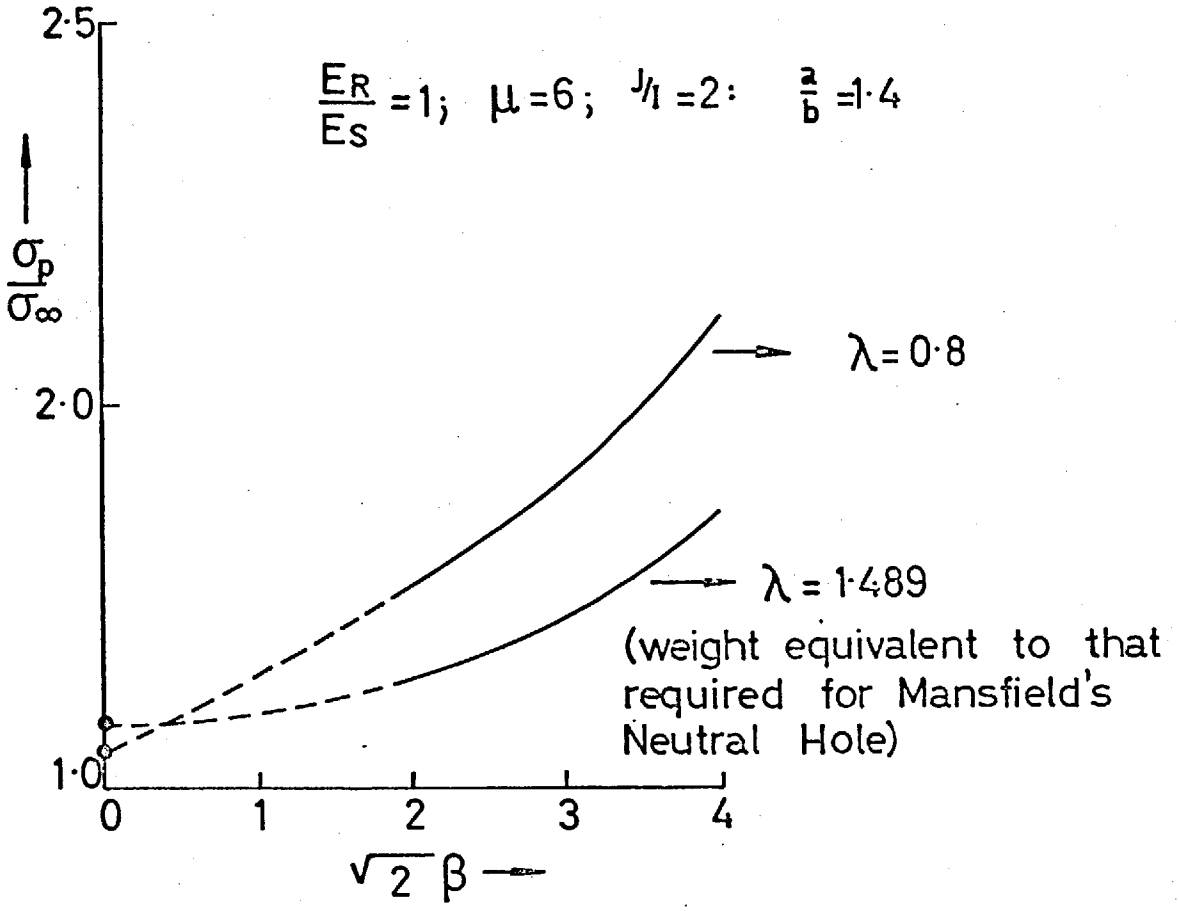

• Wittrick's Solution

FIG. 29 REINFORCED ELLIPTIC HOLE (PRESSURE LOADING)

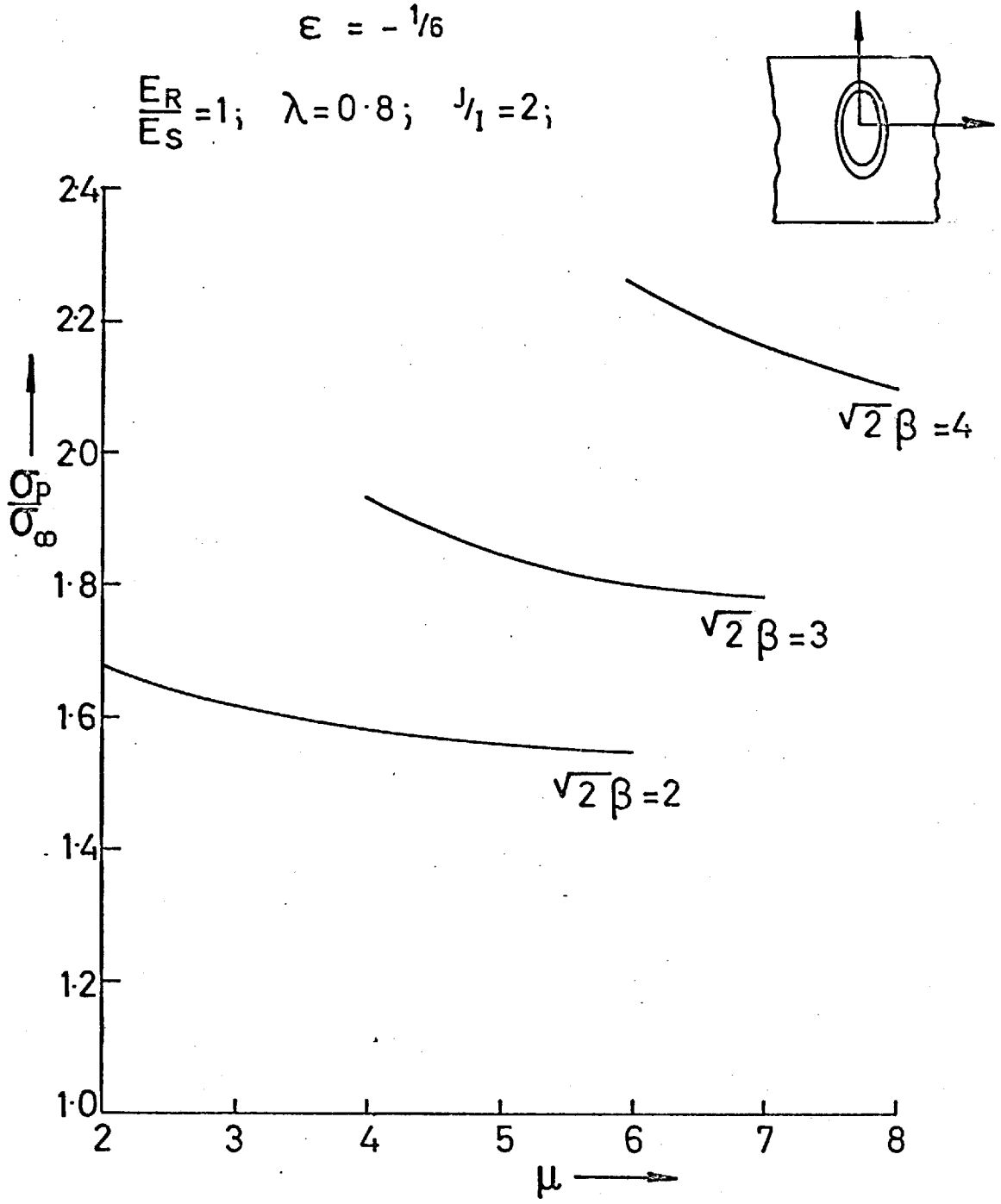

FIG. 30 REINFORCED ELLIPTIC HOLE (PRESSURE LOADING)

CHAPTER III

REINFORCED CIRCULAR HOLE IN A SPHERICAL SHELL

3.1 Introduction:

Many structures in aerospace, nuclear, marine and petrochemical industries consist of thin spherical shells. Cut-outs are introduced, for example, in case of pressure vessels for inspection purposes and in case of solid propellant motor cases, to accommodate the propellant igniters or thrust terminators. To alleviate the stress concentrations, it is necessary to reinforce the holes. In this chapter a solution is given for the case of a reinforced circular hole in a spherical shell. The shell is assumed to be shallow and the loading considered is pressure.

A shell is considered to be shallow, as postulated by Reissner (47), if the height to the base diameter ratio is 1/8. A general theory of shallow shells was formulated by Marguerre (28) and a detailed study of a shallow spherical cap was made by Reissner (47) and (50). Reissner neglects the contributions of the transverse shearing stress resultants to the equilibrium of forces in the meridional and tangential directions and the contribution of the stretching displacements to the change of curvature expressions. Reissner's assumptions regarding shallow spherical shells are identical to Donnell's assumptions for cylindrical shells and lead to an analogous set of basic equations. As a result of Donnell's assumptions, the cylindrical shell is treated as a curved rectangular plate while as a result of Reissner's assumptions, the shallow spherical shell is treated as a curved circular plate.

Theoretically it has been shown by Penny (48) that the influence of curvature on the stress concentrations around a cut-out, is not negligible in the case of a spherical shell and experiments by Houghton

and Rothwell (9) confirmed this theory. The differential equations governing the small deformations of the isotropic shallow spherical shell with constant wall thickness were obtained by Reissner (47) and these are used in this thesis. The problem of a reinforced circular opening in a spherical shell has been considered by Mansfield (17) in which the asymptotic solution was made use of. Mansfield's solution is based on Timoshenko's asymptotic solution which is not valid near the axis of symmetry of a shell and the equations thus obtained are not valid for shallow spherical shells. Also, in obtaining the stress concentration factor the increased tangential direct stresses due to the presence of the cut-out are not considered. Greszczuk (49) made an attempt to find the ideal reinforcement for a circular hole in a spherical shell by considering the effect of reinforcement geometry. In this paper however optimisation was wrongly carried out on the basis of the radial stresses and no account was taken of the more important tangentialstresses. The tangential stresses are in fact higher than the radial stresses and the optimisation as suggested does not ensure minimum tangential stresses.

The problem of an arbitrary shaped hole was considered by Guz and Savin (42) in which conformal mapping techniques were used. Later this method was extended to ring reinforced holes of arbitrary shape in spherical shells, (44). Guz and Savin do not take into account the component of bead tension, in the normal shear equilibrium. Also, the boundary conditions are expressed in terms of the displacements u, v, and w, whereas in this thesis the Airy's stress function is made use of.

It is confirmed that the area required for a neutral hole in a flat plate under uniform tension would make a circular hole neutral for a spherical shell under pressure. It is also found that, when the shear centre of the reinforcement does not lie in the shell middle surface,

the shell stresses always increase, disproving the suggestion (49) that one achieves a minimum stress level for a particular value of eccentricity. It is found that the bending rigidity of the bead can be ignored.

A spherical shell configuration is shown in figure 3 1.

3.2 Formulation of the problem and solution:

The equations governing the behaviour of the thin shallow spherical shell (47) can be written in the form,

$$\nabla^4 w' + \frac{1}{DR} \nabla^2 F' = \frac{p}{D} \qquad (3.2.1)$$

$$\nabla^4 F' - \frac{E_s t}{R} \nabla^2 w' = 0 \qquad (3.2.2)$$

The sign convention used for stress resultants and stress couples is the same as for cylindrical shell (figure 2).For the purpose of non-dimensionalising the stress resultants, a reference stress $N_{ref} = \frac{pR}{2}$, is chosen. A non-dimensionalisation is carried out so that the two differential equations could be combined to contain a single complex unknown,

$$F = F'/a^2 N_{ref}$$

$$w = (w'/a^2 N_{ref})\left(\frac{E_s t^2}{[12(1-\nu^2)]^{1/2}}\right) \qquad (3.2.3)$$

Defining $\phi = w - iF$, equations (3.2.1) and (3.2.2) can be combined to give,

$$\nabla^4 \phi + i\beta^2 \nabla^2 \phi = \beta^2 \qquad (3.2.4)$$

The effect of a hole in a shell is shown by Savin (13) to be restricted to a local region around the hole.

$$\therefore \quad F = \bar{F} + F^* \; ; \; w = \bar{w} + w^* \qquad (3.2.5)$$

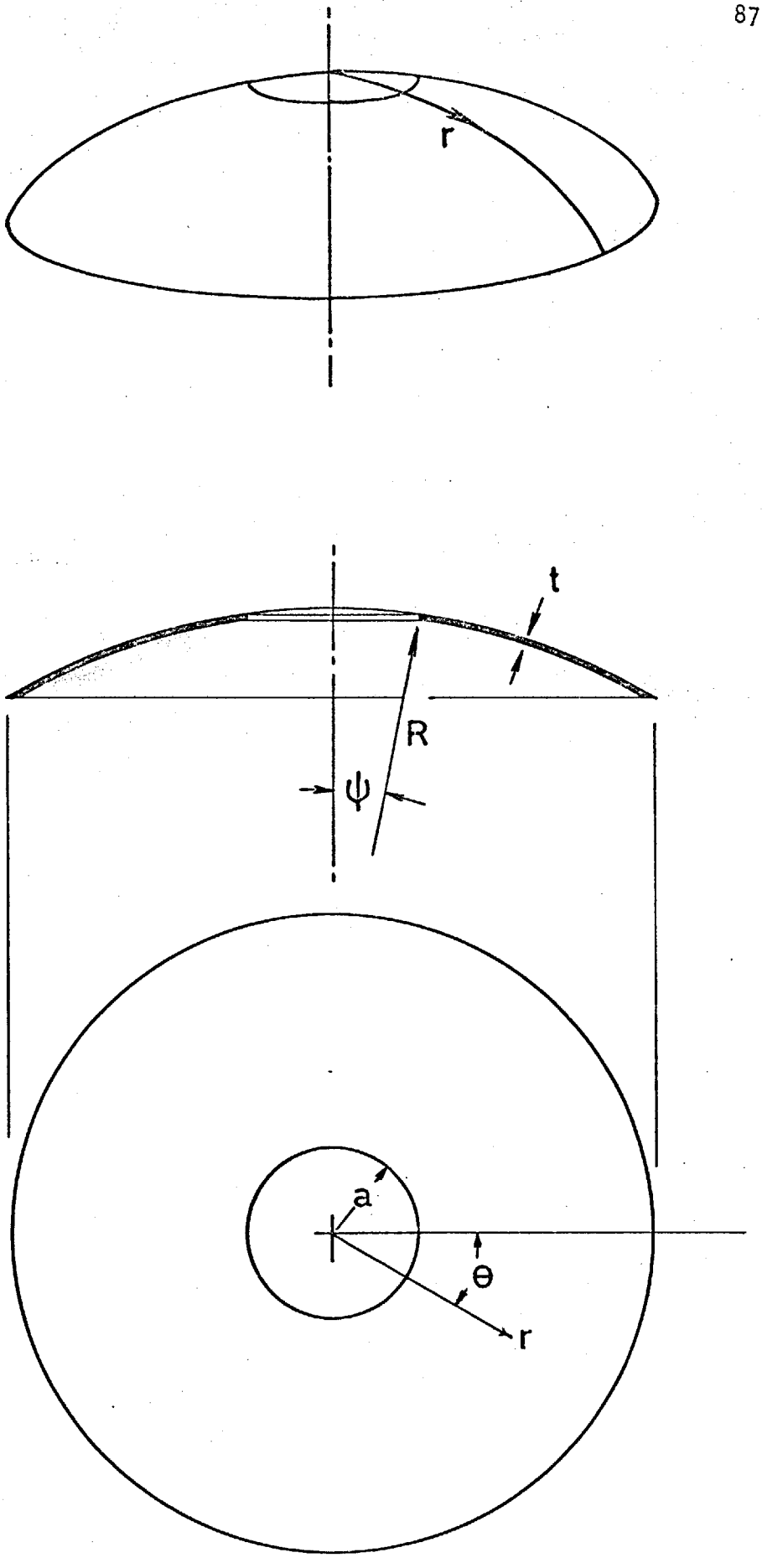

FIG. 31

where $\overline{F}$ and $\overline{w}$ are prescribed values of F and w, away from the hole, in which region F* and w* vanish.

For the case under consideration, $\overline{F} = r^2/2$ (3.2.6)

Then the residual problem reduces to the homogeneous equation,

$$\nabla^4\phi^* + i\beta^2\nabla^2\phi^* = 0 \tag{3.2.7}$$

where ϕ^* tends to zero far away from the hole.

Equation (3.2.7) can be written as,

$$\nabla^2[\nabla^2 + i\beta^2]\,\phi^* = 0 \tag{3.2.8}$$

Then $\phi^* = \phi_1^* + \phi_2^*$ where

$$\nabla^2\phi_1^* = 0 \tag{3.2.9}$$

and $$(\nabla^2 + i\beta^2)\,\phi_2^* = 0 \tag{3.2.10}$$

The solution we seek should satisfy the axisymmetry of the problem, that is, the solution is independent of θ.

Solution to (3.2.9) is $\phi_1^* = (B + iC)\log_e r$ (3.2.11)

and to (3.2.10) is $\phi_2^* = (A_1 + iA_2)\,H_o^1(\beta r\sqrt{i})$ (3.2.12)

As the real part of ϕ^* should tend to zero as r tends to infinity, B should be zero.

∴ The required solution is,

$$\phi^* = iC\log_e r + (A_1 + iA_2)\,H_o^1(\beta r\sqrt{i}) \tag{3.2.13}$$

where C, A_1 and A_2 are constants to be determined from the boundary conditions.

(Any additional constants that occur are discarded as they do not contribute to the stresses.)

Applicability of the theory is discussed in Appendix XII.

3.3 Formulation of the boundary conditions:

Here also we assume that the bending rigidity of the reinforcement in the local tangential plane of the shell is negligible and that the hole is covered by a diaphragm which transmits the pressure force to the shell as a uniform shear distributed around the hole edge but allows the hole edge to rotate and deflect freely.

Equilibrium equations:

Figure 32 shows the reinforcement forces and moments and shell forces and moments per unit length.

The equations of equilibrium are given below for the general case of eccentrically attached reinforcement. Symmetric reinforcement case can be dealt with, by putting h = b = 0.

$$N_{rr} = \frac{T}{a} \qquad (3.3.1)$$

$$M_{rr} = \frac{M}{a} - N_{rr}.h + \frac{pa}{2} \cdot b \qquad (3.3.2)$$

$$Q_r = -\frac{pa}{2} + \frac{T}{R} \qquad (3.3.3)$$

The component of tension in the reinforcement in (3.3.3) is obtained as follows.

Consider an elemental length 'ds' of the reinforcement (figure 31). The required component per unit length is

$$T \cdot \sin\psi \cdot \frac{d\theta}{ds} .$$

Using the relations $ds = ad\theta$ and $\sin\psi = a/R$, the contribution of the bead tension to normal equilibrium becomes,

$$T/R.$$

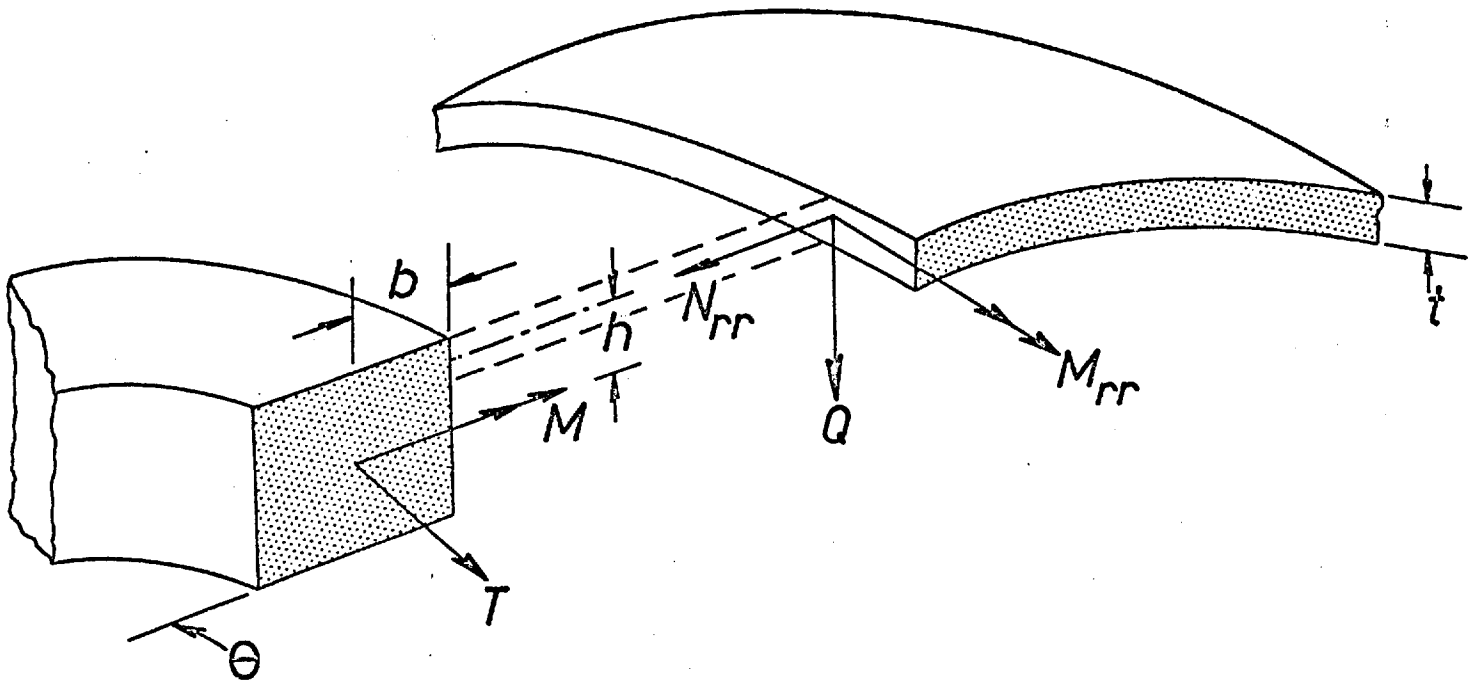

FIG. 32

Compatibility conditions:

The tangential strains of the reinforcing bead and the sheet at the junction should be equal

$$\frac{T}{AE_R} = \frac{1}{E_S t}(N_{\theta\theta} - \nu N_{rr}) - \frac{Mh}{E_R I} \tag{3.3.4}$$

Also the normal deflections and slopes for the reinforcement and the middle plane of the sheet should be the same at r = 1.

$$M = -\frac{E_R I}{a^2}\left(\frac{dw'}{dr}\right) \tag{3.3.5}$$

(For details see Appendix III.)

For the stress resultants and couples in the shell, the usual flat plate relations hold. All the moments, forces and Kirchoff shear can now be eliminated in terms of F' and w'. After non-dimensionalising the following equations result.

$$F_{,r} = \frac{E_R}{E_S}\cdot\frac{A}{at}\cdot[F_{,rr} - \nu F_{,r}] + \frac{E_R}{E_S}\cdot\frac{A}{at}\cdot\frac{h}{t}[12(1-\nu^2)]^{1/2} w_{,r} \tag{3.3.6}$$

$$w_{,rr} + \nu w_{,r} - 12(1-\nu^2)\cdot\frac{E_R}{E_S}\cdot\frac{1}{at^3} w_{,r} - (w_{,rrr} + w_{,rr} - w_{,r})\frac{b}{a}$$

$$- \frac{h}{t}[12(1-\nu^2)]^{1/2} F_{,r} = -\frac{b}{a}\cdot\beta^2 \tag{3.3.7}$$

$$w_{,rrr} + w_{,rr} - w_{,r} + \beta^2\cdot\frac{E_R}{E_S}\cdot\frac{A}{at}\cdot(F_{,rr} - \nu F_{,r})$$

$$+ \beta^2\cdot\frac{E_R}{E_S}\cdot\frac{A}{at}\cdot\frac{h}{t}[12(1-\nu^2)]^{1/2} w_{,r} = \beta^2 \tag{3.3.8}$$

3.4 Typical examples and discussion:

Expression (3.2.13) is used in equations (3.3.6), (3.3.7) and (3.3.8) to solve for the three unknowns C, A_1 and A_2.

Firstly, the problem of an unreinforced circular hole in a spherical shell is solved for $\beta^2 = 3.8$, in order to compare with experimental results obtained by Houghton and Rothwell (9). Theoretical solutions were obtained by Penny (48) for this problem. The experiments were conducted on a hemispherical aluminium alloy shell of 16" diameter, containing a 3" diameter hole and subjected to an internal pressure of 18 psi. Measurements were made using resistance strain gauges.

It can be seen from figures 33 and 34 that there is good agreement between the present theory and experiment as far as the radial and tangential direct stresses are concerned. Also it is seen that the radial bending stresses as predicted by the present method are closer to the experimental values than those given by Penny. In the theory proposed by Penny, the tangential bending moment at the edge of the hole is assumed to be zero whereas in reality it is not.

As the value of β increases, it is found that the tangential direct stresses increase as shown in figure 35. The formula for the tangential direct stress for large β given in (9)

$\frac{\sigma_{\theta\theta}}{\sigma_\infty} = 1.2 + 2.58\sqrt{\frac{a^2}{Rt}}$ seems to give very good estimates. The tangential bending stresses appear to have reached a peak value for the maximum value of β considered. This trend is similar to that found in the case of a cylinder with a circular hole subjected to tension. But the bending stresses are much smaller as compared to the case of a circular hole in a cylindrical shell. At $\beta = 6$ the bending stress is about 16% of the direct tangential stress.

In the case of symmetric reinforcement it can be seen that equations (3.3.6), (3.3.7) and (3.3.8) become homogeneous if $\frac{E_R}{E_S} = 1$; $\frac{A}{at} = 1.5$; thus making $\phi^* \equiv 0$. This implies that a reinforcement for which $\frac{E_R}{E_S} = 1$; $\frac{A}{at} = 1.5$; gives a neutral hole in a spherical

shell under pressure. The shell principal stresses for various values of $\frac{A}{at}$, have been plotted for two values of β in figure 36. As $\frac{A}{at}$ = 1.5 gives a neutral hole all such curves meet at $\frac{\sigma_{\theta\theta}}{\sigma_\infty} = 1.0$; $\frac{A}{at} = 1.5$. Mansfield (17) suggests that the stress concentration factor can be put in the form,

$$\frac{\sigma_P}{\sigma_\infty} \simeq 1 + 0.4 \left| \frac{A^*}{A} - 1 \right| \qquad (3.4.1)$$

where A* is the area required for a neutral hole.

This can be put in the form

$$\frac{\sigma_P}{\sigma_\infty} \simeq 1 + 0.4 \left| \frac{A^*/at}{A/at} - 1 \right|$$

$$\simeq 1 + 0.4 \left| \frac{1.5}{\lambda} - 1 \right| \qquad (3.4.2)$$

as the area required for the neutral hole is given by A*/at = 1.5. It can be seen from figure (36), that (3.4.2) gives lower values for the stress concentration factor and also the dependence on curvature is not predicted by this formula.

It was also observed that the parameter $\frac{I}{at^3}$ has no significant effect on the shell stresses. This can be expected to be so as the bending stresses are small compared to the membrane stresses.

Figures 37 and 38 illustrate the variation of maximum principal stress with respect to the position of bead relative to the sheet. It is seen that eccentricity always causes an increase in stresses. Thus it can be concluded that symmetric reinforcements are best for spherical shells under pressure with circular cut-outs. This result differs from (49) as the optimisation is carried out here taking into account the radial and tangential, direct and bending stresses.

Mansfield's 'Efficiency Factor':

As mentioned in (1.6), for reinforcements around holes which are neutral or nearly so, Mansfield has suggested that an eccentric reinforcement may be replaced by a symmetric reinforcement, whose cross-sectional area is reduced by a factor which turns out to be a 1/4 for a rectangular cross-section. Choosing $\beta = 4$, $\lambda = 1.5$, from figure 37, one finds that the stresses are almost the same when $\frac{h}{t} = \pm 6$, and equal to 2.6. The equivalent Mansfield's symmetric reinforcement has $\lambda = \frac{1.5}{4} = 0.375$. From figure 36, it is seen that the stress at $\lambda = 0.375$, for $\beta = 4$, is 2.6. Such good agreement should be expected as all the conditions used by Mansfield are satisfied in this example.

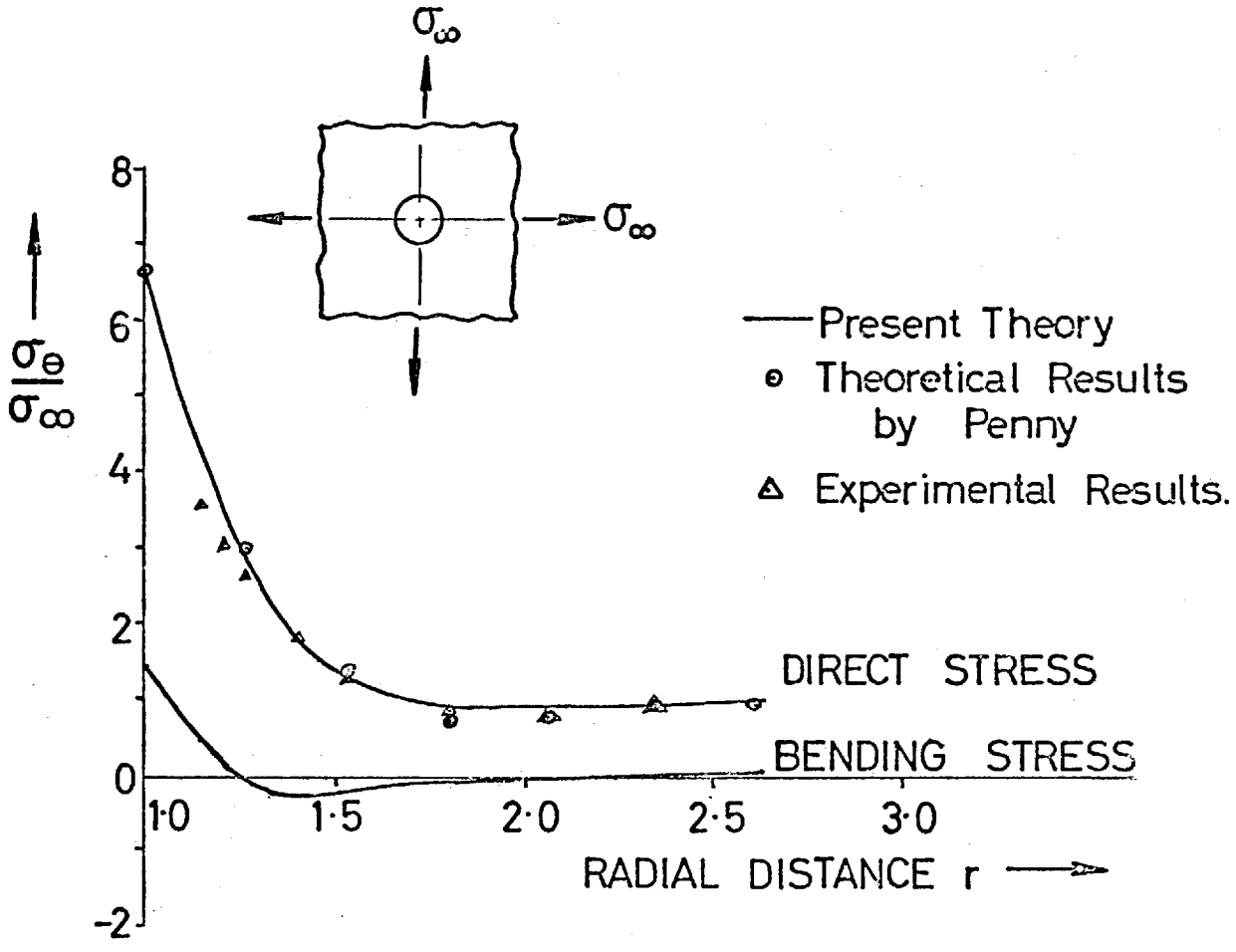

FIG.33 TANGENTIAL STRESSES AT HOLE EDGE (SPHERICAL SHELL PRESSURE)

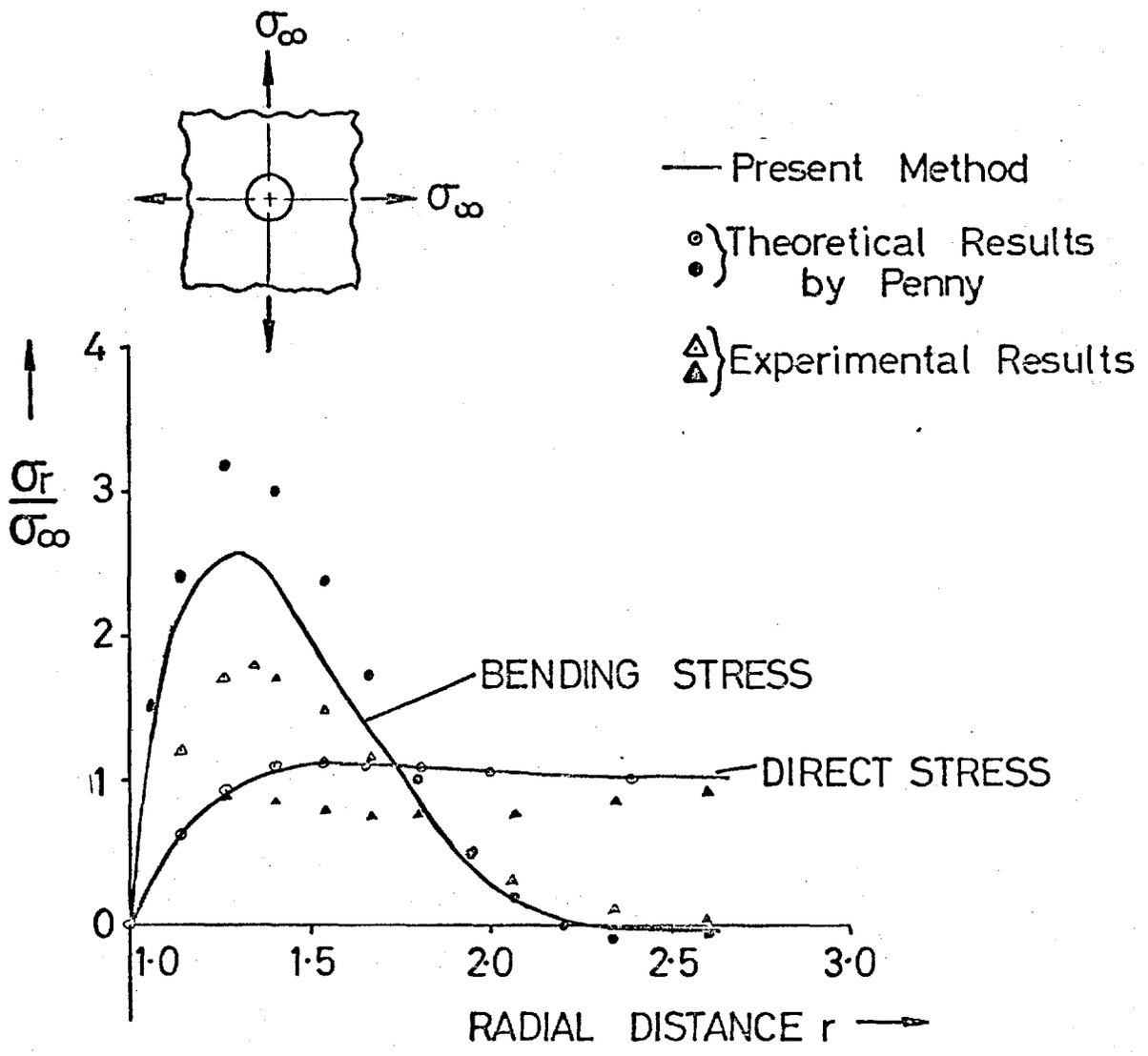

FIG. 34 RADIAL STRESSES AT HOLE EDGE (SPHERICAL SHELL - PRESSURE).

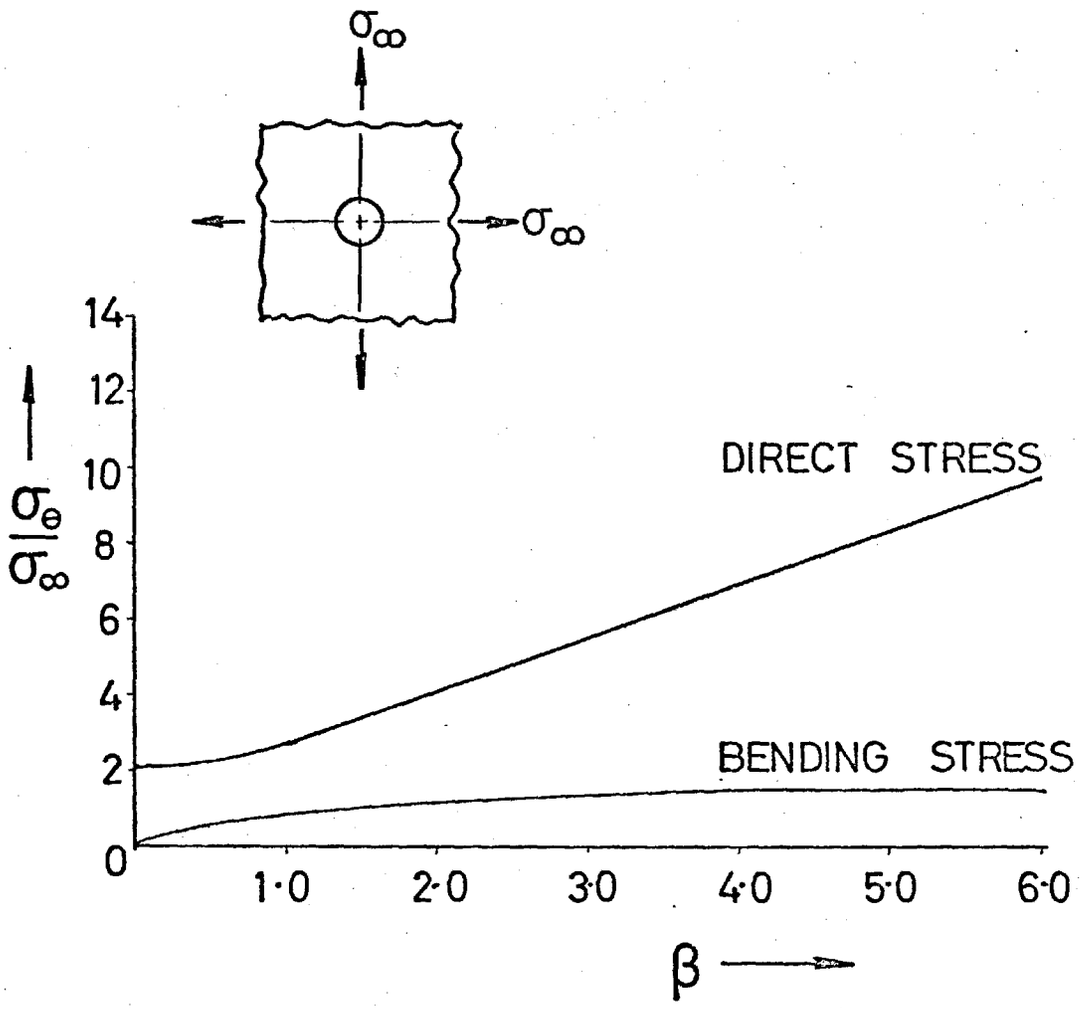

FIG. 35 TANGENTIAL STRESSES AT HOLE EDGE (SPHERICAL SHELL PRESSURE).

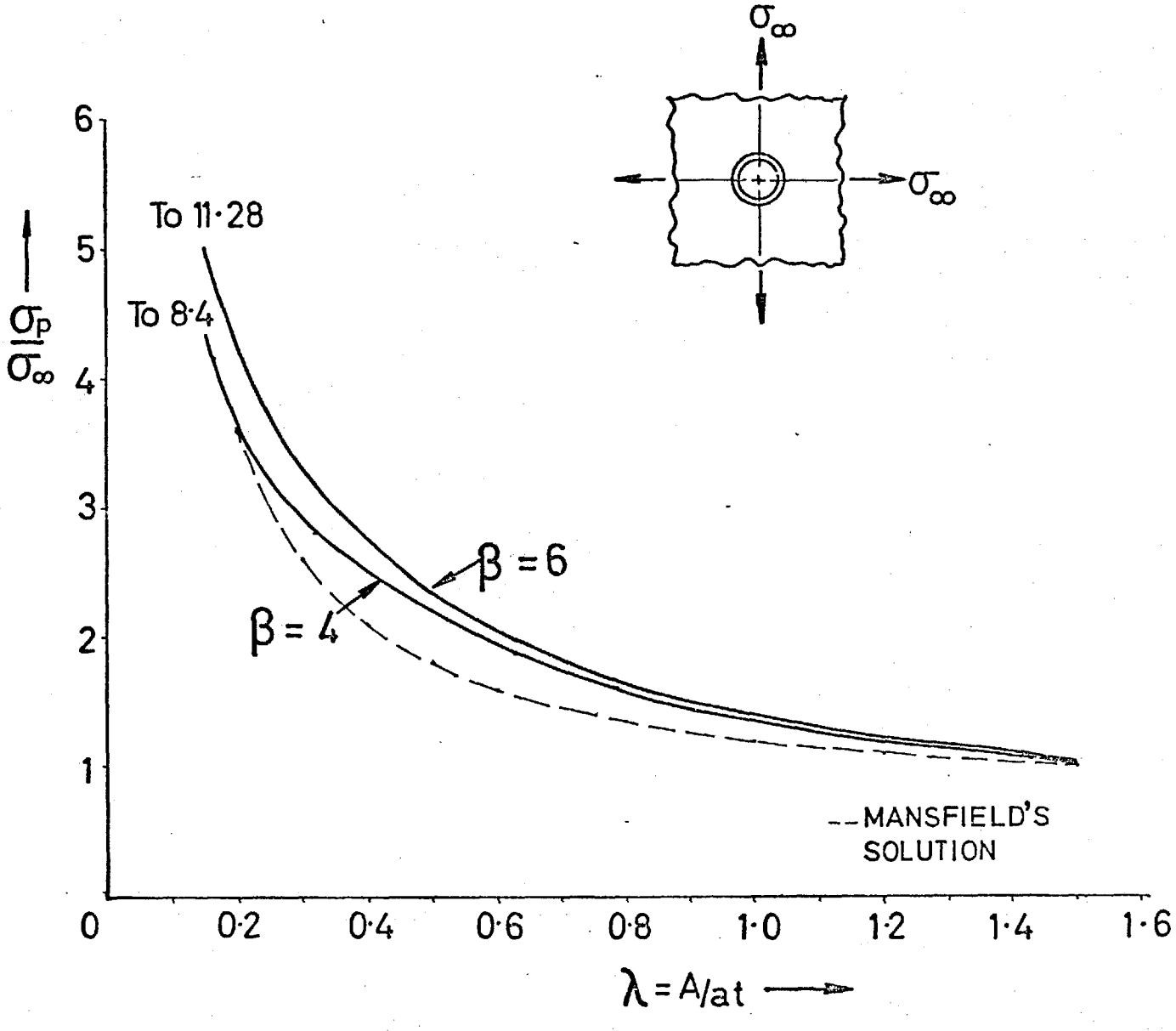

FIG. 36 VARIATION OF SHELL STRESSES WITH REINFORCEMENT.
(SPHERICAL SHELL–PRESSURE)

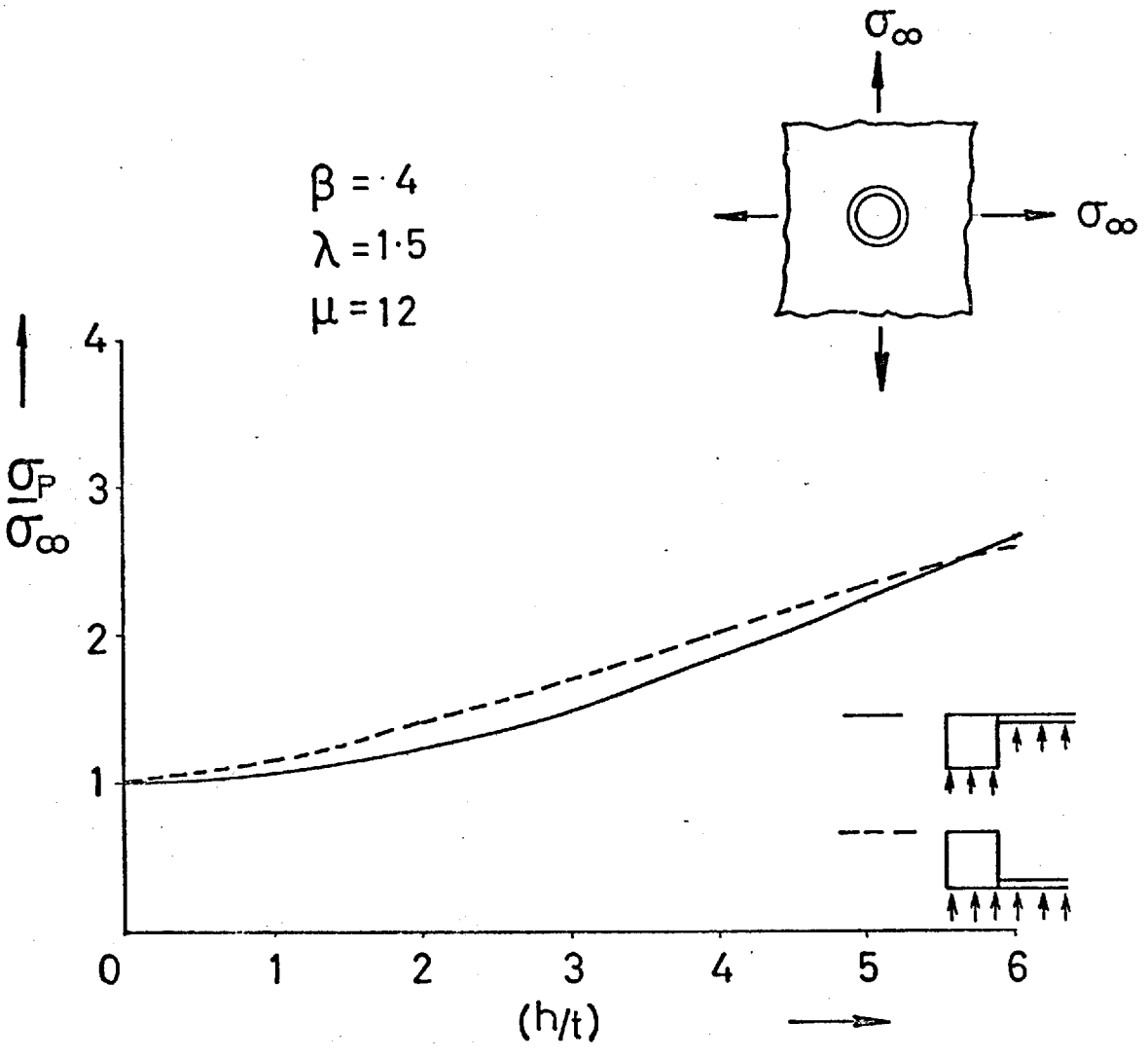

FIG. 37 INFLUENCE OF ECCENTRICITY OF REINFORCEMENT ON SHELL STRESSES (SPHERICAL SHELL-PRESSURE).

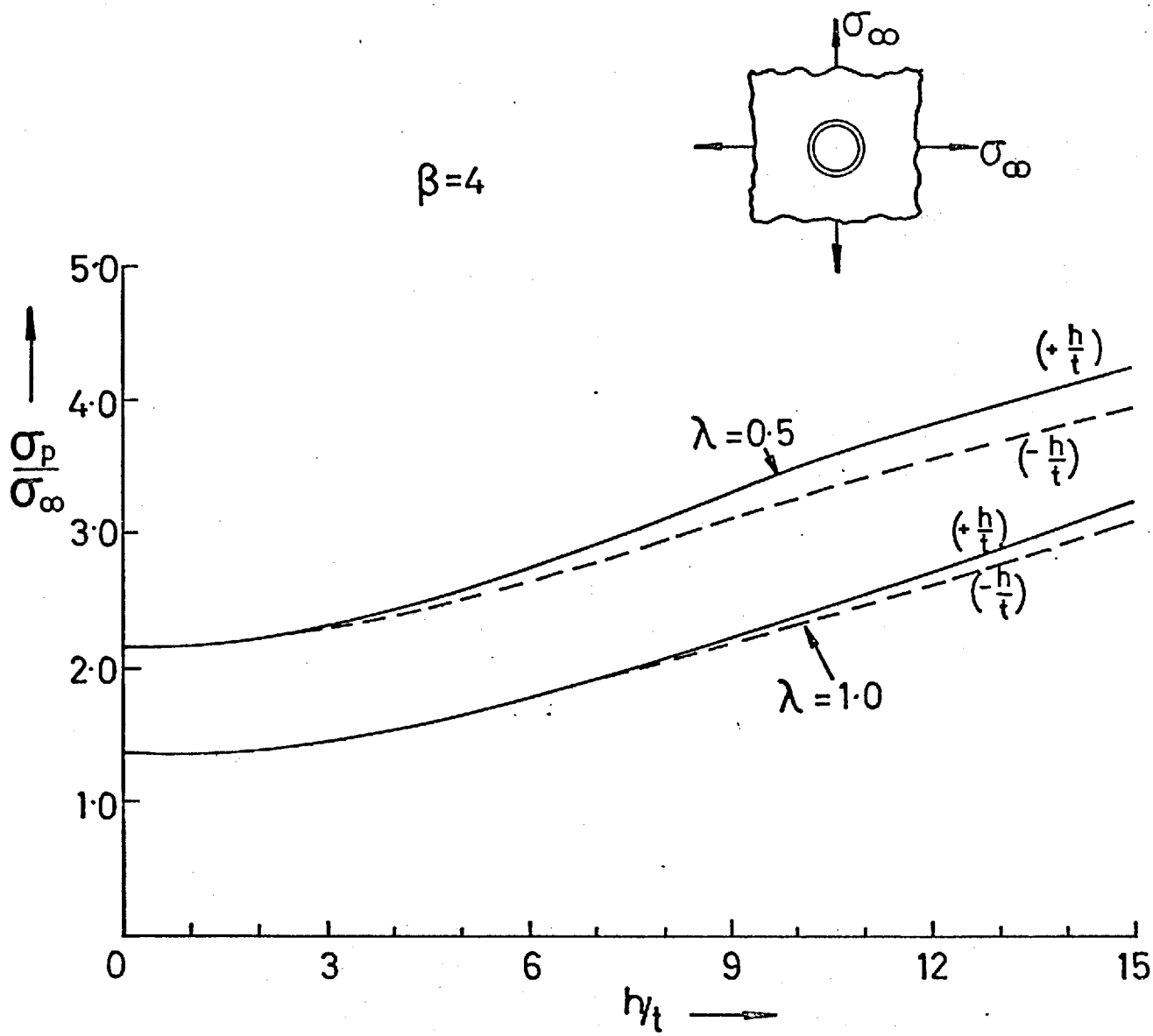

FIG. 38 INFLUENCE OF ECCENTRICITY OF REINFORCEMENT ON SHELL STRESSES. (SPHERICAL SHELL -PRESSURE)

DISCUSSION AND CONCLUSIONS

In many methods of analysis of problems concerned with reinforced or unreinforced holes in shell structures, the curvature effect is assumed to be negligible. The curvature has a very significant influence on the distribution of stresses in the shell even for the reinforced holes as shown in this thesis. In the case of torsion, the bending stresses are as important as the membrane stresses. In the case of pressure loading, the bending stresses are dependent on how the pressure load on the cut-out portion of the shell is transmitted to the shell. If it is transmitted as a uniform shear around the hole edge (Case A) the bending stresses tend to he much higher than when the shear varies as given in 'Case B'. Even so flat plate theories are in general inadequate in describing the stress field in the shell.

In the case of a cylinder under pressure with a reinforced circular hole (Case A) it was found that increasing the bending efficiency 'μ' of the reinforcement leads to a reduction in the bending stresses and hence the principal stresses with no weight penalty. It was shown that a reinforcement (λ and μ) can be chosen to give reasonably low stresses round the hole. On the other hand, under the assumption in 'Case B', the principal stresses increase with μ. These two cases represent two limits and the true values may be between them, especially for small values of β. In both cases attaching the reinforcement eccentrically increases the shell stresses.

In the case of reinforced arbitrary shaped holes the analysis presented in this thesis is applicable to any value of 'β'. The approach used by Guz and Savin (42) and (44) is valid for $\beta < 1$. Also in the case of reinforced holes, they do not take into account the component of tension in the bead, in the normal equilibrium equations. This causes an error

especially in bending stresses for large values of β, both for circular and non-circular holes. It has been found that omission of this component of tension in normal equilibrium equations does not give convergent solutions.

It is shown in (42) that for $\beta = 0.32$ and $\varepsilon = 1/9$, for a square hole in a cylinder under tension, the first approximation to the tan-

gential stress (ε terms considered) is 52% greater than the zeroeth approximation and the second (ε^2 terms considered) is 12% greater than the first. In this thesis only 'ε' order terms are considered and it is felt that the accuracy attained is sufficient for engineering purposes. For $\sqrt{2}\beta = 4$, in the case of an elliptical hole ($\frac{a}{b} = 1.4$) it was found that Wittrick's optimum bead gives a stress which is about twice that for a flat plate in case A and about 1.7 times in case B.

The analysis of a reinforced circular hole in a spherical shell shows that it is possible to find the reinforcement giving a neutral hole. This has the same area as that required for a flat plate under uniform tension. Eccentrically attaching a reinforcement always increases the shell stresses and should be avoided if possible.

The effect of large β may produce very high stresses (stress concentration factors of the order of 50) in the case of a cylinder with a cut-out and so even for low mean stresses (as are necessary to increase fatigue life) there will be yielding in a very small region. The influence of this on the history of likely crack propagation is quite unpredictable since the highly stressed yielded region will probably be very much smaller than the critical crack length.

Future work:

The theoretical analysis used for arbitrary shaped holes can be extended to other loading cases as well as to other shapes than those considered in Chapter II. Triangular holes with rounded corners (Caravelle windows) or square holes with rounded corners of given radius can be investigated. For the latter, transformation functions as given by Wittrick (38) in the form,

$$Z = \zeta - p\zeta^{-3} + q\,\zeta^{-7}$$

can be made use of. The analysis for torsion loading will be particularly useful as it is easy to conduct experiments for such a loading

in a laboratory. Also the influence of eccentric reinforcements for holes of arbitrary shape on shell stresses can be studied.

In the case of spherical sheils, under pressure loading, the problem of arbitrary shaped reinforced holes can be solved in a manner very similar to that given in Chapter II.

It is not always that one comes across compact bead type reinforcements and one may be compelled to treat the reinforcement as a plate, to be more realistic. The analysis given in this thesis can be suitably modified for a plate type reinforcement. The next step will be to extend the method to load carrying windows.

Not much experimental work has been done on reinforced holes in shells. Experiments can be conducted to check the theoretical values for the shell stresses in the case of a reinforced circular hole in a cylindrical shell under pressure loading. The main effect of a hole in a cylindrical shell is the occurrence of bending stresses and this is very much dependent on the fact whether the pressure on the cut-out portion is reacted by the shell or externally. In reality the shell reacts the pressure on the cut-out portion and the results are close to true values only when this is simulated in the experiment.

Experiments on unreinforced elliptical and square holes in cylindrical shells under torsion or pressure loadings will give an idea on the accuracy of the solution to the order of 'ε' as obtained in this thesis. In the case of tension loading the bending stresses are low when compared with membrane stresses and hence would not give an insight into the influence of curvature.

Next step will be to undertake tests on reinforced elliptical holes and square holes with rounded corners in cylindrical shells.

REFERENCES

1. Mansfield, E.M. — Neutral holes in plane sheet: Reinforced holes which are elastically equivalent to the uncut sheet. A.R.C. Technical Report. R&M No.2815, 1955.

2. Gurney, C. — An analysis of the stress in a flat plate with a reinforced circular hole under edge forces. R&M No. 1834, 1938.

3. LURIE, A.I. — Statics of thin walled elastic shells. State publishing house of technical and theoretical literature (1947). Translation AEC-tr-3798, p. 147-200, 1959.

4. Vandyke, P. — Stresses about a circular hole in a cylindrical shell. A.I.A.A. 2nd Aerospace Sciences Meeting, Paper No. 65-140, 1965.

5. Lekkerkerker, J.G. — Stress concentration around circular holes in cylindrical shells. Report presented at the Eleventh International Congress of Applied Mechanics, Munich (1964).

6. Dixon, R.C. Eringen, A.C. Jordan, N.F. and others. — Reports on stresses and stress concentrations in a circular cylindrical shell with a circular cut-out. General Technology Corporation, Technical Reports No. 3-1, 3-2, 3-3, and 3-4. (Aug. 1961 to June 1963).

7. Shevliakov, I.A.
Zigel, F.S.
The torsion of an empty cylinder with a hole in its side surface.
Dopovidi An. U.R.S.R. No.1, 41-44 (1954).

8. Withum, D.
The cylindrical shell with a circular hole under torsion.
Ingr-Arch 26, 435-446 (1956).

9. Houghton, D.S.
and
Rothwell, A.
The effect of curvature on the stress concentration around holes in shells.
College of Aeronautics Report No. 156, May, 1962.

10. Jessop, J.T.
Snell, C.
and
Allison, I.M.
The stress concentration factors in cylindrical tubes with transverse circular holes.
Aero Quarterly 10, 326-344, 1959.

11. Richards, T.H.
Stress distribution in pressurised cabins; An experimental study by means of Xylonite models.
A.R.C. 19, 360. Strut. 1999, 1957.

12. August J. Durelli,
Carlos J. del Rio,
Vincent J. Parks,
Henry Feng.
Stresses in a pressurised cylinder with a hole.
Proceeding of the American Society of Civil Engineers, Vol. 93, No. ST5, 1967,pp.383-399.

13. Savin, G.N.
Stress distribution in a thin shell weakened by a hole.
Problems of the mechanics of a continuous medium, Collection dedicated to the Seventeenth Anniversary of N.I. Muskhelishvili, IZD-VO AN SSSR, 1961.

14. Surendra, K. Dhir — Stresses around two equal reinforced circular openings in a thin plate. International Journal of Solids and Structures, Vol. 4, pp. 1093-1106, Number 11, November 1968.

15. Durelli, A.J. Park, V.J. and Hon-Chow Lee — Stresses in a perforated ribbed cylindrical shell subjected to internal pressure. International Journal of Solids and Structures, Vol. 5, pp. 573-586, June 1969.

16. Williams, D. — Pressure Cabin Design. A.R.C. CP No. 226, 1955.

17. Mansfield, E.H. — Stress considerations in the design of pressurised shells. A.R.C. CP No. 217, 1955.

18. Argyris, J.H. and Sharpf, D.W. — The SHEBA family of shell elements for the matrix displacement method. The Aeronautical Journal, October 1968.

19. Argyris, J.H. and Sharpf, D.W. — Some general considerations on the natural mode technique. (Small displacements) The Aeronautical Journal, March 1969.

20. Rothwell, A. — Private Communication 1967.

21. Timoshenko, S. — Strength of Materials, Part II. Macmillan & Co., Ltd., London (1931).

22. Reissner, H. and Morduchow, M. — Reinforced circular cut-outs in plane sheets. NACA Technical Note No. 1852, April 1949.

23. Mansfield, E.H. — Neutral holes in plane sheets. Quarterly Journal of Mechanics and Applied Mathematics, Vol. 6, p. 370, 1953.

24. Mansfield, E.H. — On the design of a row of windows in a pressurised cylindrical fuselage. R&M 336ⁿ - (1964)

25. Mansfield, E.H. — Optimum designs for reinforced circular holes. A.R.C. CP No. 239, 1956.

26. Donnell, L.H. — Stability of thin walled tubes under torsion. NACA Report No. 479.

27. Davies, G.A.O. — Plate reinforced holes. Aeronautical Quarterly, Vol. XVIII, p. 43, Feb. 1967.

28. Marguerre, K. — Zur Theorie der gekrümmten Platte grosser Formänderung. Proceedings of the Fifth International Congress of Applied Mechanics, 93-99 (1938).

29. Wittrick, W.H. — On the axisymmetrical stress concentration at an eccentrically reinforced circular hole. Aeronautical Quarterly, Vol. XVI, Feb. 1965.

30. The Royal Aeronautical Society — Structures data sheets, Volume IV. 06. 00. 07 Series.

31. The Royal Aeronautical Society — Structural principles and data. Published by Sir Isaac Pitman & Sons Ltd. (1952).

32. Wittrick, W.H. — Stresses around reinforced elliptical holes with application to pressure cabin windows. Aeronautical Quarterly, Vol. X, p. 373, November 1959.

33. Inglis, C.E. — Stresses in a plate due to the presence of cracks and sharp corners. Transactions of the Institution of Naval Architects, pp. 219, Vol. 55, 1913.

34. Hicks, R. — Reinforced elliptical holes in stressed plates. Journal of the Royal Aeronautical Society, Vol. 61, p. 688, October 1957.

35. Wells, A.A. — On the plane stress distribution in an infinite plate with a rim-stiffened elliptical opening. Quarterly Journal of Mechanics and Applied Mathematics, Vol. 3, p. 23, 1950.

36. Muskhelishvili, N.I. — Some basic problems of the mathematical theory of elasticity. Noordhoff, Groningen, Holland, 1953.

37. Wittrick, W.H. — Analysis of stress concentrations at the reinforced holes in infinite sheets. Aeronautical Quarterly, Vol. 11, Aug. 1960.

38. Wittrick, W.H. — Some simple transformation functions for square and triangular holes with rounded corners. Aeronautical Quarterly, Vol. 11, pp. 195-199, May 1960.

39. Sobey, A.J. — The estimation of stresses around unreinforced holes in infinite elastic sheets. R&M 3354 (1964).

40. Houghton, D.S. and Rothwell, A. — Stresses around some unreinforced cut-outs under various loading conditions. College of Aeronautics Report No. 146.

41. Houghton, D.S. and Rothwell, A. — The analysis of reinforced circular and elliptical cut-outs under various loading conditions. College of Aeronautics Report No. 151.

42. Guz, A.N. and Savin, G.N. — On the state of stress near curvilinear holes in shells. NASA Technical Translation TT F-423 (1966)

43. Savin, G.N. — Concentration of stresses around curvilinear holes in plates and shells. Proceedings of the 11th International Congress of Applied Mechanics, Munich, 1964.

44. Guz, A.N. and Savin, G.N. — The stress state near curvilinear reinforced orifices in shells. NASA Technical Translation TT F-424 (1966).

45. Murthy, M.V.V. — Stresses around an elliptical hole in a cylindrical shell. Journal of Applied Mechanics, March 1969, p.39.

46. Murthy, M.V.V. — Stresses around an elliptic hole in a cylindrical shell. National Aeronautical Laboratory, TN-3, 1967.

47. Reissner, E. — Stresses and small displacements of shallow spherical shells. Journal of Mathematical Physics. 25, p. 80-85, (1946); 27, p. 240 (1948).

48. Penny, R.K. — Stress concentrations at unreinforced holes in pressurised spherical shells. Referred to in College of Aeronautics Report, Cranfield, No.156.

49. Greszczuk, L.B. — Effect of reinforcement geometry on the stresses in spherical shells. SAE 578C.

50. Reissner, E. On the determination of stresses and displacements for unsymmetrical deformations of shallow spherical shells. Journal of Mathematical Physics, 38, pp.16-35, (1959).

51. Shin-Ichi-Suzuki Stress measurements in a plate containing a reinforced circular hole using a photoelastic method. International Journal of Mechanical Sciences, Vol. 6, pp. 473-477, 1964.

SUPPLEMENTARY REFERENCES

Watson, G.N.	A treatise on the theory of Bessel functions. Cambridge University Press, 1922.
Bickley, W.G.	Bessel Functions, Parts I and II.
Comrie, L.J. and others.	British Association for the Advancement of Science, Mathematical Tables Vol. X and XI. Cambridge University Press.
U.S. Works Progress Administration.	1. Tables of Bessel's functions $J_o(Z)$ and $J_1(Z)$ for complex arguments.
National Bureau of Standards.	2. Tables of Bessel's functions $Y_o(Z)$ and $Y_1(Z)$ for complex arguments.
Timoshenko, S. and Goodier, J.N.	Theory of Elasticity. McGraw-Hill Book Company (1951).
Timoshenko, S.	Theory of plates and shells. McGraw-Hill Book Company.
Prescott, J.	Applied Elasticity. Longmans, Green & Co. (1924).
Philip M. Morse and Herman Feshbach	Methods of Mathematical Physics. Parts I and II. McGraw-Hill Book Company 1953.
Novozhilov	The Theory of thin shells. Published by P. Noordhoff Ltd. The Netherlands (1959).
Wilhem Flügge	Stresses in Shells. Spring-Verlag Berlin, Göttingen, Heidelberg (1960).

Green, A.E. and Zerna, W. — Theoretical Elasticity. Second Edition (1968).

Love, A.E.H. — A treatise on Mathematical Theory of Elasticity. Cambridge University Press, 1906.

Harry Kraus — Thin elastic shells. John Wiley & Son, Inc., New York, London, 1967.

APPENDIX I

Effect of increasing sheet thickness in a fuselage shell:

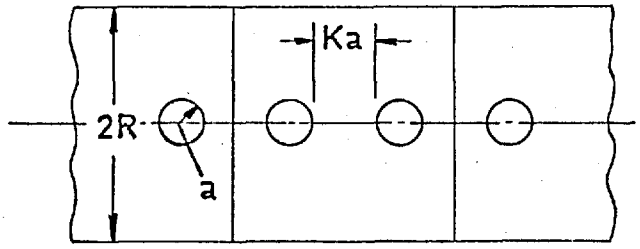

Let radius of window: a

distance between windows: ka $(k \sim 0(1))$

area of edge reinforcement: A

shell sheet thickness: t.

Total volume of structure for each frame bay = V

$$V = 4\pi Aa + 2\pi Rt(k+2)a - 2\pi a^2 t$$

$$V \simeq 4\pi a[A + (1 + k/2)Rt]$$

$(\because \frac{a}{R} << 2 + k \quad \text{as} \quad \frac{a}{R} \simeq (\frac{1}{5}))$

Considering

$$V = 4\pi a(1 + k/2)\, Rt \left\{ \frac{A}{(1 + k/2)\, Rt} + 1 \right\}$$

Let us consider the order of magnitude of

$$\frac{A}{(1 + k/2)Rt} = \frac{1}{(1 + k/2)} \frac{a}{R} \frac{A}{at} .$$

Practical limitations give, $0.1 \leqslant A/at \leqslant 2$

$$\text{If } \frac{A}{at} = 0.1; \quad \frac{A}{(1 + k/2)Rt} \simeq \frac{2}{3} \cdot \frac{1}{5} (0.1) \simeq 0.014$$

$$\text{If } \frac{A}{at} = 2, \quad \frac{A}{(1 + k/2)Rt} \simeq \frac{2}{3} \cdot \frac{1}{5} \cdot 2 \simeq 0.27$$

$\therefore$ Effect of increasing sheet thickness on structural weight is at least 4 to 10 times more drastic than increasing 'A'.

APPENDIX II

Shallow cylindrical shell equations:

With the system of axes chosen in figure 1.

Equations of equilibrium are,

$$\frac{\partial N_x}{\partial x} + \frac{\partial N_{xy}}{\partial y} = 0 \tag{1}$$

$$\frac{\partial N_{xy}}{\partial x} + \frac{\partial N_y}{\partial y} = 0 \tag{2}$$

$$\frac{\partial Q_x}{\partial x} + \frac{\partial Q_y}{\partial y} + \frac{\partial}{\partial x}\left[\frac{\partial z}{\partial x} N_x + \frac{\partial z}{\partial y} N_{xy}\right] + \frac{\partial}{\partial y}\left[\frac{\partial z}{\partial x} N_{xy} + \frac{\partial z}{\partial y} N_y\right] = -p \tag{3}$$

$$\frac{\partial M_x}{\partial x} + \frac{\partial M_{xy}}{\partial y} - Q_x = 0 \tag{4}$$

$$\frac{\partial M_{xy}}{\partial x} + \frac{\partial M_y}{\partial y} - Q_y = 0 \tag{5}$$

Substituting (4) and (5) in (3) and using (1) and (2),

$$\frac{\partial^2 M_x}{\partial x^2} + 2\frac{\partial^2 M_{xy}}{\partial x \partial y} + \frac{\partial^2 M_y}{\partial y^2} + \frac{\partial^2 z}{\partial x^2} N_x + 2\frac{\partial^2 z}{\partial x \partial y} N_{xy} + \frac{\partial^2 z}{\partial y^2} N_y = -p \tag{6}$$

Stress strain relations are,

$$\frac{N_x}{t} = \frac{E_s}{(1-\nu^2)} (\varepsilon_{xx} + \nu\varepsilon_{yy}) \tag{7}$$

$$\frac{N_y}{t} = \frac{E_s}{(1-\nu^2)} (\varepsilon_{yy} + \nu\varepsilon_{xx}) \tag{8}$$

$$\frac{N_{xy}}{t} = \frac{E_s}{2(1+\nu)} \varepsilon_{xy} \tag{9}$$

$$M_x = -D\left(\frac{\partial^2 w'}{\partial x^2} + \nu \frac{\partial^2 w'}{\partial y^2}\right) \tag{10}$$

$$M_y = -D\left(\frac{\partial^2 w'}{\partial y^2} + \nu \frac{\partial^2 w'}{\partial x^2}\right) \tag{11}$$

$$M_{xy} = -D\,(1-\nu)\,\frac{\partial^2 w'}{\partial x \partial y} \tag{12}$$

Using the above equations (10), (11) and (12) in (6) and observing that for a circular cylinder

$$\frac{\partial z}{\partial x} = \frac{\partial^2 z}{\partial x^2} = 0 \quad \text{and} \quad \frac{\partial^2 z}{\partial y^2} = -\frac{1}{R},$$

$$\nabla^4 w' + \frac{N_y}{RD} = \frac{p}{D} \tag{13}$$

Strain displacement relationships are (Donnell's approximation)

$$\varepsilon_{xx} = \frac{\partial u}{\partial x}$$

$$\varepsilon_{yy} = \frac{\partial v}{\partial y} + \frac{w'}{R}$$

$$\varepsilon_{xy} = \frac{\partial u}{\partial y} + \frac{\partial v}{\partial x} \tag{14}$$

$$-\frac{\partial^2 \varepsilon_{xy}}{\partial x \partial y} + \frac{\partial^2 \varepsilon_{xx}}{\partial y^2} + \frac{\partial^2 \varepsilon_{yy}}{\partial x^2} - \frac{1}{R} \cdot \frac{\partial^2 w'}{\partial x^2} = 0 \tag{15}$$

Using (7), (8) and (9) in (15),

$$\nabla^4 F' - \frac{E_s t}{R}\,\frac{\partial^2 w'}{\partial x^2} = 0 \tag{16}$$

APPENDIX III

Moment in a reinforcing bead due to a rotation:

The rotations of the sheet and the reinforcing bead are assumed to be the same at r = 1.

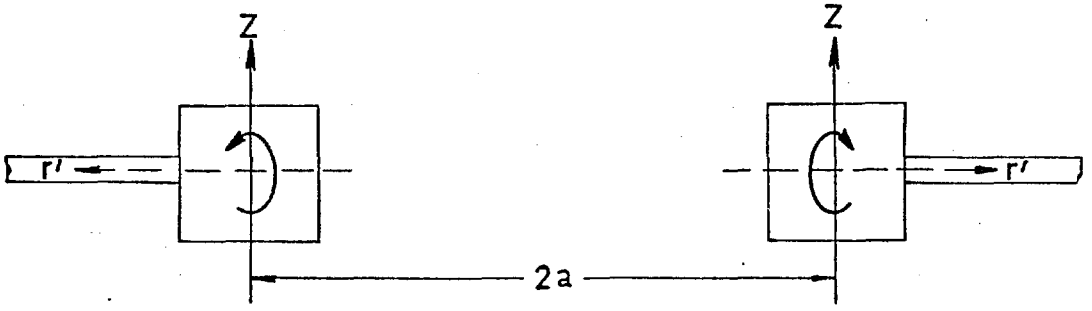

The radial displacement of a point (r',z) in the bead cross-section for a rotation as shown is,

$$-Z.w'_{,r'}$$

The corresponding vertical displacement is $(r'-a)\cdot w'_{,r'}$.

The stress at the point is

$$-E_R \frac{Z.w'_{,r'}}{a}$$

∴ The resultant moment due to this rotation is

$$= \iint_{\text{Area}} (-E_R \cdot \frac{Z}{a} \cdot w'_{,r'})(Z-[r'-a]w'_{,r'})\, dA$$

where 'dA' represents an elemental area of bead cross-section.

Noting that '$w'_{,r'}$' is independent of 'Z' and retaining only first order terms, the resultant moment becomes

$$= -\frac{E_R.I}{a} \cdot w'_{,r'}$$

As r' = ar,

$$\text{Moment} = -\frac{E_R I}{a^2} \cdot w'_{,r} .$$

APPENDIX IV

Boundary conditions for a reinforced circular hole in a cylindrical shell at r = 1:

$$3F_{,r} + 3F_{,\theta\theta} - \frac{E_R}{E_S} \cdot \frac{A}{at} (3F_{,rr} - F_{,r} - F_{,\theta\theta}) - \frac{E_R}{E_S} \cdot \frac{A}{at} \cdot \frac{h}{t} \sqrt{96}\, (w_{,r} + w_{,\theta\theta}) = 0 \qquad \text{(a)}$$

$$3F_{,\theta} - 3F_{,r\theta} + \frac{E_R}{E_S} \cdot \frac{A}{at} \left(1 - \frac{b}{a}\right)(3F_{,rr\theta} - F_{,r\theta} - F_{,\theta\theta\theta}) + \frac{A}{at} \cdot \frac{E_R}{E_S} \cdot \left(1 - \frac{b}{a}\right) \cdot \frac{h}{t} \sqrt{96}\, (w_{,\theta\theta\theta} + w_{,r\theta}) = 0 \qquad \text{(b)}$$

$$3w_{,rr} + w_{,r} + w_{,\theta\theta} - 32 \frac{E_R}{E_S} \cdot \frac{I}{at^3} (w_{,\theta\theta} + w_{,r}) - \sqrt{96} \cdot \frac{h}{t} (F_{,r} + F_{,\theta\theta}) + 12 \frac{E_R}{E_S} \cdot \frac{J}{at^3} \cdot w_{,r\theta\theta}$$

$$- \frac{b}{a} (3w_{,rrr} + 3w_{,rr} - 3w_{,r} - 8w_{,\theta\theta} + 5w_{,r\theta\theta}) = 0 \qquad \text{(c)}$$

(For tension or torsion)

$$= -12 \cdot \frac{b}{a} \cdot \beta^2 \qquad \text{(For pressure)}$$

$$3w_{,rrr} + 3w_{,rr} - 3w_{,r} + 5w_{,r\theta\theta} - 8w_{,\theta\theta} + 32 \cdot \frac{E_R}{E_S} \cdot \frac{I}{at^3} (w_{,\theta\theta\theta\theta} + w_{,r\theta\theta}) + 12 \cdot \frac{E_R}{E_S} \cdot \frac{J}{at^3} \cdot w_{,r\theta\theta}$$

$$+ 8\beta^2 \cdot \frac{E_R}{E_S} \cdot \frac{A}{at} \cdot \cos^2\theta (3F_{,rr} - F_{,r} - F_{,\theta\theta}) - \frac{h}{t} \cdot \sqrt{96} (F_{,\theta\theta} - F_{,r\theta\theta})$$

$$+ 8\beta^2 \cdot \frac{E_R}{E_S} \cdot \frac{A}{at} \cdot \frac{h}{t} \cdot \sqrt{96} \cdot \cos^2\theta (w_{,r} + w_{,\theta\theta}) = 0 \quad \text{(For tension and torsion)}$$

$$= 12\beta^2 \quad \text{(For pressure)} \qquad \text{(d)}$$

APPENDIX V
Flow Diagram for Computation
Reinforced circular hole in a cylindrical shell

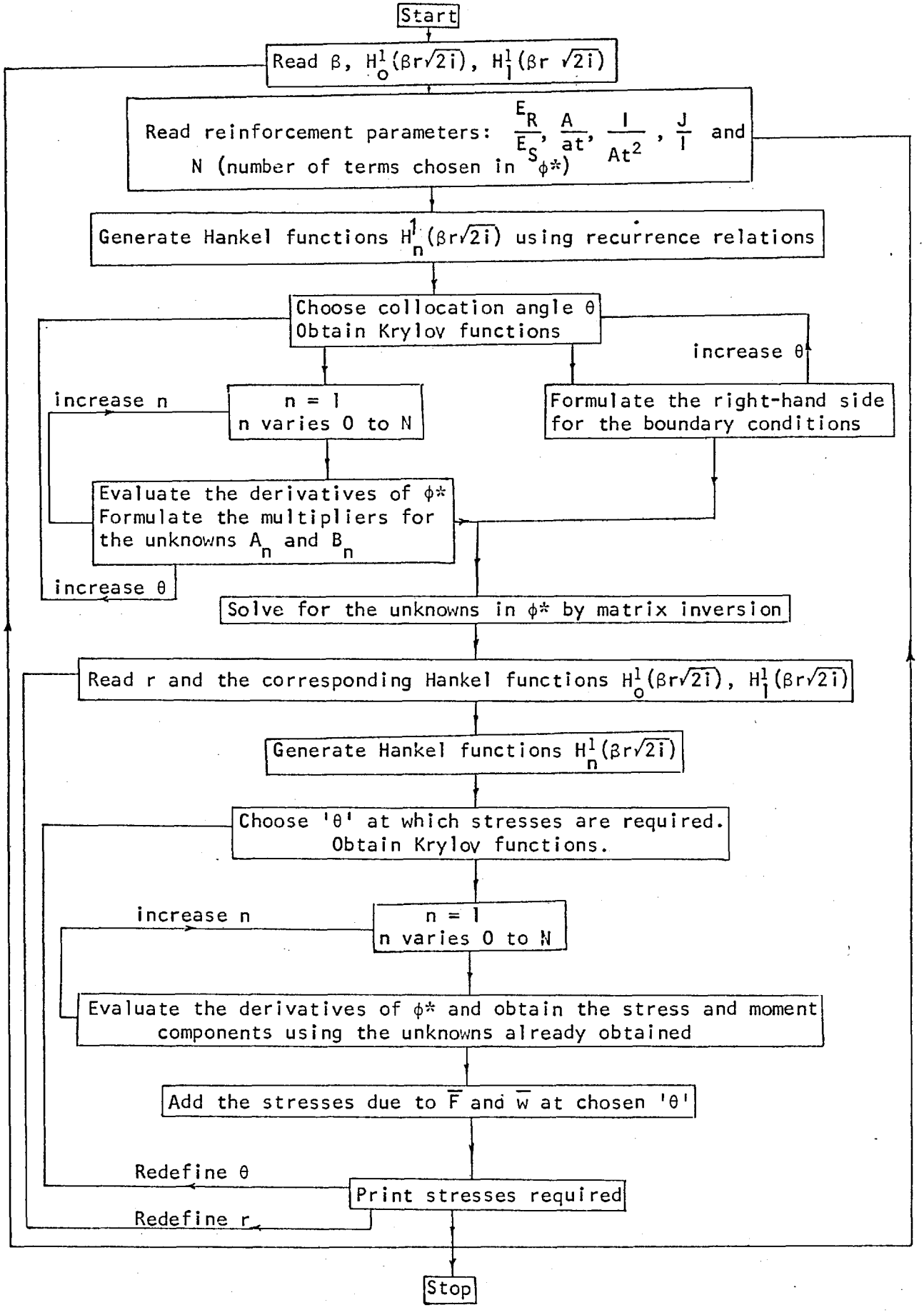

APPENDIX VI

Influence of torsion bending constant Γ

In the case of an open section,

$$H = \frac{E_R J}{2(1+\nu)a^2} \cdot w_{,r\theta} - \frac{E_R \Gamma}{a^4} \cdot w_{,r\theta\theta\theta}$$

In general Γ consists of two parts Γ_1 and Γ_2, where Γ_1 is due to the strain in the middle plane of the walls and Γ_2 is due to the direct strain across the thickness of the wall. For Z-sections, I-sections and channel sections Γ_2 can be neglected and

$$(\Gamma_1)_o = (\Gamma_1)_{s.c} + \xi_o^2 I_x + \eta_o^2 I_y - 2\xi_o \eta_o I_{xy},$$

where 'o' is the point about which the rotation takes place and ξ_o and η_o are the coordinates of 'o' with respect to orthogonal axes at the shear centre (31). I_x, I_y and I_{xy} are the moments of inertia with respect to parallel axes through the centroid.

ξ_o and η_o are of order 'd' and if we neglect the terms of order $(d/a)^2$ in the boundary conditions (which is consistent with the assumptions made so far) then,

$$\frac{(\Gamma_1)_o}{a^3 t^3} \simeq \frac{(\Gamma_1)_{s.c.}}{a^3 t^3}$$

If the open section is an angle-section or a T-section $\Gamma_1 = 0$ and Γ_2 has to be taken into account.

APPENDIX VII

Discussion of method of solution in the case of an arbitrary shaped hole in a cylindrical shell:

SECTION I:

Instead of solving (2.2.1) by separating into the form (2.2.4), the following could have been done.

The coordinate transformation effected is

$$Z = \zeta + \varepsilon f(\zeta) \tag{1}$$

The equation (2.2.1) can be put in the operational form

$$L_1 L_2 \phi^* = 0 \tag{2}$$

where $L_1 = (\nabla_Z^2 - 2(1-i)\beta\frac{\partial}{\partial\xi})$

and $L_2 = (\nabla_Z^2 + 2(1-i)\beta\frac{\partial}{\partial\xi})$ (3)

As the operators are commutative,

$$\phi^* = \phi_a^* + \phi_b^*$$

where $L_1\phi_a^* = 0 \quad ; \quad L_2\phi_b^* = 0$ (4)

Choosing $\phi_a^* = e^{(1-i)\beta\xi}\,\psi_a; \qquad \phi_b^* = e^{-(1-i)\beta\xi}\,\psi_b$ (5)

both ψ_a and ψ_b should satisfy

$$(\nabla_Z^2 + 2i\beta^2)\psi = 0 \tag{6}$$

It is convenient to form Krylov functions as follows,

$$(E_1 - iE_2)_Z = \left[e^{(1-i)\beta\xi} + e^{-(1-i)\beta\xi}\right]/2$$

$$(E_3 - iE_4)_Z = \left[e^{(1-i)\beta\xi} - e^{-(1-i)\beta\xi}\right]\frac{(1+i)}{4} \tag{7}$$

For problems symmetrical in ξ and η, the solution can be written as,

$$\phi^* = (E_1 - iE_2)_Z \psi_{symm} + (E_3 - iE_4)_Z \psi_{antisymm} \tag{8}$$

where ψ_{symm} and $\psi_{antisymm}$ are symmetric and antisymmetric solutions of equation (6).

Equation (6) in (ρ,γ) system of coordinates becomes,

$$[\{1-\varepsilon[f'(\zeta) + \overline{f'(\zeta)}]\}\nabla_\zeta^2 + 2i\beta^2]\psi = 0 \tag{9}$$

Assume $\psi = \psi_o + \varepsilon\psi_1$, and writing equation (9) to the order of ε,

$$(\nabla_\zeta^2 + 2i\beta^2)\psi_o + \varepsilon([\nabla_\zeta^2 + 2i\beta^2]\psi_1 - (f'(\zeta) + \overline{f'(\zeta)})\nabla_\zeta^2\psi_o) = 0 \tag{10}$$

To the first approximation: $\varepsilon = 0$, giving

$$(\nabla_\zeta^2 + 2i\beta^2)\psi_o = 0 \tag{11}$$

As it is the contention to get the solution to the case of a non-circular hole as a perturbation on the solution for $\rho = 1$, (11) is solved first.

The second order term in (10) now gives

$$(\nabla_\zeta^2 + 2i\beta^2)\psi_1 = (f'(\zeta) + \overline{f'(\zeta)})\nabla_\zeta^2\psi_o \tag{12}$$

Using (11),

$$(\nabla_\zeta^2 + 2i\beta^2)\psi_1 = -2i\beta^2(f'(\zeta) + \overline{f'(\zeta)})\psi_o \tag{13}$$

The solution for the equation (13) can be written as,

$$\psi_1 = \psi_{1c} + \psi_{1p}$$

where, ψ_{1c} = complementary function

ψ_{1p} = particular integral.

Solution to equation (11) for symmetrical problems, (discarding Hankel functions of the second kind as they grow large with argument) is

of the form,

$$\psi_o(\rho,\gamma) = \sum_o^\infty (A_n + iB_n)\, H_n^1(\beta\rho\sqrt{2i})\, \cos n\gamma \qquad (14)$$

and similarly

$$\psi_{1c} = \sum_o^\infty (C_n + iD_n)\, H_n^1(\beta\rho\sqrt{2i})\, \cos n\gamma \qquad (15)$$

The particular integral of equation (13) can be found using Green's function G for the Helmholtz equation,

$$(\nabla_\zeta^2 + 2i\beta^2)\psi_1 = 0$$

$$G = i\pi\, H_o^1\left(\beta\sqrt{2i}\,\sqrt{\rho^2+\rho_o^2 - 2\rho\,\rho_o \cos(\gamma-\gamma_o)}\right)$$

$$= i\pi \cdot \sum_{m=0}^\infty \varepsilon_m' \cos m(\gamma-\gamma_o)\, J_m(\beta\rho\sqrt{2i})\, H_m(\beta\rho_o\sqrt{2i})$$

(for $\rho \leqslant \rho_o$)

$$= i\pi \sum_{m=0}^\infty \varepsilon_m' \cos m(\gamma-\gamma_o)\, J_m(\beta\rho_o\sqrt{2i})\, H_m(\beta\rho\sqrt{2i})$$

(for $\rho \geqslant \rho_o$) (16)

where $\varepsilon_m' = 1$ if $m = 0$

$= 2$ if $m \neq 0$

and J_m is the Bessel's function of the first kind, order m.

$$\psi_{1p} = -\frac{1}{4\pi} \iint_{\text{Area}} G\,\{-2i\beta^2\psi_o(f'(\zeta)+\overline{f'(\zeta)})\rho_o d\rho_o d\gamma_o\} \qquad (17)$$

From (7),

$$(E_1-iE_2)_Z = (E_1-iE_2)_\zeta - 2i\beta\varepsilon\frac{(f(\zeta)+\overline{f(\zeta)})}{2}(E_3-iE_4)_\zeta$$

$$(E_3-iE_4)_Z = (E_3-iE_4)_\zeta + \beta\varepsilon\frac{(f(\zeta)+\overline{f(\zeta)})}{2}(E_1-iE_2)_\zeta \qquad (18)$$

Now the solution for ϕ^* can be written as,

$$\phi^* = \left\{ (E_1 - iE_2)_\zeta - \frac{2i\beta\varepsilon(f(\zeta)+\overline{f(\zeta)})}{2} (E_3 - iE_4)_\zeta \right\} [\psi_o + \varepsilon\psi_{1c} + \varepsilon\psi_{1p}]_{symm}$$

$$+ \left\{ (E_3 - iE_4)_\zeta + \frac{\beta\varepsilon(f(\zeta)+\overline{f(\zeta)})}{2} (E_1 - iE_2)_\zeta \right\} [\psi_o + \varepsilon\psi_{1c} + \varepsilon\psi_{1p}]_{antisymm}$$

Denoting

$$\Xi = -2i\beta\varepsilon . \frac{(f(\zeta)+\overline{f(\zeta)})}{2} (E_3 - iE_4)_\zeta \cdot \psi_{o\ symm}$$

$$+ \beta\varepsilon . \frac{(f(\zeta)+\overline{f(\zeta)})}{2} (E_1 - iE_2)_\zeta \psi_{o\ antisymm}$$

$$+ \varepsilon(E_1 - iE_2)_\zeta \psi_{1p\ symm} + \varepsilon(E_3 - iE_4)_\zeta \psi_{1p\ antisymm} \qquad (18a)$$

$$\phi^* = [(E_1 - iE_2)_\zeta \psi_{o\ symm} + (E_3 - iE_4)_\zeta \psi_{o\ antisymm}]$$

$$+ \varepsilon[(E_1 - iE_2)_\zeta \psi_{1c\ symm} + (E_3 - iE_4)_\zeta \psi_{1c\ antisymm}]$$

$$+ \Xi . \qquad (19)$$

This is the solution to the order of 'ε' in ρ and γ.

One should remember to carry out the coordinate transformation in the boundary conditions as well. If the expression for Kirchoff shear is taken as an example, it consists of derivatives, $w_{,rrr}$; $w_{,rr}$ etc. To transform these into (ρ,γ) system of coordinates is very difficult for a general transformation. In order to obviate this difficulty, it was assumed in (2.2) that

$$\phi^* = \phi_o^* + \varepsilon\phi_1^* \quad \text{where}$$

$$\nabla_Z^4\phi_o^* + 8i\beta^2\phi_{o,\xi\xi}^* = 0$$

and $$\nabla_Z^4\phi_1^* + 8i\beta^2\phi_{1,\xi\xi}^* = 0 \qquad (20)$$

Obtaining the solution to the differential equation and the boundary conditions in ρ,γ coordinates, as can be seen in this section, is very cumbersome. What we do instead is to expand N_{rr}, $N_{\theta\theta}$, etc. as a

Taylor's series around the point (ρ,γ) and use them to obtain expressions for N_{nn}, N_{ss}, etc. (Appendix VIII). For example, consider $N_{\theta\theta} = \frac{\partial^2 F(r,\theta)}{\partial r^2}$. Instead of expressing F as a function of ρ and γ, and also $\frac{\partial r^2}{\partial r^2}$ in terms of ρ and γ, $N_{\theta\theta}(r,\theta)$ can be written as,

$$N_{\theta\theta}(r,\theta) = N_{\theta\theta}(\rho,\gamma) + \Delta\rho . \frac{\partial N_{\theta\theta}(\rho,\gamma)}{\partial\rho} + \Delta\gamma . \frac{\partial N_{\theta\theta}(\rho,\gamma)}{\partial\gamma}$$

Since $r = \rho + \Delta\rho$ and $\theta = \gamma + \Delta\gamma$ (from (2.3)), where $N_{\theta\theta}(\rho,\gamma)$ $= \frac{\partial^2}{\partial\rho^2}(F_o(\rho,\gamma) + \varepsilon F_1(\rho,\gamma))$. In the final expressions that are obtained we retain only 'ε' order terms. The solution to the circular hole is got by putting $\varepsilon = 0$ and satisfying the boundary conditions on $\rho = 1$. For the case of a non-circular hole ($\varepsilon \neq 0$), the boundary conditions on additional stress resultants are satisfied on $\rho = 1$.

As a matter of fact the solution which is obtained in (2.4),

$$\begin{aligned}\phi^* = {} & (E_1 - iE_2)_Z \sum_{0,2,..}^{\infty} (A_n + iB_n)\, H_n^1(\beta r\sqrt{2i}) \cos n\theta \\ & + (E_3 - iE_4)_Z \sum_{1,3,..}^{\infty} (A_n + iB_n)\, H_n^1(\beta r\sqrt{2i}) \cos n\theta \\ & + \varepsilon\Big\{(E_1 - iE_2)_\zeta \sum_{0,2,...}^{\infty} (C_n + iD_n)\, H_n^1(\beta\rho\sqrt{2i}) \cos n\gamma \\ & + (E_3 - iE_4)_\zeta \sum_{1,3,...}^{\infty} (C_n + iD_n)\, H_n^1(\beta\rho\sqrt{2i}) \cos n\gamma \Big\} \qquad (21)\end{aligned}$$

can be shown to be identical to the expression given in (19). This is done for the elliptical hole case and is presented in Section II.

SECTION II;

From (2.4),

$$\phi_o^* = (E_1 - iE_2)_Z \sum_{0,2,4,..}^{\infty} (A_n + iB_n)\, H_n^1(\beta r\sqrt{2i})\, \cos n\theta$$

$$+ (E_3 - iE_4)_Z \sum_{1,3,..}^{\infty} (A_n + iB_n)\, H_n^1(\beta r\sqrt{2i})\, \cos n\theta$$

and

$$\phi_1^* = (E_1 - iE_2)_\zeta \sum_{0,2,4,..}^{\infty} (C_n + iD_n)\, H_n^1(\beta \rho\sqrt{2i})\, \cos n\gamma$$

$$+ (E_3 - iE_4)_\zeta \sum_{1,3,..}^{\infty} (C_n + iD_n)\, H_n^1(\beta \rho\sqrt{2i})\, \cos n\gamma \qquad (22)$$

In the case of an elliptical hole the transformation function is given by,

$$Z = \zeta + \frac{\varepsilon}{\zeta} \qquad (23)$$

which gives $$(f'(\zeta) + \overline{f'(\zeta)}) = -\frac{2\cos 2\gamma}{\rho^2} \qquad (24)$$

To the order of 'ε' using relations given in (2.3)

$$\phi_o^*(r,\theta) = \phi_o^*(\rho,\gamma) + \Delta\rho \frac{\partial \phi_o^*(\rho,\gamma)}{\partial \rho} + \Delta\gamma \cdot \frac{\partial \phi_o^*(\rho,\gamma)}{\partial \gamma} \qquad (25)$$

$\phi_o^*(\rho,\gamma)$ is the same as ϕ_o^* given in (22) but r and θ are changed to ρ and γ, which also implies Z is replaced by ζ.

$$\therefore \phi^* = \phi_o^*(\rho,\gamma) + \varepsilon\phi_1^*(\rho,\gamma) + \varepsilon\left[\frac{\cos 2\gamma}{\rho} \cdot \frac{\partial \phi_o^*(\rho,\gamma)}{\partial \rho} - \frac{\sin 2\gamma}{\rho^2} \cdot \frac{\partial \phi_o^*(\rho,\gamma)}{\partial \gamma}\right]$$

(Using 2.3) (26)

Expression obtained for ϕ^* in (19) is,

$$\phi^* = \phi_o^*(\rho,\gamma) + \varepsilon\phi_1^*(\rho,\gamma) + \Xi$$

Ξ is given in (18a). To show the identity required,

$$\Xi = \varepsilon\left[\frac{\cos 2\gamma}{\rho}\cdot\frac{\partial\phi_o^*(\rho,\gamma)}{\partial\rho} - \frac{\sin 2\gamma}{\rho^2}\,\frac{\partial\phi_o^*(\rho,\gamma)}{\partial\gamma}\right] \tag{27}$$

Substituting the expression for ψ_o from (1.4), G from (16) and using (24); (17) gives,

$$\psi_{1p} = i\beta^2(A_1+iB_1)\frac{\cos\gamma}{\rho}\cdot\frac{H_o^1(\beta\rho\sqrt{2i})}{\beta\sqrt{2i}} - i\beta^2(A_o+iB_o)\cos 2\gamma.H_o^1(\beta\rho\sqrt{2i})$$

$$+ 2i\beta^2\sum_{2,\ldots}^{\infty}(A_m+iB_m)\frac{H_m^1(\beta\rho\sqrt{2i})\cos(m-2)\gamma}{4(m-1)}$$

$$- 2i\beta^2\sum_{1,\ldots}^{\infty}(A_m+iB_m)\frac{(H_m^1(\beta\rho\sqrt{2i})\cos\overline{m+2}\,\gamma)}{4(m+1)} \tag{28}$$

(For details see Section III.)

$$\Xi = \frac{-2i\beta\varepsilon}{\rho}\cdot\cos\gamma.(E_3-iE_4)_\zeta\sum_{0,2,..}^{\infty}(A_n+iB_m)\,H_n^1(\beta\rho\sqrt{2i})\cos n\gamma$$

$$+ \frac{\beta\varepsilon}{\rho}\cdot\cos\gamma.(E_1-iE_2)_\zeta\sum_{1,3,..}^{\infty}(A_n+iB_n)\,H_n^1(\beta\rho\sqrt{2i})\cos n\gamma$$

$$+ \varepsilon(E_1-iE_2)_\zeta\left\{-i\beta^2(A_o+iB_o)\,H_o^1(\beta\rho\sqrt{2i})\cos 2\gamma\right.$$

$$+ 2i\beta^2\sum_{2,4\ldots}^{\infty}(A_m+iB_m)\frac{H_m^1(\beta\rho\sqrt{2i})\cos\overline{m-2}\,\gamma}{4(m-1)}$$

$$\left.- 2i\beta^2\sum_{2,4,..}^{\infty}(A_m+iB_m)\frac{H_m^1(\beta\rho\sqrt{2i})\cos\overline{m+2}\,\gamma}{4(m+1)}\right\}$$

$$+ \varepsilon(E_3-iE_4)_\zeta\left\{i\beta^2(A_1+iB_1)\frac{H_o^1(\beta\rho\sqrt{2i})}{\beta\rho\sqrt{2i}}\cos\gamma\right.$$

$$+ 2i\beta^2\sum_{3,\ldots}^{\infty}(A_m+iB_m)\frac{H_m^1(\beta\rho\sqrt{2i})\cos\overline{m-2}\,\gamma}{4(m-1)}$$

$$\left.- 2i\beta^2\sum_{1,3,..}^{\infty}(A_m+iB_m)\frac{H_m^1(\beta\rho\sqrt{2i})\cos\overline{m+2}\,\gamma}{4(m+1)}\right\} \tag{29}$$

Consider the right-hand side of (27)

$$\frac{\varepsilon}{\rho}\left\{(E_1-iE_2)_\zeta \sum_{0,2,..}^{\infty}(A_n+iB_n)\left[\frac{(\cos\overline{n+2}\gamma+\cos\overline{n-2}\gamma)}{2}\frac{\partial H_n^1(\beta\rho\sqrt{2i})}{\partial\rho}\right.\right.$$

$$\left.+\frac{(\cos\overline{n-2}\gamma-\cos\overline{n+2}\gamma)}{2}\frac{n}{\rho}.H_n^1(\beta\rho\sqrt{2i})\right]$$

$$+(E_3-iE_4)_\zeta\sum_{1,3,..}^{\infty}(A_n+iB_n)\left[\frac{(\cos\overline{n+2}\gamma+\cos\overline{n-2}\gamma)}{2}\frac{\partial H_n^1(\beta\rho\sqrt{2i})}{\partial\rho}\right.$$

$$\left.\left.+\frac{(\cos\overline{n-2}\gamma-\cos\overline{n+2}\gamma)}{2}.\frac{n}{\rho}.H_n^1(\beta\rho\sqrt{2i})\right]\right\}$$

$$-\frac{2i\beta\varepsilon}{\rho}.\cos\gamma.(E_3-iE_4)_\zeta\sum_{0,2,...}^{\infty}(A_n+iB_n)\,H_n^1(\beta\rho\sqrt{2i})\cos n\gamma$$

$$+\frac{\beta\varepsilon}{\rho}\cos\gamma.(E_1-iE_2)_\zeta\sum_{1,3,..}^{\infty}(A_n+iB_n)\,H_n^1(\beta\rho\sqrt{2i})\cos n\gamma \qquad (30)$$

Let us consider a typical term in (30) and show that it is identical to the corresponding term in (29).

$$\frac{\varepsilon}{\rho}.(E_1-iE_2)_\zeta.(A_n+iB_n)\left[\frac{(\cos\overline{n+2}\gamma+\cos\overline{n-2}\gamma)}{2}\frac{\partial H_n^1(\beta\rho\sqrt{2i})}{\partial\rho}\right.$$

$$\left.+\frac{(\cos\overline{n-2}\gamma-\cos\overline{n+2}\gamma)}{2}.\frac{n}{\rho}.H_n^1(\beta\rho\sqrt{2i})\right]$$

i.e. $$\frac{\varepsilon}{2\rho}(A_n+iB_n)(E_1-iE_2)_\zeta\left\{\cos\overline{n+2}\gamma\;[-\beta\sqrt{2i}\,H_{n+1}^1(\beta\rho\sqrt{2i})]\right.$$

$$\left.+\cos\overline{n-2}\gamma\;[\beta\sqrt{2i}\,H_{n-1}^1(\beta\rho\sqrt{2i})]\right\}$$

i.e. $$\frac{\varepsilon}{2}(A_n+iB_n)(E_1-iE_2)_\zeta\left\{+\beta^2 2i\left[\frac{-H_n^1-H_{n+2}^1}{2(n+1)}\right]\cos\overline{n+2}\gamma\right.$$

$$\left.+\cos\overline{n-2}\gamma.\beta^2 2i\left[\frac{H_{n-2}^1+H_n^1}{2(n-1)}\right]\right\}$$

i.e. $$\varepsilon.(E_1-iE_2)_\zeta\left\{2i\beta^2\frac{(A_n+iB_n)\,H_n^1(\beta\rho\sqrt{2i})\cos\overline{n-2}\gamma}{4(n-1)}\right.$$

$$- 2i\beta^2 (A_n+iB_n) \frac{H_n^1(\beta\rho\sqrt{2i}) \cos \overline{n+2}\,\gamma}{4(n+1)} \Bigg\}$$

+ terms of the type included in $\phi_1^*(\rho,\gamma)$.

This term can be readily seen in (29) and this is so, for each term.

Hence the identity is proved.

SECTION III:

To find the particular integral of equation,

$$(\nabla_\zeta^2 + 2i\beta^2)\,\psi_1 = -2i\beta^2(f'(\zeta) + \overline{f'(\zeta)})\psi_o$$

$$\psi_{1p} = -\frac{1}{4\pi} \iint_{\text{Area}} \{G\,[-2i\beta^2\psi_o(f'(\zeta) + \overline{f'(\zeta)})\,\rho_o d\rho_o d\gamma_o]\}$$

and for the elliptical hole: $f'(\zeta) + \overline{f'(\zeta)} = \frac{-2\cos 2\gamma}{\rho^2}$ (31)

Using (16) and (17)

$$= \beta^2\Bigg[\int_\rho^\infty \int_o^{2\pi} \Big\{\sum_{m=0}^{\infty} \varepsilon_m' \cos m(\gamma-\gamma_o)\, J_m(\beta\rho\sqrt{2i})\, H_m(\beta\rho_o\sqrt{2i})\Big\}$$

$$\times \Big\{\sum_{n=0}^{\infty} (A_n+iB_n)\, H_n(\beta\rho_o\sqrt{2i}) \cos n\,\gamma_o\Big\} \frac{\cos 2\gamma_o}{\rho_o}\, d\rho_o\, d\gamma_o$$

$$+ \int_1^\rho \int_o^{2\pi} \Big\{\sum_{m=0}^{\infty} \varepsilon_m' \cos m(\gamma-\gamma_o)\, J_m(\beta\rho_o\sqrt{2i})\, H_m(\beta\rho\sqrt{2i})\Big\}$$

$$\times \Big\{\sum_{n=0}^{\infty} (A_n+iB_n)\, H_n(\beta\rho_o\sqrt{2i}) \cos n\gamma_o\Big\} \frac{\cos 2\gamma_o}{\rho_o}\, d\rho_o d\gamma_o\Bigg] \tag{32}$$

As the problem under consideration is symmetric in 'γ' 'sin $m\gamma$' terms can be discarded in (32).

For evaluating the various integrals that result the following relations are made use of.

$$J_{n+1}(Z)\ Y_n(Z) - J_n(Z)\ Y_{n+1}(Z) = \frac{2}{\pi Z} \tag{33}$$

(Hankel function $H_n(Z) = J_n(Z) + iY_n(Z)$)

If K_m, $\overline{K}_n$ represent Bessel's functions or Hankel functions of order m and n respectively, then,

$$\int_Z K_m(Z)\ \overline{K}_n(Z)\ \frac{dZ}{Z} = -Z\ \frac{K_{m+1}(Z).\overline{K}_n(Z) - K_m(Z).\overline{K_{n+1}}(Z)}{(m^2 - n^2)} + \frac{K_m(Z).\overline{K_n}(Z)}{m+n} \tag{34}$$

$$\int_Z Z^{-m-n-1}\ K_{m+1}(Z).\ \overline{K_{n+1}}(Z)\ dZ$$

$$= -\frac{Z^{-m-n}}{2(m+n+1)}\left[K_m(Z)\ \overline{K_n}(Z) + K_{m+1}(Z)\ \overline{K_{n+1}}(Z)\right] \tag{35}$$

$$\int_Z Z^{m+n+1}\ K_m(Z)\ \overline{K_n(Z)}\ dZ$$

$$= \frac{Z^{m+n+2}}{2(m+n+1)}\left[K_m(Z)\ \overline{K_n(Z)} + K_{m+1}(Z)\ \overline{K_{n+1}(Z)}\right] \tag{36}$$

Also $$\int_0^{2\pi} \cos(\ell\gamma_o)\ d\gamma_o = 0 \quad \text{if } \ell \neq 0$$

$$= 2\pi \quad \text{if } \ell = 0: \tag{37}$$

Using these relations in (32), and noting that the integrals involved in E_n, F_n in terms of the type,

$$(E_n + iF_n)\ H_n^1(\beta\rho\sqrt{2i})\ \cos n\gamma$$

need not be evaluated as these terms could be merged into the series for ψ_{1c}, ψ_{1p} is obtained in the form given in (28).

APPENDIX VIII

Stress and moment resultants in terms of complex stress function

Define, $N_{nn} = N_{nn}^{(o)} + \varepsilon N_{nn}^{(1)}$

$$= (\overline{N_{nn}^{(o)}} + N_{nn}^{(o)*}) + \varepsilon(\overline{N_{nn}^{(1)}} + N_{nn}^{(1)*})$$

$$N_{ss} = N_{ss}^{(o)} + \varepsilon N_{ss}^{(1)}$$

$$= \overline{N_{ss}^{(o)}} + N_{ss}^{(o)*}) + \varepsilon(\overline{N_{ss}^{(1)}} + N_{ss}^{(1)*})$$

$$N_{ns} = (N_{ns}^{(o)} + \varepsilon N_{ns}^{(1)})$$

$$= (\overline{N_{ns}^{(o)}} + N_{ns}^{(o)*}) + \varepsilon(\overline{N_{ns}^{(1)}} + N_{ns}^{(1)*}) \qquad (1)$$

Where — denotes the values far away from the hole and * denotes the perturbations due to the presence of the cut-out.

To obtain the stress transformation equations from (r,θ) coordinates to (ρ,γ) coordinates, we proceed as follows. (Refer to figures 20 and 21)

$$N_{nn} = N_{rr}\cos^2\psi + N_{\theta\theta}.\sin^2\psi + N_{r\theta}.\sin 2\psi$$

$$N_{ss} = N_{rr}\sin^2\psi + N_{\theta\theta}.\cos^2\psi - N_{r\theta}.\sin 2\psi$$

$$N_{ns} = (N_{\theta\theta}-N_{rr})\sin\psi\cos\psi + N_{r\theta}.\cos 2\psi$$

$$M_{nn} = M_{rr}\cos^2\psi + M_{\theta\theta}.\sin^2\psi + M_{r\theta}\sin 2\psi$$

$$M_{ss} = M_{rr}\sin^2\psi + M_{\theta\theta}.\cos^2\psi - M_{r\theta}.\sin 2\psi$$

$$M_{ns} = (M_{\theta\theta}-M_{rr})\sin\psi\cos\psi + M_{r\theta}.\cos 2\psi$$

$$Q_n = Q_r\cos\psi + Q_\theta.\sin\psi + \frac{\partial M_{ns}}{\partial s} \qquad (2)$$

Define;

$$N^j_{rr} = - \text{Imag}\left[\frac{1}{\rho}.\phi_{j,\rho} + \frac{1}{\rho^2}\phi_{j,\gamma\gamma}\right]$$

$$N^j_{\theta\theta} = - \text{Imag}\left[\phi_{j,\rho\rho}\right]$$

$$N^j_{r\theta} = - \text{Imag}\left[\frac{1}{\rho^2}.\phi_{j,\gamma} - \frac{1}{\rho}.\phi_{j,\rho\gamma}\right]$$

$$M^j_{rr} = - \text{Real}\left[\phi_{j,\rho\rho} + \frac{\nu}{\rho}.\phi_{j,\rho} + \frac{\nu}{\rho^2}\phi_{j,\gamma\gamma}\right]$$

$$M^j_{\theta\theta} = - \text{Real}\left[\frac{1}{\rho}.\phi_{j,\rho} + \frac{1}{\rho^2}\phi_{j,\gamma\gamma} + \nu\phi_{j,\rho\rho}\right]$$

$$M^j_{r\theta} = + \text{Real}\left[(1-\nu)\left(\frac{1}{\rho^2}.\phi_{j,\gamma} - \frac{1}{\rho}.\phi_{j,\rho\gamma}\right)\right]$$

$$Q^j_r = - \text{Real}\left[(\nabla^2\phi_j)_{,\rho}\right]$$

$$Q^j_\theta = - \text{Real}\left[\left(\frac{1}{\rho}.\nabla^2\phi_j\right)_{,\gamma}\right] \qquad (3)$$

Also, let

$$L_1 = \frac{\bar{\zeta}f(\zeta) + \zeta\overline{f(\zeta)}}{2\rho}.\frac{\partial}{\partial\rho} + \left[\frac{(f(\zeta) - \overline{f(\zeta)})}{2i\varrho}\cos\gamma - \frac{(f(\zeta) + \overline{f(\zeta)})}{2\rho}.\sin\gamma\right]\frac{\partial}{\partial\gamma}.$$

and $\varepsilon L_2 = 2\psi = 2\varepsilon\left[\frac{\zeta\overline{f(\zeta)} - \bar{\zeta}f(\zeta)}{2i\rho^2} + \frac{f'(\zeta) - \overline{f'(\zeta)}}{2i}\right]$

(from 2.3)) (4)

The stresses N_{rr}, $N_{\theta\theta}$, $N_{r\theta}$ and the moments M_{rr}, $M_{\theta\theta}$, $M_{r\theta}$ as well as the Kirchoff shears Q_r, Q_θ can be expanded as a Taylor's series around the point (ρ,γ) to the order of 'ε'.

$$K = K^{(o)} + \varepsilon K^{(1)} + \Delta\rho\,\frac{\partial K^{(o)}}{\partial\rho} + \Delta\gamma.\frac{\partial K^{(o)}}{\partial\gamma} \qquad (5)$$

where K represents any of N_{rr}, $N_{\theta\theta}$, $N_{r\theta}$, M_{rr}, $M_{\theta\theta}$, $M_{r\theta}$, Q_r or Q_θ.

$\Delta\rho$, and $\Delta\gamma$ are obtained from (2.3) since

$$r = \rho + \Delta\rho;$$

$$\theta = \gamma + \Delta\gamma.$$

Using (4) and (5) in (2), one obtains,

$$N_{nn} = N_{nn}^{(o)} + \varepsilon N_{nn}^{(1)} = N_{rr}^{(o)} + \varepsilon[N_{rr}^{(1)} + L_1 N_{rr}^{(o)} + L_2 N_{r\theta}^{(o)}]$$

$$N_{ss} = N_{ss}^{(o)} + \varepsilon N_{ss}^{(1)} = N_{\theta\theta}^{(o)} + \varepsilon[N_{\theta\theta}^{(1)} + L_1 N_{\theta\theta}^{(o)} - L_2 N_{r\theta}^{(o)}]$$

$$N_{ns} = N_{ns}^{(o)} + \varepsilon N_{ns}^{(1)} = N_{r\theta}^{(o)} + \varepsilon[N_{r\theta}^{(1)} + L_1 N_{r\theta}^{(o)} + \frac{L_2}{2}(N_{\theta\theta}^{(o)} - N_{rr}^{(o)})]$$

$$M_{nn} = M_{nn}^{(o)} + \varepsilon M_{nn}^{(1)} = M_{rr}^{(o)} + \varepsilon[M_{rr}^{(1)} + L_1 M_{rr}^{(o)} + L_2 M_{r\theta}^{(o)}]$$

$$M_{ss} = M_{ss}^{(o)} + \varepsilon M_{ss}^{(1)} = M_{\theta\theta}^{(o)} + \varepsilon[M_{\theta\theta}^{(1)} + L_1 M_{\theta\theta}^{(o)} - L_2 M_{r\theta}^{(o)}]$$

$$M_{ns} = M_{ns}^{(o)} + \varepsilon M_{ns}^{(1)} = M_{r\theta}^{(o)} + \varepsilon[M_{r\theta}^{(1)} + L_1 M_{r\theta}^{(o)} + \frac{L_2}{2}(M_{\theta\theta}^{(o)} - M_{rr}^{(o)})]$$

$$Q_n = Q_n^{(o)} + \varepsilon Q_n^{(1)} = Q_r^{(o)} + \varepsilon[Q_r^{(1)} + L_1 Q_r^{(o)} + \frac{L_2}{2} Q_\theta^{(o)}]$$

$$\frac{\partial w}{\partial n} = \frac{\partial w^{(o)}}{\partial n} + \varepsilon\frac{\partial w^{(1)}}{\partial n} = \frac{\partial w^{(o)}}{\partial \rho} + \varepsilon[\frac{\partial w^{(1)}}{\partial \rho} + L_1 \frac{\partial w^{(o)}}{\partial \rho} + \frac{L_2}{2\rho} \cdot \frac{\partial w^{(o)}}{\partial \gamma}]$$

$$w = w^{(o)} + \varepsilon[w^{(1)} + L_1 w^{(o)}] \qquad (6)$$

APPENDIX IX

Boundary conditions for a reinforced elliptical hole in a cylindrical shell:

$$\text{Image}\left\{-(6+2\Lambda)(\phi^{*}_{1,\gamma\gamma}+\phi^{*}_{1,\rho})+6\Lambda\phi^{*}_{1,\rho\rho}\right\} = \text{Imag}\left\{(6+2\Lambda)\left[\cos 2\gamma\,(+\phi^{*}_{o,\rho\rho}-\phi^{*}_{o,\rho}-2\phi^{*}_{o,\gamma\gamma}+\phi^{*}_{o,\rho\gamma\gamma}\right.\right.$$

$$-\sin 2\gamma\,(\phi^{*}_{o,\rho\gamma}+\phi^{*}_{o,\gamma\gamma\gamma})+4\sin 2\gamma\,(\phi^{*}_{o,\gamma}-\phi^{*}_{o,\rho\gamma})]-6\Lambda\,[\cos 2\gamma\,.\,\phi^{*}_{o,\rho\rho\rho}-\sin 2\gamma.\phi^{*}_{o,\rho\rho\gamma}$$

$$\left.\left.-4\sin 2\gamma\,(\phi^{*}_{o,\gamma}-\phi^{*}_{o,\rho\gamma})]-18\cos 2\gamma\,(\phi^{*}_{o,\rho}+\phi^{*}_{o,\gamma\gamma})\right\}+18\,\overline{N^{(o)}_{nn}}\cos 2\gamma-(6+2\Lambda)\,\overline{N^{(1)}_{nn}}+6\Lambda\,\overline{N^{(1)}_{ss}}\,.$$

$$\text{Where}\quad \Lambda = \frac{E_R}{E_S}\cdot\frac{A}{r_o t}\,;$$

$$\text{Imag}\left\{6(\phi^{*}_{1,\gamma} - \phi^{*}_{1,\rho\gamma}) - 2\Lambda(\phi^{*}_{1,\gamma\gamma\gamma} + \phi^{*}_{1,\rho\gamma}) + 6\Lambda\phi^{*}_{1,\rho\rho\gamma}\right\}$$

$$= \text{Image}\Bigg[-2\Big\{3\Big(\cos 2\gamma\,(-2\phi^{*}_{o,\gamma} + 2\phi^{*}_{o,\rho\gamma} - \phi^{*}_{o,\rho\rho\gamma}) - \sin 2\gamma\,(\phi^{*}_{o,\gamma\gamma} - \phi^{*}_{o,\rho\gamma\gamma}) + 2\sin 2\gamma(\phi^{*}_{o,\rho\rho} - \phi^{*}_{o,\rho} - \phi^{*}_{o,\gamma\gamma})\Big)$$

$$- \Lambda\Big[\Big(\cos 2\gamma(-\phi^{*}_{o,\rho\gamma} + \phi^{*}_{o,\rho\rho\gamma} + \phi^{*}_{o,\rho\gamma\gamma\gamma} - 2\phi^{*}_{o,\gamma\gamma\gamma}) - 2\sin 2\gamma(-\phi^{*}_{o,\rho} + \phi^{*}_{o,\rho\rho} - 2\phi^{*}_{o,\gamma\gamma} + \phi^{*}_{o,\rho\gamma\gamma})$$

$$- \sin 2\gamma(\phi^{*}_{o,\rho\gamma\gamma} + \phi^{*}_{o,\gamma\gamma\gamma\gamma}) - 2\cos 2\gamma(\phi^{*}_{o,\rho\gamma} + \phi^{*}_{o,\gamma\gamma\gamma}) + 4\sin 2\gamma(\phi^{*}_{o,\gamma\gamma} - \phi^{*}_{o,\rho\gamma\gamma})$$

$$+ 8\cos 2\gamma\,(\phi^{*}_{o,\gamma} - \phi^{*}_{o,\rho\gamma})\Big)$$

$$- 3\Big(\cos 2\gamma.\phi^{*}_{o,\rho\rho\rho\gamma} - 2\sin 2\gamma.\phi^{*}_{o,\rho\rho\rho} - \sin 2\gamma.\phi^{*}_{o,\rho\rho\gamma\gamma} - 2\cos 2\gamma.\phi^{*}_{o,\rho\rho\gamma}$$

$$- 4\sin 2\gamma.(\phi^{*}_{o,\gamma\gamma} - \phi^{*}_{o,\rho\gamma\gamma}) - 8\cos 2\gamma.(\phi^{*}_{o,\gamma} - \phi^{*}_{o,\rho\gamma})\Big)\Big] - 3\cos 2\gamma.(\phi^{*}_{o,\gamma} - \phi^{*}_{o,\rho\gamma})\Big\}\Bigg]$$

$$+ 6\,\overline{N^{(1)}_{ns}} + 2\Lambda\frac{\partial}{\partial\gamma}(3\overline{N^{(1)}_{ss}} - \overline{N^{(1)}_{nn}}) - 6\,\overline{N^{(o)}_{ns}}\cos 2\gamma\,.$$

$$\text{Real}\left\{(3\phi_{1,\rho\rho}^{*}+\phi_{1,\rho}^{*}+\phi_{1,\gamma\gamma}^{*})-32\Pi(\phi_{1,\gamma\gamma}^{*}+\phi_{1,\rho}^{*})+12\Omega\,\phi_{1,\rho\gamma\gamma}^{*}\right\}=$$

$$+\ \text{Real}\left\{-\cos 2\gamma\,(3\phi_{o,\rho\rho\rho}^{*}+\phi_{o,\rho\rho}^{*}-\phi_{o,\rho}^{*}-2\phi_{o,\gamma\gamma}^{*}+\phi_{o,\rho\gamma\gamma}^{*})+\sin 2\gamma\,(3\phi_{o,\rho\rho\gamma}^{*}+\phi_{o,\rho\gamma}^{*}+\phi_{o,\gamma\gamma\gamma}^{*})\right.$$

$$+8\sin 2\gamma(\phi_{o,\gamma}^{*}-\phi_{o,\rho\gamma}^{*})+32\,\Pi\left[(5\cos 2\gamma\phi_{o,\gamma\gamma}^{*}-2\sin 2\gamma.\phi_{o,\gamma}^{*})+\cos 2\gamma\phi_{o,\rho\rho}^{*}-\sin 2\gamma.\phi_{o,\rho\gamma}^{*}+2\sin 2\gamma.\phi_{o,\gamma}^{*}\right]$$

$$-12\,\Omega\left[-2\cos 2\gamma\phi_{o,\rho\gamma\gamma}^{*}+2\sin 2\gamma\phi_{o,\rho\gamma}^{*}+\cos 2\gamma\phi_{o,\rho\rho\gamma\gamma}^{*}-4\sin 2\gamma.\phi_{o,\rho\rho\gamma}^{*}-4\cos 2\gamma.\phi_{o,\rho\rho}^{*}\right.$$

$$\left.-\sin 2\gamma\phi_{o,\rho\gamma\gamma\gamma}^{*}+2\sin 2\gamma\phi_{o,\gamma\gamma\gamma}^{*}+8\cos 2\gamma.\phi_{o,\gamma\gamma}^{*}-8\sin 2\gamma\,\phi_{o,\gamma}^{*}\right]$$

$$\left.+32\Pi\,(L_1\phi_o^{*})_{,\gamma\gamma}\right\}$$

$$\text{Where}\quad \Omega=\frac{E_R}{E_S}\frac{J}{r_o t^3};\quad \Pi=\frac{E_R}{E_S}\frac{I}{r_o t^3}\quad .$$

$$\text{Real}\left\{3\phi^{*}_{1,\rho\rho\rho} + 3\phi^{*}_{1,\rho\rho} - 3\phi^{*}_{1,\rho} - 8\phi^{*}_{1,\gamma\gamma} + 5\phi^{*}_{1,\rho\gamma\gamma} + 32\Pi\phi^{*}_{1,\gamma\gamma\gamma\gamma} + (32\Pi + 12\Omega)\,\phi^{*}_{1,\rho\gamma\gamma}\right\}$$

$$+ \text{Imag}\left\{-8\beta^2\Lambda\cos^2\gamma(3\phi^{*}_{1,\rho\rho} - \phi^{*}_{1,\rho} - \phi^{*}_{1,\gamma\gamma})\right\} = \text{Real}\left\{-3\cos 2\gamma(\phi^{*}_{o,\rho\rho\rho\rho} + \phi^{*}_{o,\rho\rho\rho} - 2\phi^{*}_{o,\rho\rho} + 2\phi^{*}_{o,\rho} + \phi^{*}_{o,\rho\rho\gamma\gamma}\right.$$

$$- 4\phi^{*}_{o,\rho\gamma\gamma} + 6\phi^{*}_{o,\gamma\gamma}) + 3\sin 2\gamma(\phi^{*}_{o,\rho\rho\rho\gamma} + \phi^{*}_{o,\rho\rho\gamma} - \phi^{*}_{o,\rho\gamma} + \phi^{*}_{o,\rho\gamma\gamma\gamma} - 2\phi^{*}_{o,\gamma\gamma\gamma})$$

$$-6\sin 2\gamma(\phi^{*}_{o,\rho\rho\gamma} + \phi^{*}_{o,\rho\gamma} + \phi^{*}_{o,\gamma\gamma\gamma}) - 2\Big[\cos 2\gamma(2\phi^{*}_{o,\gamma\gamma} - 2\phi^{*}_{o,\rho\gamma\gamma} + \phi^{*}_{o,\rho\rho\gamma\gamma}) - 2\sin 2\gamma(2\phi^{*}_{o,\gamma} - 2\phi^{*}_{o,\rho\gamma} + \phi^{*}_{o,\rho\rho\gamma})$$

$$-2\cos 2\gamma\,(-\phi^{*}_{o,\gamma\gamma} + \phi^{*}_{o,\rho\gamma\gamma}) - \sin 2\gamma(-\phi^{*}_{o,\gamma\gamma\gamma} + \phi^{*}_{o,\rho\gamma\gamma\gamma}) + \cos 2\gamma(-\phi^{*}_{o,\gamma\gamma} + \phi^{*}_{o,\rho\gamma\gamma}) + 2\sin 2\gamma(-\phi^{*}_{o,\rho\rho\gamma} + \phi^{*}_{o,\rho\gamma} + \phi^{*}_{o,\gamma\gamma\gamma})$$

$$+4\cos 2\gamma(-\phi^{*}_{o,\rho\rho} + \phi^{*}_{o,\rho} + \phi^{*}_{o,\gamma\gamma})\Big] - 32\Pi(4\cos 2\gamma\phi^{*}_{o,\gamma\gamma\gamma\gamma} - 12\sin 2\gamma\phi^{*}_{o,\gamma\gamma\gamma} - 16\cos 2\gamma.\phi^{*}_{o,\gamma\gamma} + 8\sin 2\gamma.\phi^{*}_{o,\gamma})$$

$$-(12\Omega + 32\Pi)(\cos 2\gamma.\phi^{*}_{o,\rho\gamma\gamma} - 4\sin 2\gamma.\phi^{*}_{o,\rho\gamma} + \cos 2\gamma.\phi^{*}_{o,\rho\rho\gamma\gamma} - \sin 2\gamma.\phi^{*}_{o,\rho\gamma\gamma\gamma} + 2\sin 2\gamma.\phi^{*}_{o,\gamma\gamma\gamma} - 4\sin 2\gamma.\phi^{*}_{o,\rho\rho\gamma}$$

$$\left. - 4\cos 2\gamma.\phi^{*}_{o,\rho\rho} + 8\cos 2\gamma.\phi^{*}_{o,\gamma\gamma} - 8\sin 2\gamma.\phi^{*}_{o,\gamma}) - 32\Pi\,(L_1\phi_o^{*})_{,\gamma\gamma\gamma\gamma}\right\}$$

$$+ \text{Imag}\quad 8\beta^2.\Lambda\cos^2\gamma\left\{-\cos 2\gamma.(-\phi^{*}_{o,\rho} + \phi^{*}_{o,\rho\rho} - 2\phi^{*}_{o,\gamma\gamma} + \phi^{*}_{o,\rho\gamma\gamma}) + \sin 2\gamma(\phi^{*}_{o,\rho\gamma} + \phi^{*}_{o,\gamma\gamma\gamma}) - 4\sin 2\gamma(\phi^{*}_{o,\gamma} - \phi^{*}_{o,\rho\gamma})\right.$$

$$\left. + 3\cos 2\gamma\phi^{*}_{o,\rho\rho\rho} - 3\sin 2\gamma\phi^{*}_{o,\rho\rho\gamma} - 12\sin 2\gamma(\phi^{*}_{o,\gamma} - \phi^{*}_{o,\rho\gamma})\right\}$$

$$+ \text{Imag}\,[-8\beta^2\Lambda\sin^2 2\gamma]\left\{3\phi^{*}_{o,\rho\rho} - \phi^{*}_{o,\rho} - \phi^{*}_{o,\gamma\gamma}\right\} + 8\beta^2\Lambda\sin^2 2\gamma(3\,\overline{N^{(o)}_{ss}} - \overline{N^{(o)}_{nn}}) - 8\beta^2\Lambda\cos^2\gamma.(3\overline{N^{(1)}_{ss}} - \overline{N^{(1)}_{nn}})$$

APPENDIX X

Boundary conditions for a reinforced square hole with rounded corners in a cylindrical shell:

$$\text{Imag}\left\{-(6+2\Lambda)(\phi^{*}_{1,\gamma\gamma}+\phi^{*}_{1,\rho})+6\Lambda\,\phi^{*}_{1,\rho\rho}\right\} = \text{Image}\left\{(6+2\Lambda)\left[(-\phi^{*}_{o,\rho}+\phi^{*}_{o,\rho\rho}-2\phi^{*}_{o,\gamma\gamma}+\phi^{*}_{o,\rho\gamma\gamma})\cos 4\gamma\right.\right.$$

$$\left.-\sin 4\gamma(\phi^{*}_{o,\rho\gamma}+\phi^{*}_{o,\gamma\gamma\gamma})+8\sin 4\gamma(\phi^{*}_{o,\gamma}-\phi^{*}_{o,\rho\gamma})\right]-6\Lambda\left[\cos 4\gamma.\phi^{*}_{o,\rho\rho\rho}-\sin 4\gamma.\phi^{*}_{o,\rho\rho\gamma}\right.$$

$$\left.\left.-8\sin 4\gamma(\phi^{*}_{o,\gamma}-\phi^{*}_{o,\rho\gamma})\right]-90\cos 4\gamma(\phi^{*}_{o,\rho.}+\phi^{*}_{o,\gamma\gamma})\right\}+90\cos 4\gamma.\ \overline{N^{(o)}_{nn}}-(6+2\Lambda)\,\overline{N^{(1)}_{nn}}+6\Lambda\,\overline{N^{(1)}_{ss}}$$

$$\text{Where}\quad \Lambda = \frac{E_R}{E_S}\cdot\frac{A}{r_o t}$$

$$\text{Imag}\left\{6(\phi^{*}_{1,\gamma} - \phi^{*}_{1,\rho\gamma}) - 2\Lambda\,(\phi^{*}_{1,\gamma\gamma\gamma} + \phi^{*}_{1,\rho\gamma} - 3\phi^{*}_{1,\rho\rho\gamma})\right\}$$

$$= \text{Imag}\left\{-2\left[3\left(\cos 4\gamma(-2\phi^{*}_{o,\gamma} + 2\phi^{*}_{o,\rho\gamma} - \phi^{*}_{o,\rho\rho\gamma}) - \sin 4\gamma(\phi^{*}_{o,\gamma\gamma} - \phi^{*}_{o,\rho\gamma\gamma}) + 4\sin 4\gamma(\phi^{*}_{o,\rho\rho} - \phi^{*}_{o,\rho} - \phi^{*}_{o,\gamma\gamma})\right)\right.\right.$$

$$- \Lambda\left\{\cos 4\gamma\,(-\phi^{*}_{o,\rho\gamma} + \phi^{*}_{o,\rho\rho\gamma} - 2\phi^{*}_{o,\gamma\gamma\gamma} + \phi^{*}_{o,\rho\gamma\gamma\gamma}) - 4\sin 4\gamma(-\phi^{*}_{o,\rho} + \phi^{*}_{o,\rho\rho} - 2\phi^{*}_{o,\gamma\gamma} + \phi^{*}_{o,\rho\gamma\gamma})\right.$$

$$- \sin 4\gamma(\phi^{*}_{o,\rho\gamma\gamma} + \phi^{*}_{o,\gamma\gamma\gamma\gamma}) - 4\cos 4\gamma(\phi^{*}_{o,\rho\gamma} + \phi^{*}_{o,\gamma\gamma\gamma}) + 8\sin 4\gamma(\phi^{*}_{o,\gamma\gamma} - \phi^{*}_{o,\rho\gamma\gamma}) + 32\cos 4\gamma(\phi^{*}_{o,\gamma} - \phi^{*}_{o,\rho\gamma})$$

$$\left.- 3\left(\cos 4\gamma.\phi^{*}_{o,\rho\rho\rho\gamma} - 4\sin 4\gamma\phi^{*}_{o,\rho\rho\rho} - \sin 4\gamma.\phi^{*}_{o,\rho\rho\gamma\gamma} - 4\cos 4\gamma.\phi^{*}_{o,\rho\rho\gamma} - 8\sin 4\gamma(\phi^{*}_{o,\gamma\gamma} - \phi^{*}_{o,\rho\gamma\gamma}) - 32\cos 4\gamma(\phi^{*}_{o,\gamma} - \phi^{*}_{o,\rho\gamma})\right)\right\}$$

$$\left.- 9\cos 4\gamma(\phi^{*}_{o,\gamma} - \phi^{*}_{o,\rho\gamma})\right]\Big\} + 6\,\overline{N^{(o)}_{ns}} + 2\Lambda\,.\,\frac{\partial}{\partial\gamma}\,(3\overline{N^{(1)}_{ss}} - \overline{N^{(1)}_{nn}}) - 18\cos 4\gamma.\,\overline{N^{(o)}_{ns}}\,.$$

$$\text{Real}\left\{3\phi_{1,\rho\rho}^{*}+\phi_{1,\rho}^{*}+\phi_{1,\gamma\gamma}^{*}-32\Pi\phi_{1,\gamma\gamma}^{*}+12\Omega\phi_{1,\rho\gamma\gamma}^{*}-32\Pi\phi_{1,\rho}^{*}\right\}$$

$$=\text{Real}\left\{-\cos 4\gamma\left(3\phi_{o,\rho\rho\rho}^{*}+\phi_{o,\rho\rho}^{*}-\phi_{o,\rho}^{*}-2\phi_{o,\gamma\gamma}^{*}+\phi_{o,\rho\gamma\gamma}^{*}\right)+\sin 4\gamma\left(3\phi_{o,\rho\rho\gamma}^{*}+\phi_{o,\rho\gamma}^{*}+\phi_{o,\gamma\gamma\gamma}^{*}\right)\right.$$

$$+16\sin 4\gamma\left(\phi_{o,\gamma}^{*}-\phi_{o,\rho\gamma}^{*}\right)+32\Pi\left[\left(21\cos 4\gamma.\phi_{o,\gamma\gamma}^{*}-12\sin 4\gamma.\phi_{o,\gamma}^{*}\right)+\cos 4\gamma.\phi_{o,\rho\rho}^{*}-\sin 4\gamma.\phi_{o,\rho\gamma}^{*}+4\sin 4\gamma.\phi_{o,\gamma}^{*}\right]$$

$$-12\Omega\left[-2\cos 4\gamma\phi_{o,\rho\gamma\gamma}^{*}+4\sin 4\gamma\,\phi_{o,\rho\gamma}^{*}+\cos 4\gamma.\phi_{o,\rho\rho\gamma\gamma}^{*}-8\sin 4\gamma.\phi_{o,\rho\rho\gamma}^{*}-16\cos 4\gamma.\phi_{o,\rho\rho}^{*}\right.$$

$$\left.\left.-\sin 4\gamma\phi_{o,\rho\gamma\gamma\gamma}^{*}+4\sin 4\gamma\phi_{o,\gamma\gamma\gamma}^{*}+32\cos 4\gamma\phi_{o,\gamma\gamma}^{*}-64\sin 4\gamma\phi_{o,\gamma}^{*}\right]+32\Pi\;\left(L_1\phi_o^{*}\right)_{,\gamma\gamma}\right\}$$

$$\text{Where}\quad \Omega=\frac{E_R}{E_S}\cdot\frac{J}{r_o t^3};\qquad \Pi=\frac{E_R}{E_S}\cdot\frac{I}{r_o t^3}\ .$$

$$\text{Real}\left\{3\phi^{*}_{1,\rho\rho\rho} + 3\phi^{*}_{1,\rho\rho} - 3\phi^{*}_{1,\rho} - 8\phi^{*}_{1,\gamma\gamma} + 5\phi^{*}_{1,\rho\gamma\gamma} + 32\Pi\,\phi^{*}_{1,\gamma\gamma\gamma\gamma} + (32\Pi + 12\Omega)\,\phi^{*}_{1,\rho\gamma\gamma}\right\}$$

$$+ \text{Imag}\left\{-8\beta^2\Lambda\cos^2\gamma\,(3\phi^{*}_{1,\rho\rho} - \phi^{*}_{1,\gamma\gamma} - \phi^{*}_{1,\rho})\right\} = \text{Real}\Big\{-3\cos 4\gamma\left[\phi^{*}_{o,\rho\rho\rho\rho} + \phi^{*}_{o,\rho\rho\rho} - 2\phi^{*}_{o,\rho\rho} + 2\phi^{*}_{o,\rho} + \phi^{*}_{o,\rho\rho\gamma\gamma}\right.$$

$$\left. - 4\phi^{*}_{o,\rho\gamma\gamma} + 6\phi^{*}_{o,\gamma\gamma}\right] + 3\sin 4\gamma\left[\phi^{*}_{o,\rho\rho\rho\gamma} + \phi^{*}_{o,\rho\rho\gamma} - \phi^{*}_{o,\rho\gamma} + \phi^{*}_{o,\rho\gamma\gamma\gamma} - 2\phi^{*}_{o,\gamma\gamma\gamma}\right] - 12\sin 4\gamma\left[\phi^{*}_{o,\rho\rho\gamma} + \phi^{*}_{o,\rho\gamma} + \phi^{*}_{o,\gamma\gamma\gamma}\right]$$

$$- 2\Big(\cos 4\gamma\left[2\phi^{*}_{o,\gamma\gamma} - 2\phi^{*}_{o,\rho\gamma\gamma} + \phi^{*}_{o,\rho\rho\gamma\gamma}\right] - 4\sin 4\gamma\left[2\phi^{*}_{o,\gamma} - 2\phi^{*}_{o,\rho\gamma} + \phi^{*}_{o,\rho\rho\gamma}\right] - 4\cos 4\gamma\left[-\phi^{*}_{o,\gamma\gamma} + \phi^{*}_{o,\rho\gamma\gamma}\right]$$

$$- \sin 4\gamma\left[-\phi^{*}_{o,\gamma\gamma\gamma} + \phi^{*}_{o,\rho\gamma\gamma\gamma}\right] + 3\cos 4\gamma\left[-\phi^{*}_{o,\gamma\gamma} + \phi^{*}_{o,\rho\gamma\gamma}\right] + 4\sin 4\gamma\left[-\phi^{*}_{o,\rho\rho\gamma} + \phi^{*}_{o,\rho\gamma} + \phi^{*}_{o,\gamma\gamma\gamma}\right]$$

$$+ 16\cos 4\gamma\left[-\phi^{*}_{o,\rho\rho} + \phi^{*}_{o,\rho} + \phi^{*}_{o,\gamma\gamma}\right]\Big) - 32\Pi\,(12\cos 4\gamma\cdot\phi^{*}_{o,\gamma\gamma\gamma\gamma} - 72\sin 4\gamma\phi^{*}_{o,\gamma\gamma\gamma} - 192\cos 4\gamma\cdot\phi^{*}_{o,\gamma\gamma} + 192\sin 4\gamma\cdot\phi^{*}_{o,\gamma})$$

$$-(12\Omega + 32\Pi)\left[13\cos 4\gamma\cdot\phi^{*}_{o,\rho\gamma\gamma} - 56\phi^{*}_{o,\rho\gamma} + \cos 4\gamma\cdot\phi^{*}_{o,\rho\rho\gamma\gamma} - 8\sin 4\gamma\cdot\phi^{*}_{o,\rho\rho\gamma} - 16\cos 4\gamma\cdot\phi^{*}_{o,\rho\rho} - \sin 4\gamma\cdot\phi^{*}_{o,\rho\gamma\gamma\gamma}\right.$$

$$\left. + 4\sin 4\gamma\cdot\phi^{*}_{o,\gamma\gamma\gamma} + 32\cos 4\gamma\cdot\phi^{*}_{o,\gamma\gamma} - 64\sin 4\gamma\cdot\phi^{*}_{o,\gamma}\right] - 32\Pi\,(L_1\phi_o^{*})_{,\gamma\gamma\gamma\gamma}\Big\}$$

$$+ \text{Imag}\;\; 8\beta^2\Lambda\cos^2\gamma\left[3\cos 4\gamma\cdot\phi^{*}_{o,\rho\rho\rho} - 3\sin 4\gamma\cdot\phi^{*}_{o,\rho\rho\gamma} - 24\sin 4\gamma\left[\phi^{*}_{o,\gamma} - \phi^{*}_{o,\rho\gamma}\right] - \cos 4\gamma\left[-\phi^{*}_{o,\rho} + \phi^{*}_{o,\rho\rho} - 2\phi^{*}_{o,\gamma\gamma} + \phi^{*}_{o,\rho\gamma\gamma}\right]\right.$$

$$\left. + \sin 4\gamma\,(\phi^{*}_{o,\rho\gamma} + \phi^{*}_{o,\gamma\gamma\gamma}) - 8\sin 4\gamma(\phi^{*}_{o,\gamma} - \phi^{*}_{o,\rho\gamma})\right]$$

$$+ \text{Imag}\;\left[-24\beta^2\Lambda\sin 2\gamma\cdot\sin 4\gamma\cdot(3\phi^{*}_{o,\rho\rho} - \phi^{*}_{o,\rho} - \phi^{*}_{o,\gamma\gamma})\right]$$

$$+ 24\beta^2\Lambda\sin 2\gamma\cdot\sin 4\gamma\cdot(3\overline{N^{(o)}_{ss}} - \overline{N^{(o)}_{nn}}) - 8\beta^2\Lambda\cos^2\gamma\,(3\overline{N^{(1)}_{ss}} - \overline{N^{(1)}_{nn}})$$

APPENDIX XI

Flow Diagram for Computation
Reinforced arbitrary shaped hole in a cylindrical shell

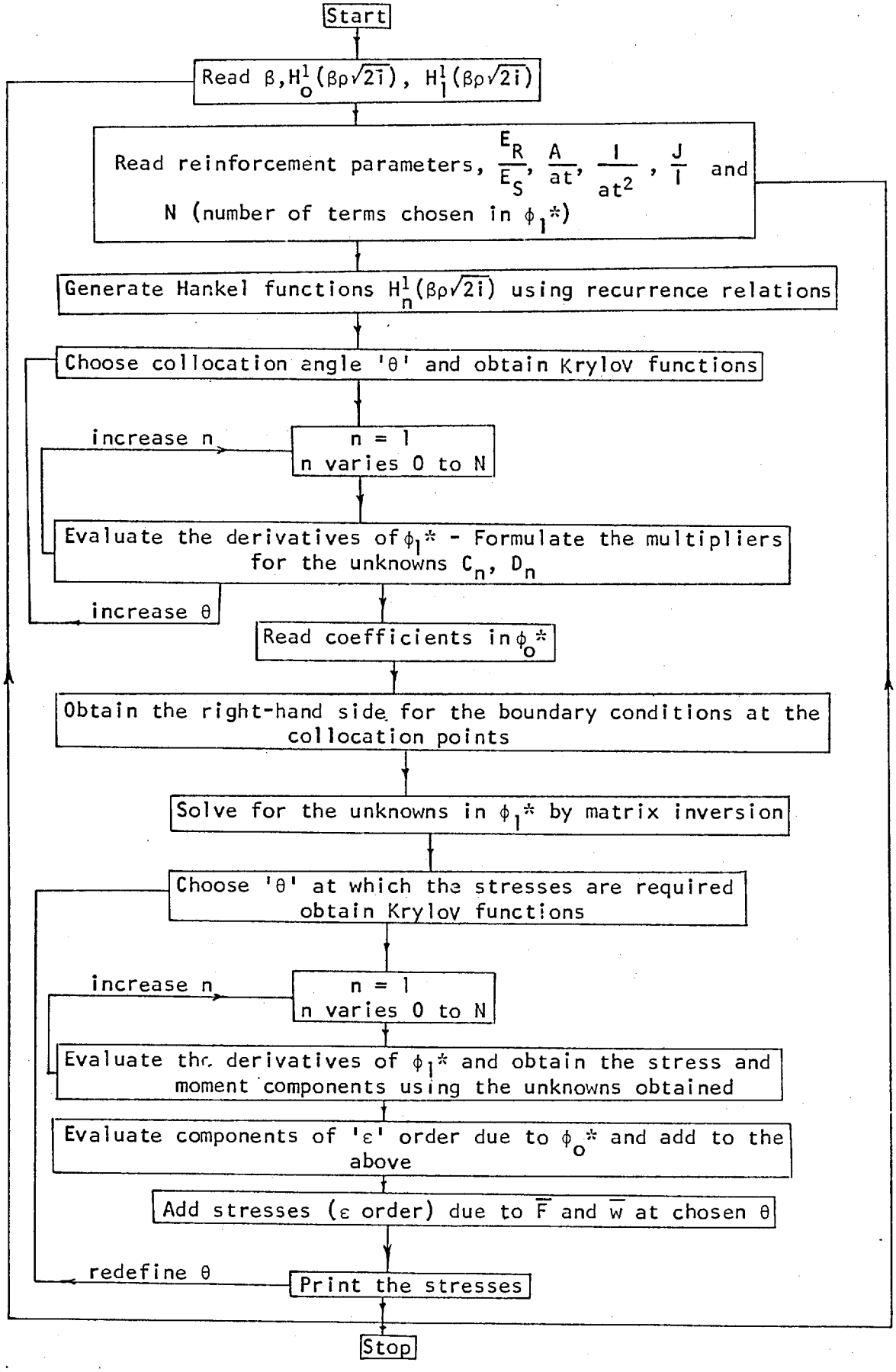

APPENDIX XII

Applicability of the present theory:

The range of applicability of shallow shell theory has been discussed by Vandyke (4).

Hankel functions of the first kind behave like

$$H_n^1(\beta r\sqrt{2i}) \sim e^{-\beta r} \Big/ (\beta r)^{1/2}$$

and KryloV functions behave like

$$(E_1 - iE_2) \sim (E_3 - iE_4) \sim e^{\beta r \cos\theta}$$

for large arguments.

$$\therefore \quad (E_1 - iE_2) H_n^1(\beta r\sqrt{2i}) \sim (E_3 - iE_4) H_n^1(\beta r\sqrt{2i})$$

$$\sim \frac{e^{-\beta r(1 - |\cos\theta|)}}{(\beta r)^{1/2}}$$

Consider the decay in $\theta = \pm \pi/2$, direction,

$$\phi^* \sim e^{-\beta r} \Big/ (\beta r)^{1/2} \qquad \text{(a)}$$

For a shallow shell, the ratio of the rise 'δ' to base length '$2\bar{y}$' is less than 1/8.

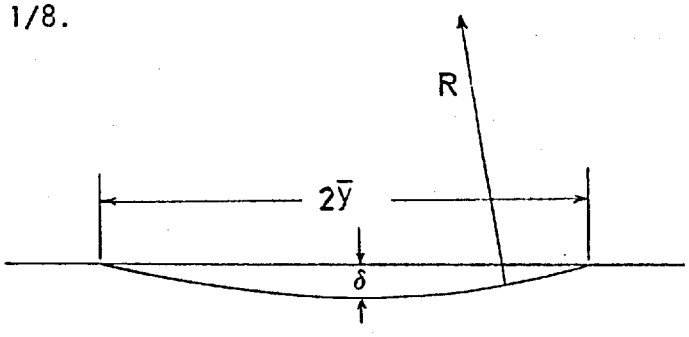

For a circular cylinder, $\delta(2R - \delta) = \bar{y}^2$

Neglecting 'δ^2', $\quad \frac{\delta}{2\bar{y}} = \frac{\bar{y}}{4R}$ $\qquad$ (b)

Using the shallow shell criterion and the fact that $\bar{y} = a\bar{r}$, (b) becomes,

$$\frac{\bar{y}}{4R} = \frac{a\bar{r}}{4R} < \frac{1}{8} \qquad (c)$$

As the hole must lie in the shallow shell region,

$$\frac{a}{R} < \frac{1}{2} \qquad (d)$$

Let us assume that at $r = \bar{r}$, the hole effects have died down to one tenth of their values at the hole edge.

Using (a)

$$\frac{e^{-\beta(\bar{r}-1)}}{(\bar{r})^{1/2}} = \frac{1}{10} \qquad (e)$$

Using (c) and (e), a relation between $\frac{a}{R}$ and $\frac{t}{R}$ is got which is plotted in figure 39.

However, for large values of 'β', we can assume that the entire decay is caused by the exponential term in (e) which gives,

$$\beta(\bar{r} - 1) = 2.3 \qquad (f)$$

i.e. $$\bar{r} = \frac{2.3 + \beta}{\beta} < \frac{R}{2a} \text{ (using (c))}$$

This leads to: $$\frac{a}{R} < \frac{1}{2} - \frac{1.15}{\beta}$$

Using the definition of 'β' and (d), this reduces to,

$$\frac{a}{R} < \frac{1}{2} - 3.6 \left(\frac{t}{R}\right)^{1/2} \qquad (g)$$

Relation (g) is true for large values of β, that is small vaues of (t/R), and has been plotted in figure 39. The analysis given holds for the cylindrical shell. In the case of spherical shell, the same figure 39 applies, except that the y axis represents t/8R instead of t/R.

Variation of Poisson's ratio was shown to have no significant effect on the shell stresses in (6). Hence the results are applicable to cases where the value of ν is around 1/3.

Donnell's assumptions are not satisfactory if the deformations 'w' longitudinally or peripherally consist of modes whose wave length is of the order of the length of the cylinder or perimeter of the cross-section of the cylinder. In the problem considered in this thesis the deformations die away at distances of r = 1.5 from the centre of the hole and hence do not contain large components from modes for which Donnell's assumptions are unsatisfactory.

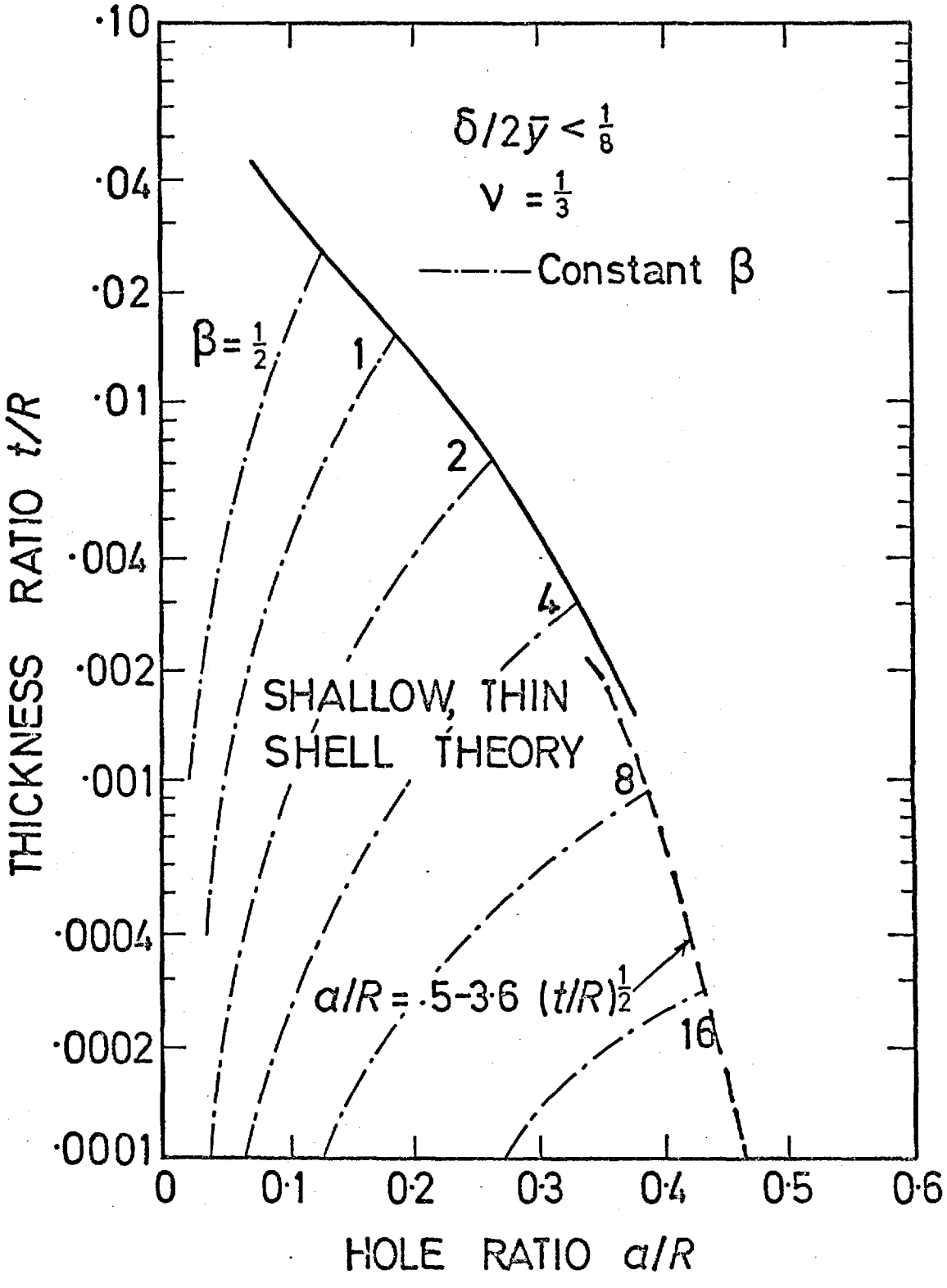

FIG. 39 REGION OF VALIDITY OF SHALLOW SHELL THEORY.

APPENDIX XIII

Reinforced circular hole in a cylindrical shell (loading 'Case B')

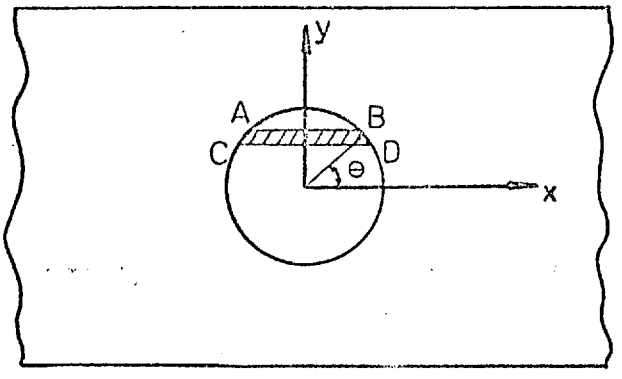

Results are obtained in this appendix assuming that the pressure load acting on the cut-outportion of the shell is distributed as the varying shear round the hole edge referred to as 'Case (B)' on page 26.

If the relative bending stiffness of the curved window in the 'x' and 'y' directions are so dissimilar, we may ignore bending moments and therefore normal shears on generators such as AB and CD. If the edge of the window is free to slide radially then the membrane action is zero here and may be ignored over the whole of the shallow window shell. Under these assumptions the pressure on an element ABDC is resisted entirely by shear on the edges AC and BD, giving rise to the shear per unit length = $pa\cos^2\theta$.

For this case, the equations of equilibrium (1.4.1), (1.4.2) and (1.4.4) remain the same whereas (1.4.3) becomes

$$M_{rr} + N_{rr}h = \frac{M}{a} + \frac{1}{a}H_{,\theta} + Q.b + pa\cos^2\theta.b$$

and (1.4.5) becomes

$$Q = \frac{1}{a}P_{,\theta} + \frac{T}{R}\cos^2\theta - pa\cos^2\theta.$$

The right-hand side of the four boundary conditions in Appendix IV consequently contain

$-24 \cdot \frac{b}{a} \cdot \beta^2 \cdot \cos^2\theta$ instead of $-12 \cdot \frac{b}{a} \cdot \beta^2$ in (c)

and

$24\beta^2\cos^2\theta$ instead of $12\beta^2$ in (d).

In this case also we assume as in (1.6) that $E_R/E_S = 1$ and $J/I = 2$ leaving the three parameters defining the problem β, $\lambda = \frac{A}{at}$ and $\mu = \frac{I}{At^2}$.

(It is found that the stresses increase if J/I is increased for some typical sections. Most of the change occurs in the range $0 \leq \frac{J}{I} \leq 1$ as in Chapter I and in the range $1 \leq \frac{J}{I} \leq 3$, the stresses remain almost constant. Very small J/I implies that the section must be a thin-walled open tube and it is found again that the torsion bending rigidity of the section cannot then be ignored.)

The carpet diagrams in figures 40, 41 and 42 show the variation of stresses with β, λ and μ. For a constant μ the stresses reduce with increasing λ and for a constant λ stresses increase with μ. Stresses also increase with β and for $\sqrt{2}\beta = 2$ the minimum stress concentration obtained is 1.785 at $\lambda = 1.8$. This compares with Wittrick's (32) solution for a flat plate ($\beta = 0$) of 1.306 for $\lambda = 1.0$.

As in (1.6) by assuming an eccentric reinforcement to be of a doubly symmetrical rectangular cross-section whose centre is offset distances 'b' and 'h' (figure 3), the stresses obtained are plotted in figures 43, 44 and 45. The stresses for the eccentric reinforcement are in all cases higher than those for symmetrical reinforcement.

Comparing the two Cases (A) and (B) it is found that the bending stresses are very much lower in 'Case B' and it seems that this is because the window load is being concentrated in the regions where the reinforcement and the shell have the curvature necessary to resist normal loads by a predominantly membrane action. The differences between the two cases are most pronounced for higher values of β as was predicted. In fact for the lowest value $\sqrt{2}\beta = 2$, in the optimum region $1 < \lambda < 1.8$ and $\mu > 3$ there is

very little difference between the two cases.

Mansfield's efficiency factor: (See (1.6))

Table III gives the maximum principal stresses for symmetrical ($\lambda = 0.4$) and eccentric ($\lambda = 1.6$) reinforcements. The agreement with Mansfield's suggested formula seems good though the stress system is very complex. The agreement is much better for 'Case B' as compared with 'Case A' due to the lower bending stresses previously mentioned.

It appears that for 'Case B' figures 40, 41 and 42 may be confidently used for symmetric as well as eccentric reinforcements for other than rectangular cross-sections.

Table III

	$\sqrt{2}\beta = 2$		$\sqrt{2}\beta = 3$		$\sqrt{2}\beta = 4$	
μ	$\lambda = 0.4$ Symmetric	$\lambda = 1.6$ Eccentric	$\lambda = 0.4$ Symmetric	$\lambda = 1.6$ Eccentric	$\lambda = 0.4$ Symmetric	$\lambda = 1.6$ Eccentric
1	2.466	2.151				
2	2.565	2.351	2.851	2.585		
3	2.628	2.465	2.953	2.723	3.176	2.932
4	2.672	2.534	3.026	2.829	3.254	3.018
5	2.704	2.581	3.081	2.907	3.312	3.108
6	2.728	2.613	3.125	2.964	3.398	3.184
7			3.159	3.009	3.455	3.248
8					3.502	3.303

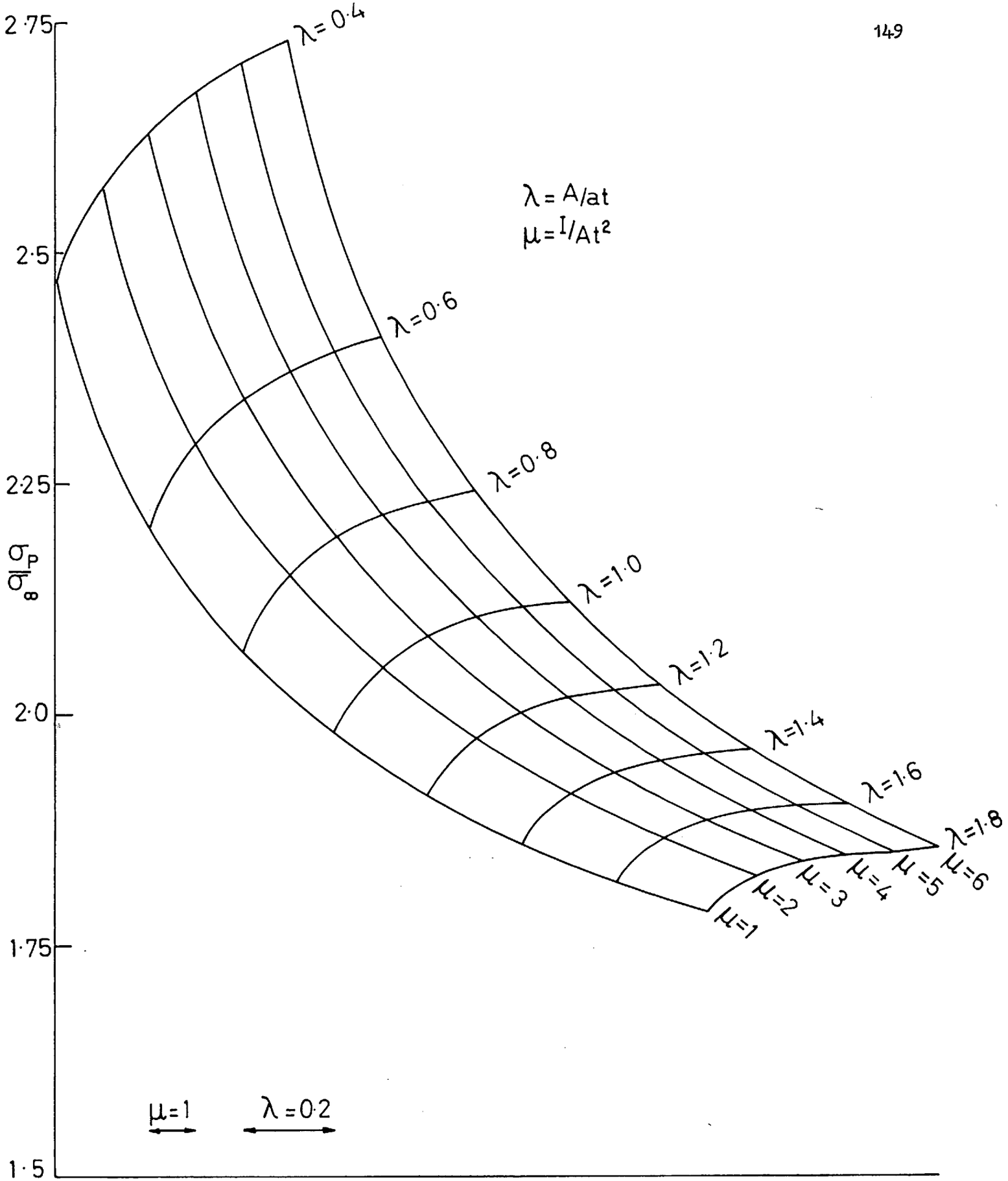

FIG. 40 SYMMETRIC REINFORCEMENT $\sqrt{2}\beta = 2$

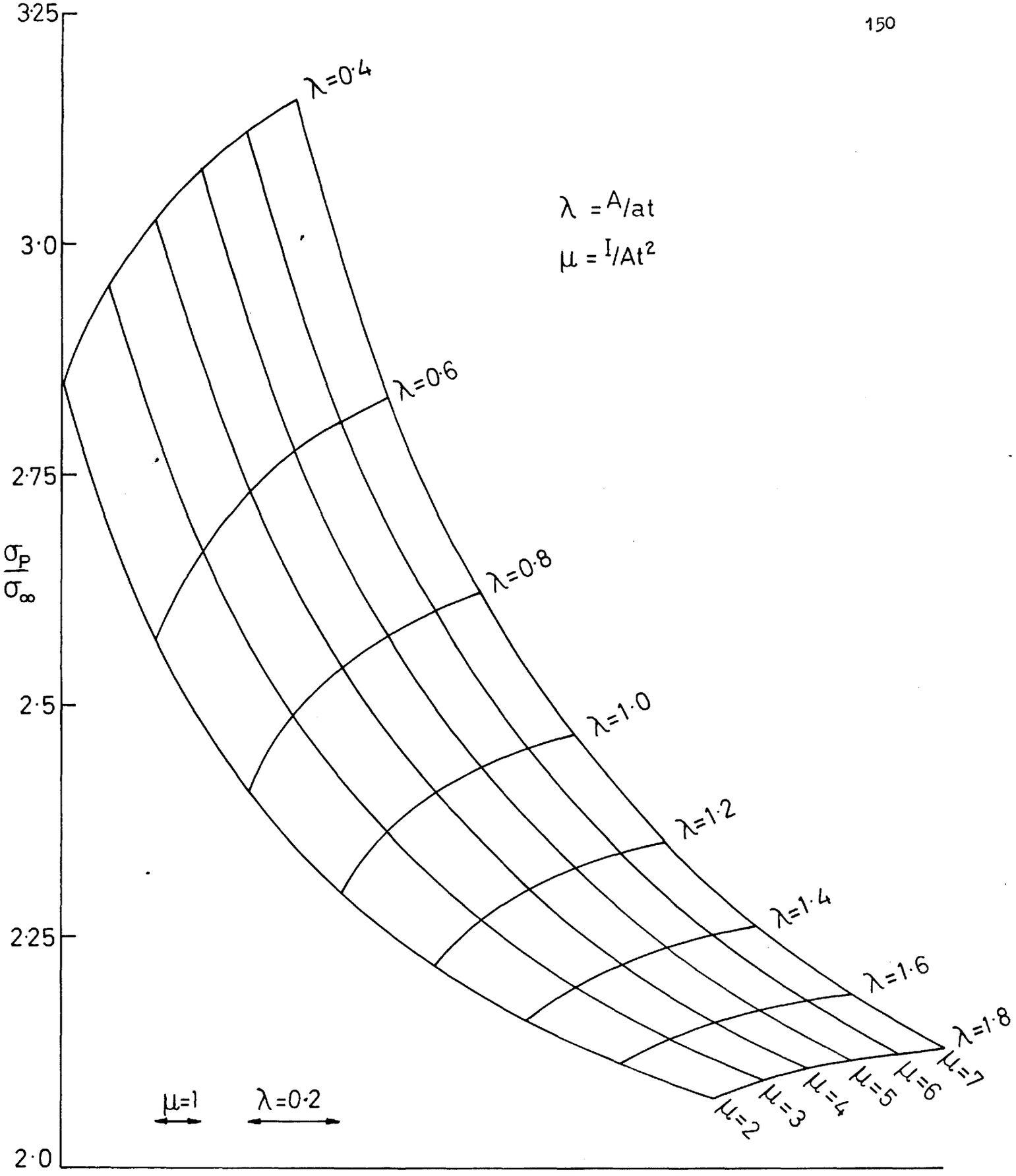

FIG. 41 SYMMETRIC REINFORCEMENT $\sqrt{2}\beta = 3$

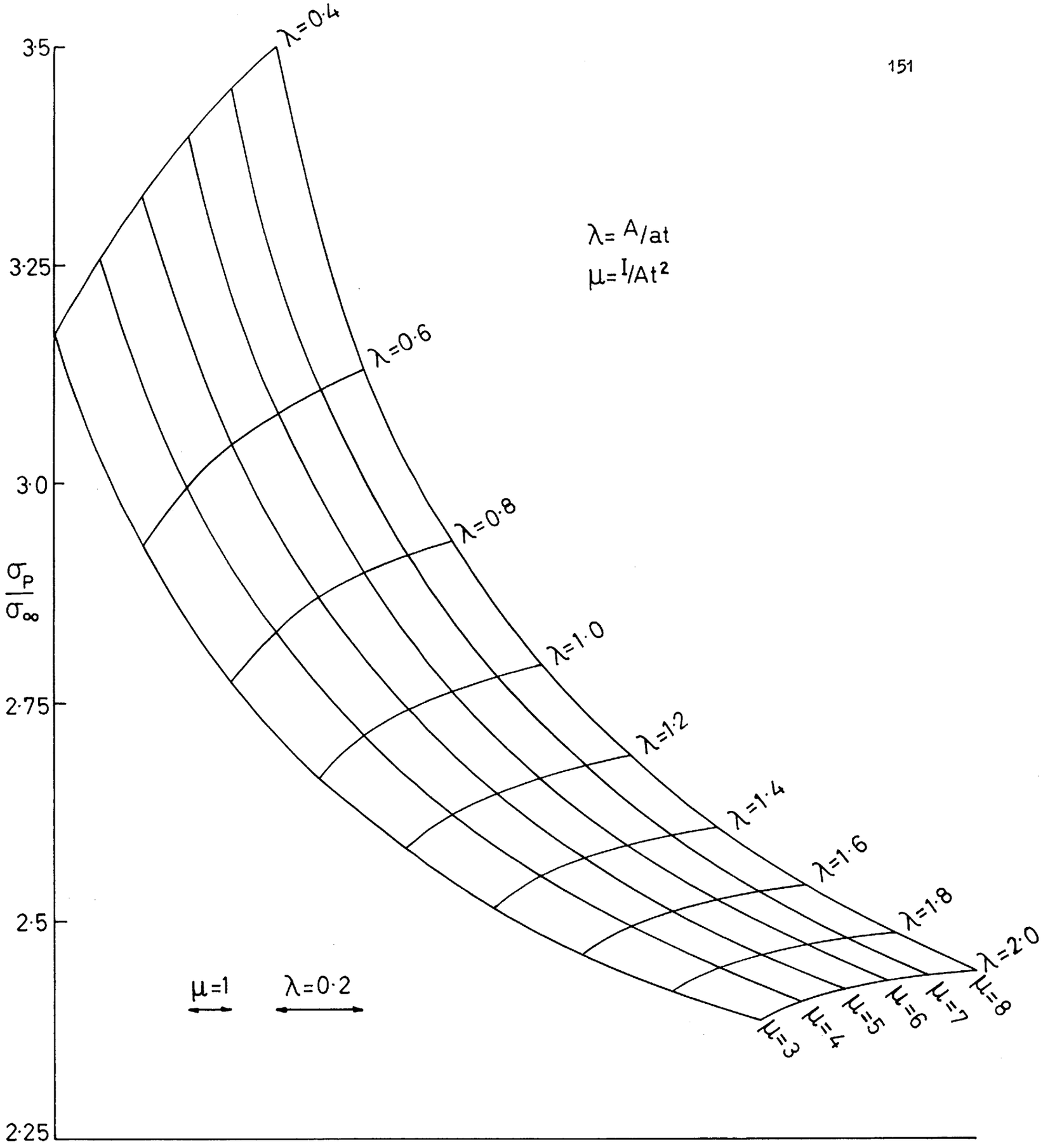

FIG. 42 SYMMETRIC REINFORCEMENT $\sqrt{2}\beta = 4$

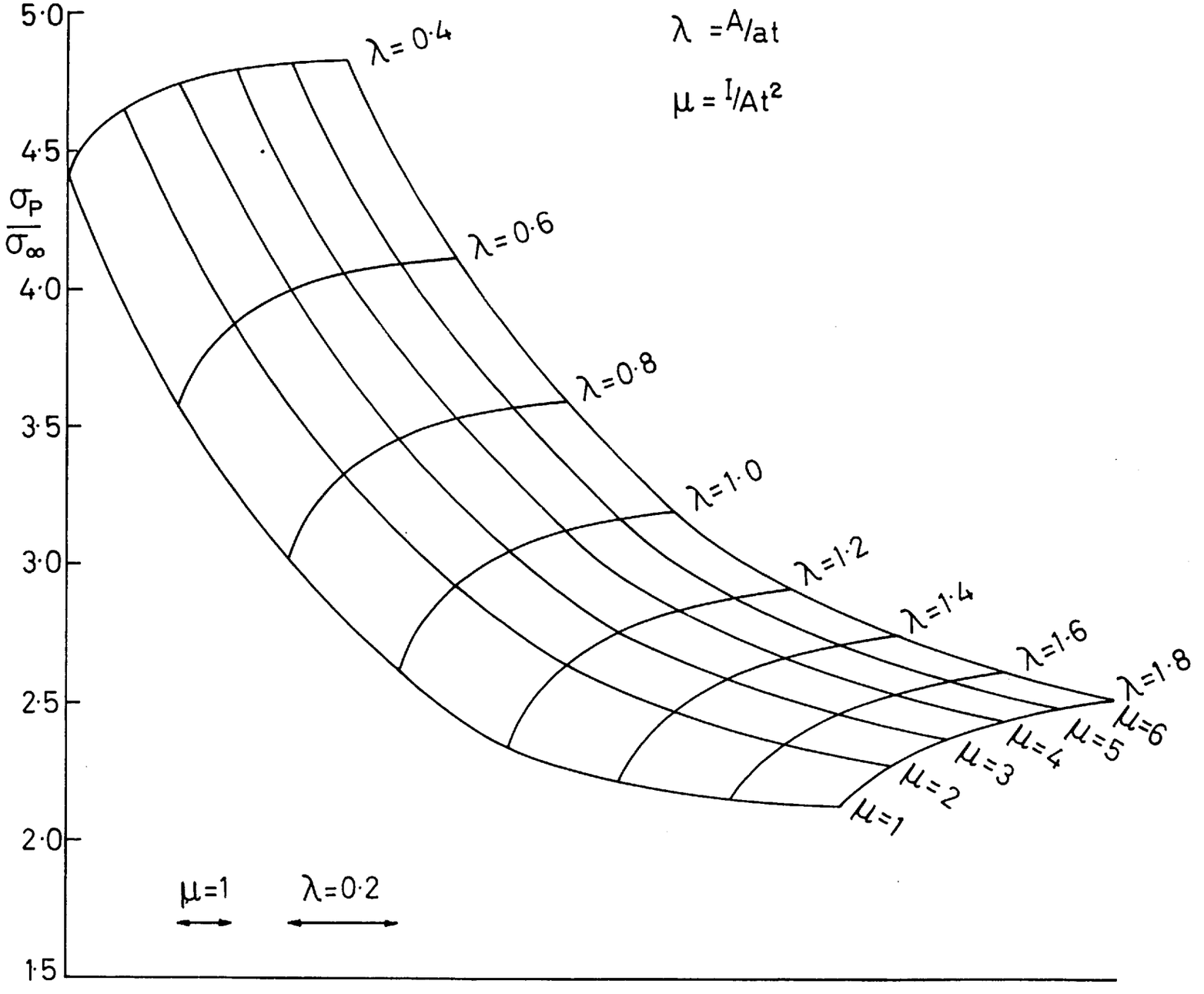

FIG. 43 ECCENTRIC REINFORCEMENT $\sqrt{2}\beta = 2$

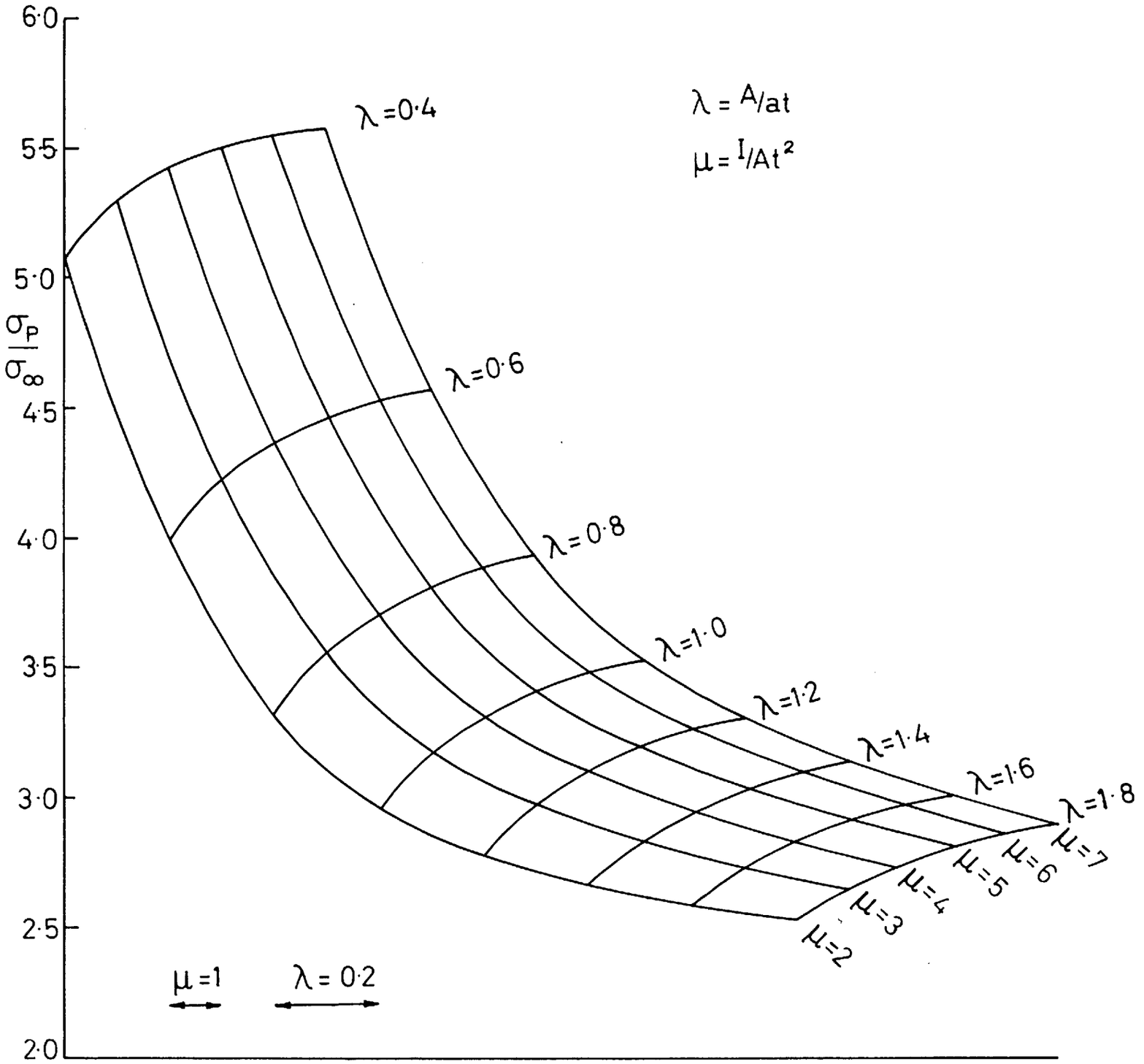

FIG. 44 ECCENTRIC REINFORCEMENT $\sqrt{2}\beta = 3$

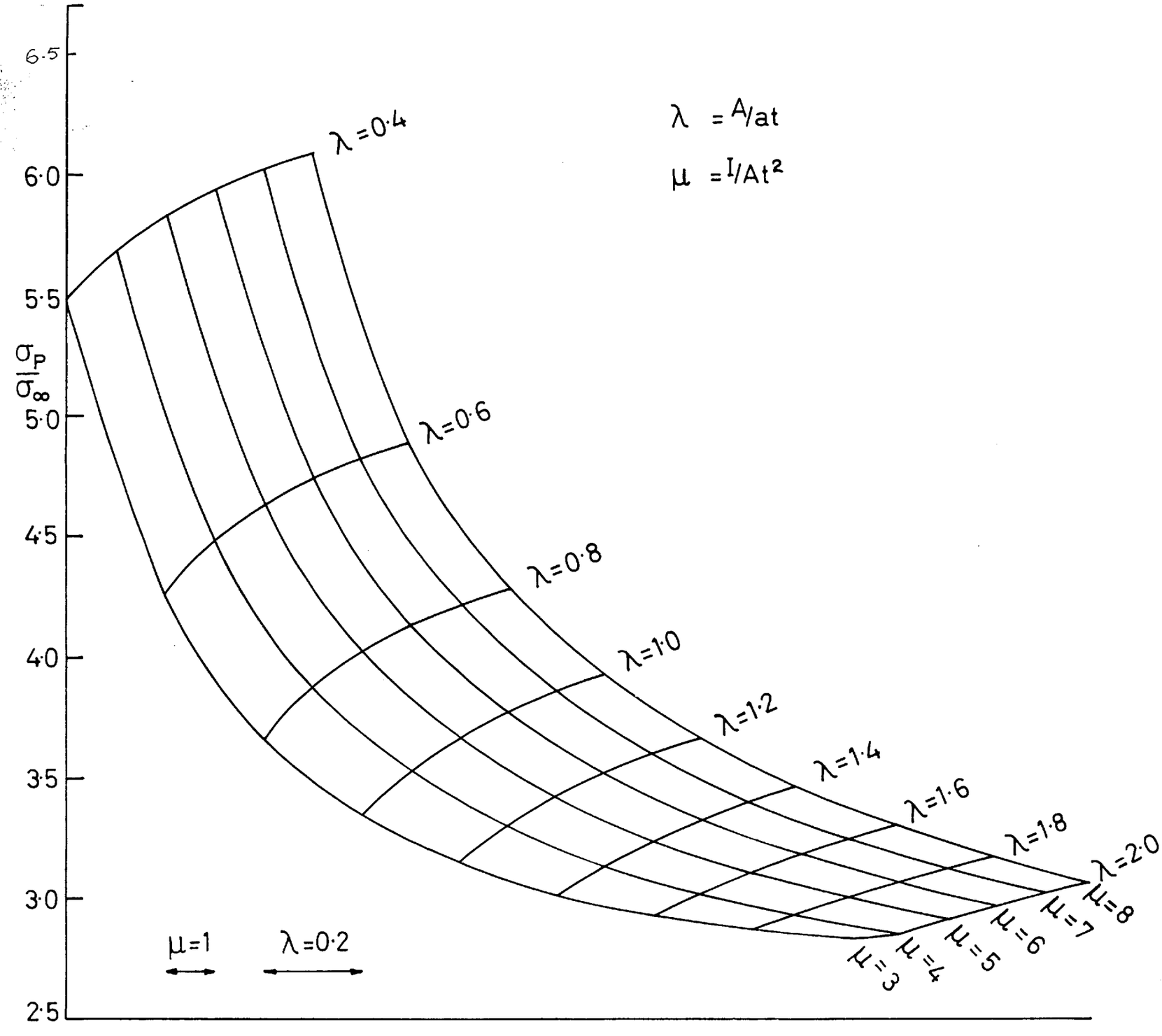

FIG. 45 ECCENTRIC REINFORCEMENT $\sqrt{2}\beta = 4$.

APPENDIX XIV

Reinforced elliptical hole in a cylindrical shell (loading 'Case B')

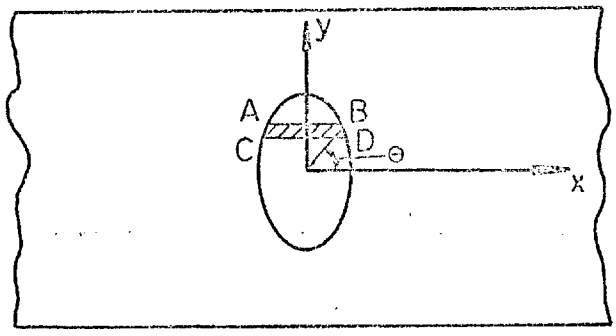

It can be assumed as in Appendix XIII that the pressure load acting on the region ABCD is transmitted as shears distributed along AC and BD.

The shear per unit length = $pr_o.r\ \cos\theta.\cos\alpha$, which using (2.3) reduces (to the order of ε) at $\rho = 1$ to,

$$pr_o \cos^2\gamma + \varepsilon pr_o \cos 2\gamma.\cos^2\gamma.$$

The equations of equilibrium (2.5.1), (2.5.2), (2.5.3) and (2.5.4) remain the same whereas (2.5.5) becomes,

$$Q_n = P_{,s} + T.\cos\alpha.\eta_{o,s} - pr_o\cos^2\gamma - \varepsilon pr_o\cos 2\gamma.\cos^2\gamma.$$

(This change gives rise to an additional term on the right-hand side of (2.7.8) as

$$- pr_o \cos 2\gamma \cos^2\gamma$$

There is a corresponding change in Appendix IX, page 136, where the additional term is

$$+ 24\beta^2 \cos 2\gamma.\cos^2\gamma.)$$

To study the influence of reinforcement Wittrick's (32) optimum, almost neutral hole, ($\lambda = 0.8$, $\frac{a}{b} = 1.4$) is chosen. It was found that the variation of the maximum principal stress with μ was very small as the bending stresses in the shell were very small. For example for $\sqrt{2}\beta = 2$, the variation of σ_p/σ_∞ was from 1.446 to 1.457 as μ varied between 2 and

7. The points corresponding to 'Case B' have been plotted for comparison with "Case A' in figure 46.

Even though the bending stresses are small, the reinforcement in the curved shell is not as efficient as in the flat plate. Considering Wittrick's (32) optimum cut-out again, at $\theta = 0$, the imbalance between the window shear and the normal component of reinforcement is only about 10%. But the shell is very sensitive to such an effect as is apparent in the high stress concentrations around a circular hole in a cylinder under simple tension. The reduction in stress is seen in figure 46 to be most pronounced for large β where 'Case B' is a more realistic model. For smaller values of β the two cases approach the same value.

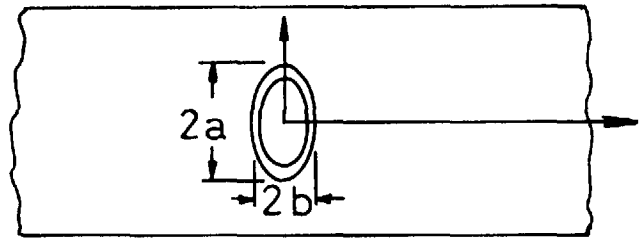

$\frac{E_R}{E_s} = 1;\ \lambda = 0{\cdot}8;\quad \mu = 6;\quad {}^{J}/_{I} = 2;\quad \frac{a}{b} = 1{\cdot}4$

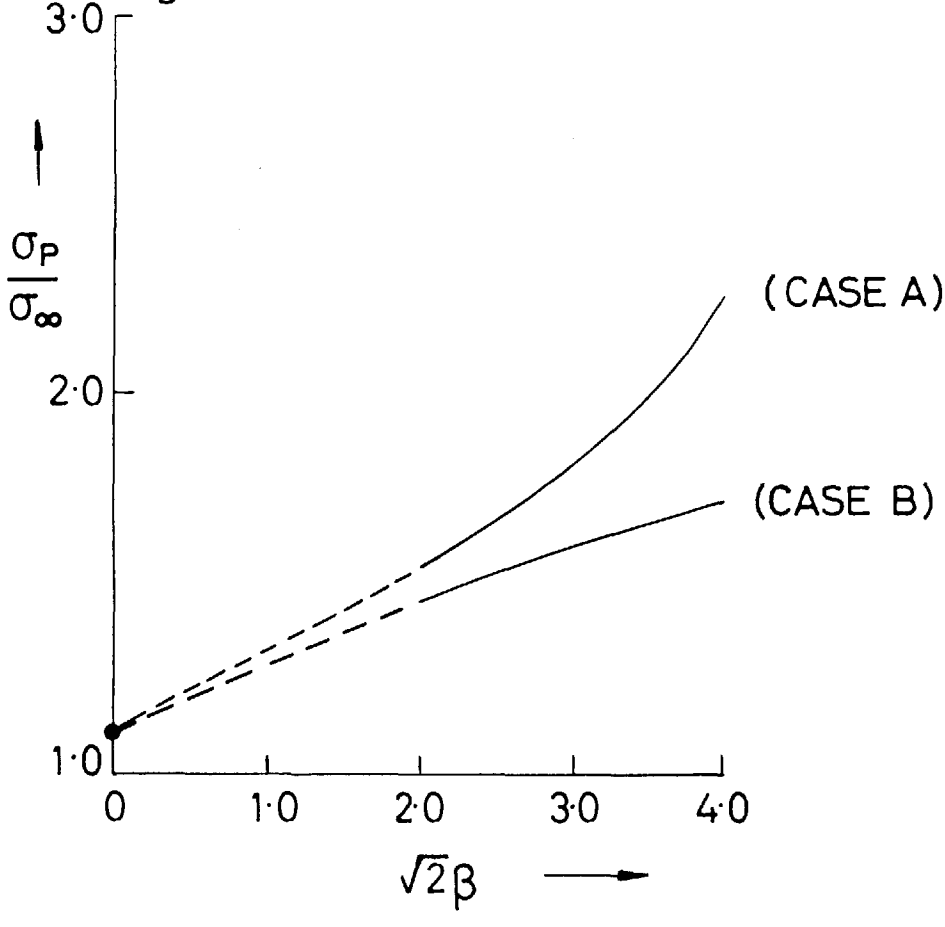

• Wittrick's solution

FIG. 46 REINFORCED ELLIPTICAL HOLE (PRESSURE LOADING)